3-2021

Improving Airfield Pavement Degradation Prediction Skill with Local Climate and Traffic

Evan M. Fortney

IMPROVING AIRFIELD PAVEMENT DEGRADATION PREDICTION SKILL WITH LOCAL CLIMATE AND TRAFFIC

THESIS

Evan M. Fortney, Captain, USAF

AFIT-ENV-MS-21-M-228

DEPARTMENT OF THE AIR FORCE
AIR UNIVERSITY
AIR FORCE INSTITUTE OF TECHNOLOGY

Wright-Patterson Air Force Base, Ohio

AFIT-ENV-MS-21-228

IMPROVING AIRFIELD PAVEMENT DEGRADATION PREDICTION SKILL WITH LOCAL CLIMATE AND TRAFFIC

THESIS

Presented to the Faculty

Department of Engineering and Management

Graduate School of Engineering and Management

Air Force Institute of Technology

Air University

Air Education and Training Command

In Partial Fulfillment of the Requirements for the

Degree of Master of Science in Engineering Management

Evan M. Fortney, BS

Captain, USAF

March 2021

AFIT-ENV-MS-21-228

IMPROVING AIRFIELD PAVEMENT DEGRADATION PREDICTION SKILL WITH LOCAL CLIMATE AND TRAFFIC

Evan M. Fortney, BS

Captain, USAF

Committee Membership:

Lt Col Steven J. Schuldt, PhD, PE
Chair

Maj Justin D. Delorit, PhD, PE
Member

COL James P. Allen, PE, MSS
Member

Lt Col Ryan A. Howell, PhD
Member

Abstract

Airfield pavements are a critical component of the global transportation network that provide a platform for national defense. Accurate predictions of rigid and flexible pavement condition reduce the need for costly, time-intensive physical inspections that disrupt operations. In practice, the leading pavement management software creates degradation predictions from like-type pavement groups using age as the independent variable and current state conditions as the dependent variable. Calibration by location is limited to the grouping of pavement families and is not influenced by the array of local condition effects such as climate and aircraft passes. For this work, a framework is created and implemented on three data sets to create unique and comparable model set results that reveal compelling ways in which time and condition interact. This framework utilizes a bias-reduced, principal component regression model that builds upon accepted practices for degradation modeling to enhance and possibly augment future prediction capabilities. The model was individually applied to each pair of location and pavement family and reveals several novel findings: the selected climatic variables describe 74-93% of pavement degradation across a dataset of 1,995 pavement sections constructed between 1985 and 2019 from 14 CONUS Air Force installations; the effects from climatic factors are temporally nonstationary, as discovered through fluctuations of variable significance throughout the observed time period, and further confirmed by climate change projections that should drive renewed research into adaptable condition prediction capability; and environmental factors are more impactful than aircraft passes,

with between 2-15% improvement of model skill in the pavement family that supports the most aircraft operations when comparing two datasets of 266 pavement sections constructed between 2010 and 2019 from 9 CONUS AF installations. More data collection of the same and different data fields will increase the confidence in model results since many data gaps existed due to a short temporal scale of some data. The created framework revealed that freeze-thaw, solar irradiance, precipitation, and sustained wind were commonly significant factors in describing degradation variability. This framework can be applied to any large airport with available data to determine local sources of degradation and improve pavement design sustainability.

Acknowledgments

I would like to express my sincere appreciation and love to my wife and girls who sacrificed the most. Also, to my faculty advisor, Lt Col Steven Schuldt, thank you for your guidance and support throughout the course of this thesis effort. Maj Justin Delorit was also critical in helping guide me through the depth of critical thinking required to complete this thesis. Sarah Brown and Kurt Lamm gave so much of their time to help support the creation of my methodology. The Pavements community is large and supportive, and I would not have been able to do this without the voices of many. I am especially thankful for the help from Lt Col Ryan Howell and Capt John Kulikowski. I would also like to thank COL Jim Allen, and those at the Construction Engineering Research Lab both for the support and latitude provided to me in this collaborative endeavor.

Evan M. Fortney

Table of Contents

Page

List of Figures

Page

List of Tables

Page

IMPROVING AIRFIELD PAVEMENT DEGRADATION PREDICTION SKILL WITH LOCAL CLIMATE AND TRAFFIC

I. Introduction

Background

Airfield pavements are a critical component of the global transportation network that provide a platform for national defense. Accurate predictions of rigid and flexible pavement condition reduce the need for costly, time-intensive physical inspections that disrupt operations. (Mulry et al. 2015). Preventative and corrective maintenance activities are founded upon accurate expectations of degradation. In practice, the leading data-driven airport pavement management systems (APMS) create degradation predictions from like-type pavement groups using age as the independent variable and current state conditions as the dependent variable. Decision makers rely on APMSs to predict pavement condition to better plan investiture and rehabilitation of pavements between physical inspections (Gendreau and Soriano 1998; Shahin 2005). Nearly all state aviation agencies worldwide use APMSs to provide a comprehensive, objective, structured approach to improve decision-making efficiency and justify remedial actions necessary to maintain safe and serviceable pavements (Ismail et al. 2009). Several pavement management systems evaluate highway pavements, but few APMSs have robust databases and prediction capabilities (Ismail et al. 2009).

PAVER™ is the leading, fully-functional APMS used by the US Department of Defense (DoD) and Federal Aviation Administration (FAA) since the 1970s (Federal Aviation Administration 2014; Shahin and Rozanski 1978). PAVER™ is a database, planning tool, and modeling system that uses polynomial-fit regression to approximate future pavement conditions

for user-defined, like-type pavement families and helps plan maintenance for nearly 2.2 billion square feet of airfield pavement valued at $20B (Kemeny 2018; Shahin 1994; Shahin and Rozanski 1978). The database and internal processes in PAVER™ will be used for this research to develop an adaptable framework that has the potential to increase prediction capability and improve condition-aware pavement design.

Researchers have conglomerated pavement distress and condition data into spatial and family categories to investigate distress trends on a larger scale using climatic (Meihaus 2013; Parsons and Pullen 2016) or geographic zones (Sahagun et al. 2017). Still, location-specific research has been limited due to coarse data resolution. Pavement engineers understand distress sources for pavements, such as age, environment, traffic, maintenance history, pavement substructure, and construction quality (Haas 2001). Aircraft traffic-related variables like loading (Ameri et al. 2011; Sawant 2009), tire configuration (Shafabakhsh and Kashi 2015; Wang and Al-Qadi 2011), and frequency (White et al. 1997) are among the leading causes of deterioration. Pavement age and environmental factors also significantly affect the deterioration rate due to senescence and exposure to weather impacts (Ankit et al. 2011; Chinowsky et al. 2013).

Problem Statement

It is difficult to quantify and attribute sources of degradation across time since conditions are stochastic and dynamic. Prediction capability could be expanded by addressing which deterioration sources are prevalent at each airport, attributing that source's effect on pavement condition, and tailoring rehabilitation plans and future pavement design efforts for that airport's specific needs.

Limitations exist in APMS due to the selection and scope of independent variables used to drive predictions, which are not locally calibrated and cannot adapt to likely future conditions,

such as nonstationary climate or changes in use patterns. As climate continues to change and aircraft operations fluctuate with new aircraft implementation according to changing mission requirements, the importance of accurate, reliable, and sustainable considerations within APMSs will continue to increase.

Research Objectives

This thesis seeks to achieve the following objectives:

1. Conduct a thorough review of the current literature surrounding pavement distresses and condition prediction capabilities.
2. Utilize datasets and established processes from PAVER™ to group similar pavements and create degradation functions for further modeling and analysis.
3. Develop and implement a novel framework to apply an unbiased, statistical tool to datasets to identify the amount of the discovered effect on pavement condition from select climatic and aircraft traffic variables.

Thesis Organization

This thesis follows the scholarly article format in which Chapters 3, 4, and 5 serve as stand-alone academic conference or journal publications. Chapter 2 is a high-level literature review summarizing recent, relevant academic literature and establishes support for the research methodology used in further chapters. Chapters 3 and 4 are applications of the created framework using datasets from USAF installations, PAVER™ condition data, Air Traffic Activity Report (ATAR) traffic pass data, and continental United States (CONUS) weather station data. This framework applies to all large military and civilian airports or pavement systems with continual climatic exposure and high loading conditions. Each article individually contains an abstract, introduction, literature review, data description, methodology, results,

discussion, and conclusion. Chapter 5 is a stand-alone article plus conclusions section that summarizes potential future work along with the significance of this research for pavement asset managers and decision makers.

Chapter 3, "Improving Airfield Pavement Degradation Prediction Skill with Local Climate," achieves research objectives #2 and 3 by describing the methodology used to select pavement families and applying similar logic from PAVER™ to create predictive degradation curves on a dataset of USAF installations. A bias-reduced statistical model determines the variation described in linear approximations of pavement degradation by the specific base and family pairings using only climatic independent variables. The climatic variables utilized were freeze-thaw (days), water equivalent precipitation (inches), snowfall depth (inches), sustained wind speed above 10 miles per hour (days), and solar irradiance (W/m^2), which were compiled annually and normalized. This paper was submitted to the American Society of Civil Engineers (ASCE) *Journal of Infrastructure Systems* on 15 Feb 2021 and is pending acceptance.

Chapter 4, "Accounting for the Combined Effects of Local Climate and Traffic on Airfield Pavements Using Principal Component Regression" also accomplishes research objectives #2 and 3 by following the system framework outlined in Chapter 3 for two separate datasets with a shorter temporal scale that incorporates both aircraft traffic and climatic independent variables. These two model sets, one without traffic passes, are compared to display the increase in percent variation described by an unbiased, principal component regression model and therefore display the individual contributions to pavement deterioration variability for both climate and aircraft passes separately. This paper's target journal is the ASCE *Journal of Transportation Engineering, Part B: Pavements* with an impact factor of 1.5 and common application among pavement professionals and asset managers in the field.

Chapter 5, “Creating Condition Aware Pavement Predictions,” details the significance of the results and provides a summative conclusion with its overall potential impact on the field of knowledge. This article is intended for publication in *The Military Engineer* 2021 September/October “Asset Management,” published by the Society of American Military Engineers (SAME). This article is directed towards a US Government employee audience with the purpose of plainly conveying the benefit of having localized predictive modeling capabilities that describe and attribute the leading sources of airfield pavement deterioration. The additional research significance, research contributions, and recommendation for future research sections serve as a conclusion that displays how the novel framework created in Chapter 3 and implemented further in Chapter 4 can be used to plan more efficient maintenance regimes, design sturdier pavements, and adapt to future projections of condition with increased mission output and changing climate conditions that may not resemble historical observations.

II. Literature Review

Chapter Overview

A comprehensive literature review has been conducted to establish a firm foundation for the proposed study. This literature review focuses on investigating the current practices and relevant research studies in airfield pavement life-cycle management and planning. This chapter summarizes and organizes the reviewed literature in three main sections: (1) a summary of airport pavement management systems (APMS) that maintain databases and create pavement degradation predictions, with an added focus on the capabilities of PAVER™; (2) common distress types and studies about potential degradation variables; and (3) pavement sustainability considerations that integrate the triad of environment, finance, and social values, including effects from climate change forecasts.

Pavement Management Systems

An analysis of existing asset management tools and models at the turn of the century highlighted risk areas and recommended changes to better manage bridge health data (Frangopol et al. 2001). It concluded that a modern, computerized, reliability-based approach was necessary for life-cycle asset management. Many pavement management systems exist for road pavements that all seek to provide a systematic and justifiable procedure to determine repair priorities and allocate resources for maintenance and rehabilitation (Ismail et al. 2009). Although different management systems are used to evaluate highway pavements and create predictions of degradation using varying independent variables, only a few airport pavement management systems (APMS) have as many robust qualities. Several prototype tools exist, such as AIRPACS (Seiler et al. 1991), that uses professionally-acquired heuristics to help select rehabilitation options, but PAVER™ is the leading, fully-functional APMS.

The DoD primarily uses PAVER™ to provide proactive infrastructure management pathways for pavement. PAVER™ was created by the U.S. Army Construction Engineering Research Laboratory (CERL) in the late 1970s and is currently supported by the Federal Aviation Administration (FAA), Federal Highway Administration (FHA), US Army, US Air Force (USAF), and US Navy (Federal Aviation Administration 2014). PAVER™ is a database, planning tool, and modeling system that uses polynomial-fit regression to approximate future pavement conditions for user-defined, like-type pavement families (Shahin 1994; Shahin and Rozanski 1978). Airfield pavement families within PAVER™ are determined by three factors: pavement material type, priority, and use (Shahin 1994). The foundation of asset condition is the Pavement Condition Index (PCI), a numerical index from 0 to 100 that is determined by visual inspection from pavement experts guided by specific ASTMs (Greene et al. 2004). The international roughness index (IRI) is another common quantifier of pavement condition and ride quality that focuses on vibrational effects from longitudinal road roughness (Múčka 2016). PCI is a more encompassing metric that describes full-thickness pavement performance and is used by PAVER™. In contrast, IRI is more descriptive of surface conditions, so PCI will be used to quantify pavement conditions for the rest of this research.

Analysts use several theoretical curves to understand asset degradation. Shahin (2005) highlights a curve correlated to PCI that degrades sharply at first, maintains a steady score for most of the asset's life, and then rapidly declines at the critical point near the end of its life. A robust APMS can better predict the critical point of degradation so that maintenance and repair (M&R) resources will be most efficiently spent. Figure 1 demonstrates the theoretical, critical condition point and corresponding PCI scale.

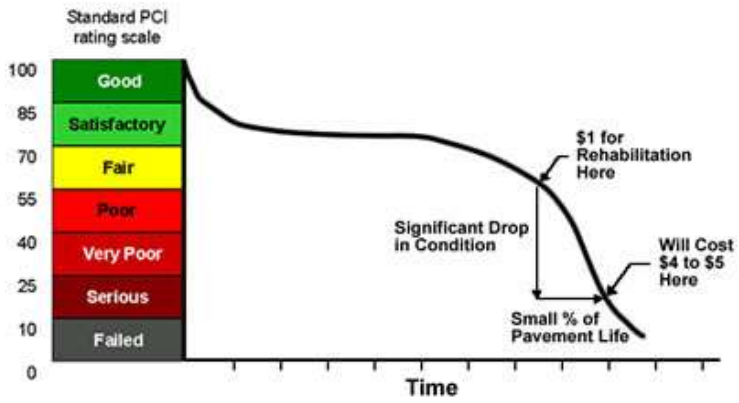

Figure 1. Typical life cycle of pavements (Colorado State University 2019)

Parsons and Pullen (2017) studied whether a curve fit (polynomial, Gaussian, or otherwise) is unnecessary and if a linear representation would suffice for predicting degradation. Visual inspection supported their hypothesis, so they performed a statistical analysis of variance (ANOVA) between the mean PCI scores by year and the decay rate (change in PCI per year). Their conclusions show that despite some pavement families which "do not exhibit the conceptual S-shaped deterioration curve," linear approximations should be avoided for both flexible and rigid pavements (Parsons and Pullen 2017). Pavement degradation generally follows a curve, but a linear degradation approximation is necessary if there is not enough data to support the formulation of a higher-order function.

The accuracy of PCI predictions by the PAVER™ internal software was validated within only a few percentage points, which is considered a reasonable degree of accuracy in the forecasting community (Knost and Mishalani 2019). Knost and Mishalani (2019) gathered historical pavement predictions, eliminated any pavement sections that received major rehabilitation during the examination period, and compared those historical predictions with current actual scores for Air Force installations in four diverse climate zones across the contiguous United States (Meihaus 2013). Even though PCI determination is standardized,

subjectivity from the rater can still slightly influence the PCI outcome. For example, pavements with lower initial ratings produced pessimistic forecasts (Knost and Mishalani 2019).

Pavement Distress Types

There are many different pavement distress types as listed in ASTM D5340 that pavement inspection experts reference to determine the PCI of a pavement section (American Society for Testing and Materials. 2012). The most prevalent causes for distress on airfield pavements are age, environment, traffic, maintenance history, pavement substructure, and construction quality, as shown in Figure 2 (Haas 2001)

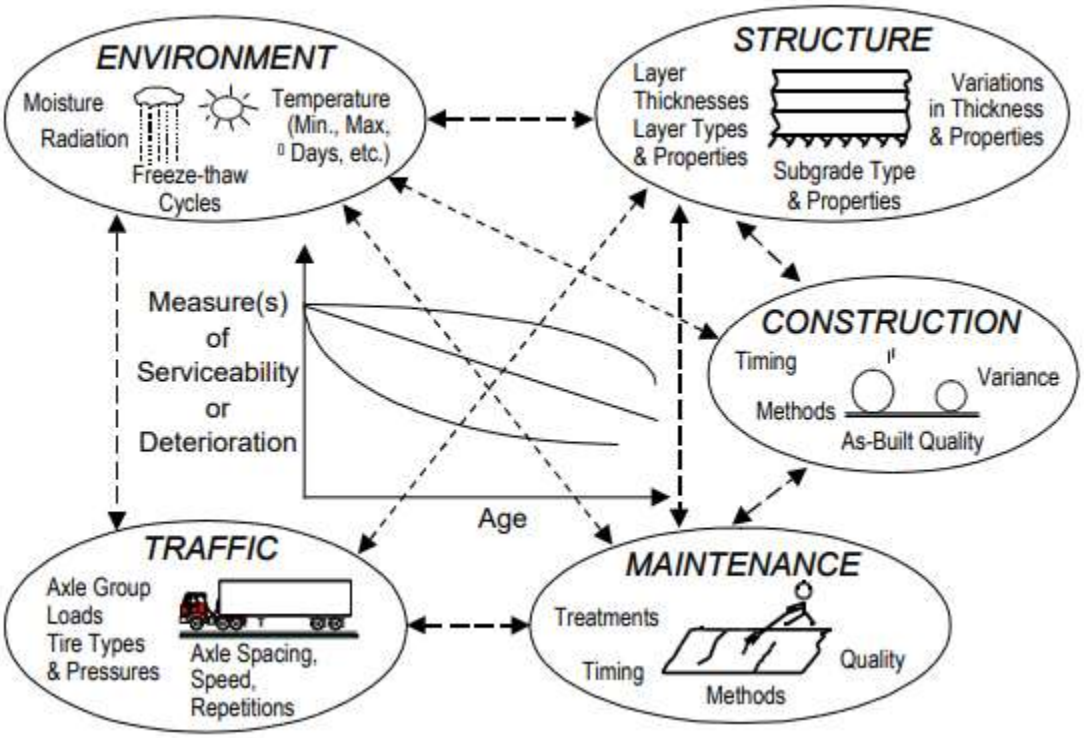

Figure 2. Factors affecting pavement performance (Haas 2001)

Ankit et al. (2011) performed a detailed review of the effects of various environmental factors on pavement performance and found commonalities between them. They concluded that the encompassing term ‘remaining service life,’ as determined by forecasting models, is the most

significant predictor of serviceability; however, the determination of this variable encompasses many other factors. As expressed by their responses to environmental factors, the behaviors of the pavement material play a secondary role in forecasting pavement deterioration. Of the environmental factors reviewed, freeze-thaw, precipitation, wind speed, air temperature, relative humidity, atmospheric pressure, and solar radiation had significant effects on the material's resilient modulus and its degradation (Ankit et al. 2011).

The weight, type, loading, and frequency of aircraft are a leading cause of pavement deterioration. The landing gear configuration of large commercial aircraft was studied to determine that specific wheel shape and main gear configurations have a more extensive damage factor than channelized landing gear (Shafabakhsh and Kashi 2015). Research has been performed to analyze, model, and test the response of pavement performance to aircraft tire pressure, weight, and repetitive passes (Sawant 2009; Wang and Al-Qadi 2011). Pavement substructure and mix design are important in reducing rutting and shear failure due to aircraft traffic. However, the uncertainty and stochasticity of actual aircraft patterns mean little is known about aircraft traffic's life-cycle effects (White et al. 1997). Pavement engineers use software such as PCASE (DoD), FAARFIELD (FAA), and Alize-Airfield (French Aviation Authority) to design pavements with accurate thickness, strength, and subgrade strength required to meet the expected load capacity for the selected location, pavement type, traffic area, and controlling aircraft (Adolf 2010; Heymsfield and Tingle 2019). Empirical tables exist for all combinations of current aircraft and pavement types and are used internally by pavement design software, an example of which is shown in Figure 3 (Adolf 2010). When multiple aircraft are present, the allowable passes can be converted and summed from each aircraft into equivalent passes related

to the controlling aircraft, which is commonly set with a design standard of 50,000 passes of a C-17 (US DoD 2001a).

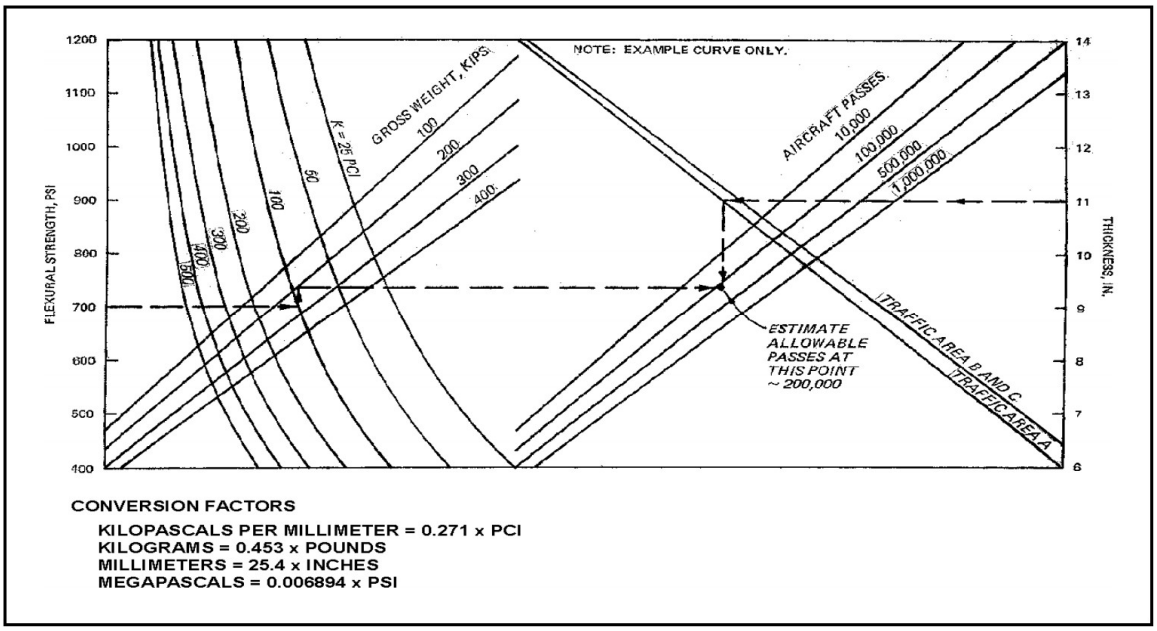

Figure 3. Example empirical plot to determine allowable passes (AFI 32-1041 2019)

It is clear that pavement life cycle is affected by weather factors. A common approach for analyzing climatic trends is by conglomerating pavement distress and condition data into familial and spatial categories to improve data resolution and increase model significance. Köppen-Geiger's (KG) established climatic types are often referenced to study differences in performance in similar climates. These climatic types can be simplified into five major regions, three of which cover almost the entire contiguous US, which share primary weather patterns without reducing climate analysis capability (Delorit et al. 2020). Figure 4 displays these KG zones with many USAF installations that typically have airport pavements.

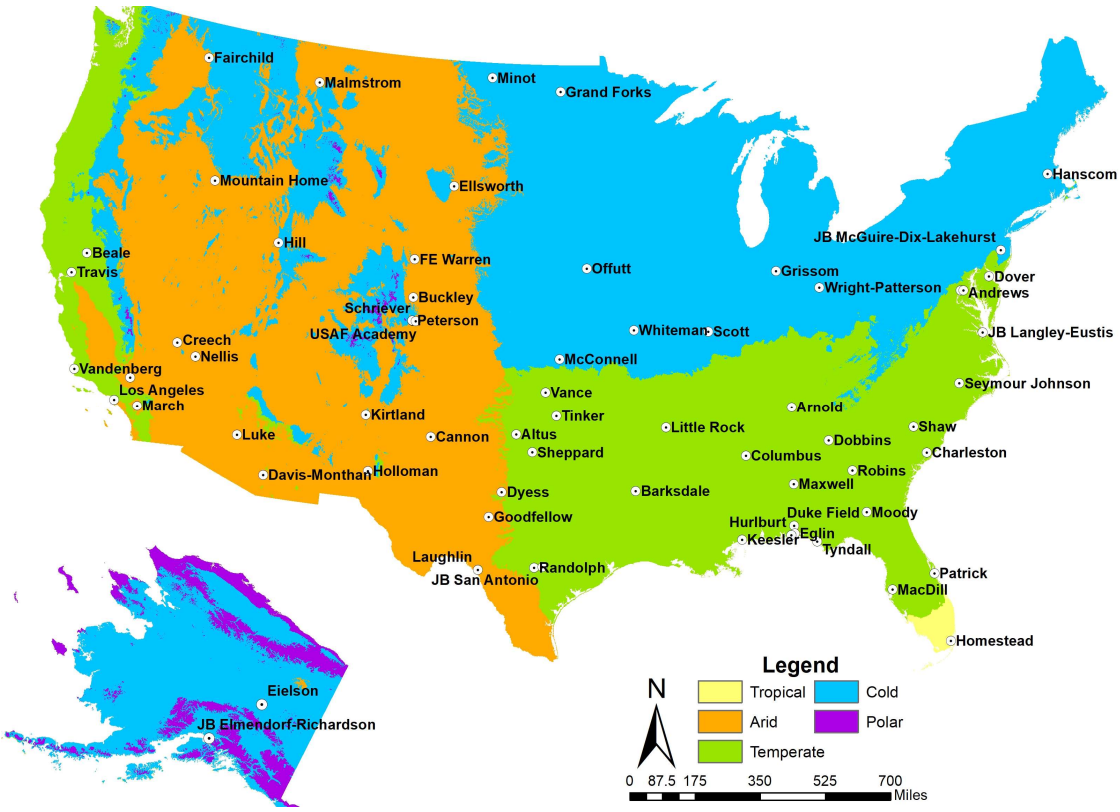

Figure 4. Major Köppen-Geiger climatic zones with USAF airfields overlaid.

Meihaus (2013) supports the hypothesis that climate zones determined solely by temperature and humidity threshold have common pavement distress trends. They propose zones that compare wet and dry with freeze and no-freeze to create four diverse climate regions, as seen in Figure 5 (Meihaus 2013). The thresholds utilized to determine wet and freezing combinations were: greater than 25 inches of average annual precipitation and greater than 750 average annual freezing degree days, respectively. By considering the change in PCI between AF installations within each of the four zones, Meihaus concluded that PCC pavement families show significantly higher deterioration rates in the freeze-dry climate.

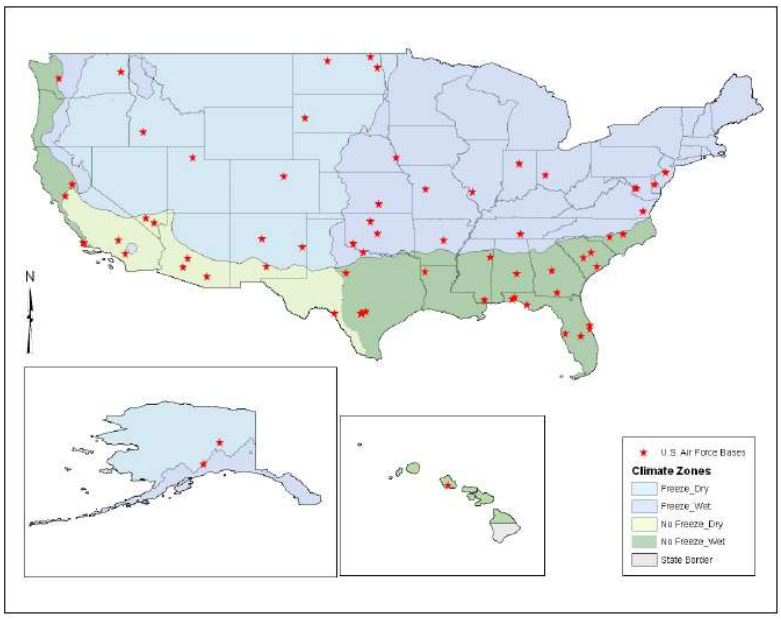

Figure 5. Climate zone map for the US using temperature and precipitation thresholds (Meihaus 2013).

Further research suggests that weather-related distresses share commonality in patterns that divide the United States into only two zones and that pavement behavior improves with time in the freeze-dry zone (Sahagun et al. 2017). This research concluded that climate is the leading cause of pavement degradation by highlighting distress types with the highest frequencies of occurrence that tie directly to weather. This finding implies that the traditional model based on humidity and temperature data is not appropriate to evaluate pavement behavior at the individual distress level (Sahagun et al. 2017). Assuming that the PCI deduct value accounts for all other distress contributors, the following distress types showed decreased PCI deduct values over time in the freeze-dry climate zone: corner spalling, joint spalling, shrinkage cracking, scaling, large patch/utility cut, small patch, joint seal damage, durability cracking, and linear cracking. Although many similar types of distresses correlated to geographic regions, the researchers could not conclude that those climates caused distresses due to limitations in the data provided.

So far, the literature ignores other frequent distress contributors besides residual effects that may have been included in each climate zone. This assumption presents a concern, but Bennett (2019) also considered pavement structure factors. Although Bennet did not generate a regression model, an analysis of trends revealed which distress types had the most substantial cumulative reduction in pavement conditions throughout all Air Force installations. Each distress type was statistically analyzed to determine if pavement structure or climatic variables influenced the likelihood of each distress. They revealed several factors that shared statistical significance among the top seven distress types. Table 1 below shows how the age of the pavement is the most common factor; thickness, feature type, subgrade, and freeze-thaw cycles share the next level of significance; and average maximum temperature, average days above freezing, and the freeze index share the next lower level of significance (Bennett 2019). This ranking suggests that the number of freeze-thaw cycles is the most significant climatic factor.

Table 1. Common significant factors in PCC distresses (adapted from Bennett 2019).

Factors Common Among	Statistically Significant Factors
7 of the 7 Distresses	Years Since Major Work (Age)
6 of the 7 Distresses	None
5 of the 7 Distresses	Thickness Feature Subgrade Freeze-thaw Cycles
4 of the 7 Distresses	Average Maximum Temperature Average Days Above 32° C (Extreme Heat) Freeze Index
3 of the 7 Distresses	Average Precipitation Average Mean Temperature
2 of the 7 Distresses	None
1 of the 7 Distresses	Average Minimum Temperature Average Days Below Freezing (Extreme Cold)
0 of the 7 Distresses	None

Ultimately, they concluded that current design and management policies do not adequately compensate pavement maintenance organizations for the actual cost of repairing

these issues (Bennett 2019). Linear cracking, joint seal damage, large patches, and shattered slabs were the top four most abundant identified PCC distress types. Meanwhile, asphalt suffers more from longitudinal cracking, transverse cracking, weathering, block cracking, and alligator cracking.

Sustainability Considerations and Climate Change

Life-cycle cost analysis began as research to examine pavement performance and long-term cost over time to optimize financial investment. However, life-cycle assessment (LCA) considerations have evolved into a holistic sustainability approach to pavement analysis (Allen and Albert 2014). Sustainable pavement practices consider economic factors and environmental and social value impacts from original pavement materials through construction and operations to end-of-pavement-life decisions. Pavement sustainability and APMS decisions are combined in life-cycle assessment tools to consider climate change-related variables and impacts on society based on balancing the aspects of economy, environment, and social values with a key objective for improved resilience (Harvey et al. 2016).

Experts spanning many academic fields agree that the global average temperature will continue to increase over the next century, with aggressive projections showing a global temperature change (GTC) of 2.7 ^{0}C by the end of the century (Kjellstrom et al. 2018). To best communicate the potential impacts of varying climate change conditions, researchers reference several common scenarios called representative concentration pathways (RCP) containing emission, concentration, and land-use trajectories (van Vuuren et al. 2011). Commonly referenced RCP projections represent mitigation levels of greenhouse gas emissions and their effect on population and gross domestic product (GDP). The ultimate impact of these scenarios on pavement deterioration is increased aircraft traffic due to population increase and harsher

climatic conditions such as increased freeze-thaw days near the poles and higher temperatures with more solar irradiance near the equator (van Vuuren et al. 2011).

Chinowsky et al. (2013) researched predictions for climate change on expected maintenance costs of highway infrastructure. Pessimistic projections show increases of up to $2.8 billion annually for maintenance costs in the U.S. for all paved and unpaved roads by 2050 when measuring the following three separate types of deterioration: rutting caused by precipitation, rutting caused by freeze-thaw, and cracking of roads due to high temperatures. However, some conservative projections have no realizable difference in maintenance costs because warmer temperatures offset expected damages by cold weather events (Chinowsky et al. 2013).

Taylor and Philp (2015) proposed the Thornwaite Moisture Index climate indicator as an effective measure to account for climatic conditions. They created a model using this data that considered the amount of rutting and surface cracking in terms of a change in the international roughness index (IRI). Moreover, they performed a systematic review on climate change policies and pavement-focused literature to portray how receptive and ready many nations are to adapt politically and socially (Taylor and Philp 2015). If degradation effects can be attributed to specific climate factors, decision makers could better prepare and adapt to the breakdown of their pavement infrastructure.

Research Limitations and Areas of Opportunity

Despite the significant contributions of these studies and the effectiveness of current airport pavement management systems, little reported research attributes distress with life-cycle pavement performance and allows APMS software to adjust assessment predictions due to local climatic and aircraft traffic effects, whether historical or as projected conditions.

Accordingly, the following research contributions will present and implement a novel framework that applies a bias-reduced, statistical tool to specific pairs of location and pavement family, ultimately identifying the contribution from select climatic and aircraft traffic on pavement condition. Moreover, the varied temporal selections of the datasets analyzed will display changes in climatic effect on pavement performance across time. This systems framework that accounts for varying potential conditions such as mission change, new aircraft, or climatic change can improve the current spectrum of APMSs by incorporating condition-aware degradation predictions, whereas current approaches are age-centric. Ultimately, improved accuracy, fidelity, and granularity in degradation prediction could lead to more informed rehabilitation planning and design capability that includes customized agents for creating sustainable pavement management decisions.

III. Scholarly Article 1: Improving Airfield Pavement Degradation Prediction Skill with Local Climate

Evan M. Fortney; Steven J. Schuldt, Ph.D., PE; James P. Allen, PE, MSS; Sarah L. Brown; Justin D. Delorit, Ph.D., PE

Abstract

Transportation networks rely on serviceable airfield pavements to support economic security and national defense. Accurate predictions of rigid and flexible pavement conditions reduce the need for costly, time-intensive physical inspections that disrupt operations. In practice, airfield pavement predictions are made using statistical analogs based on current-state conditions from groups of similar assets across a broad geographic region, mainly using pavement age. Most predictions are not locally calibrated and are not easily adaptable to account for likely future conditions, like changes in use patterns or climate. This work addressed these limitations by applying a bias-free statistical model to pairs of locations and pavement families to reveal which aspects of climate skillfully explain local variability in pavement deterioration. Selected climate variables explain 74-93% of pavement degradation variation across 1,995 individual pavement sections, from 14 Air Force installations spanning three major Köppen-Geiger climatic types in the Contiguous United States. The adaptable framework created in this study suggests that locally calibrated, climate-driven models could improve pavement design resiliency and justify extending the time between inspections.

Introduction

Airfield pavements are a critical component of the global transportation network and are a cornerstone of national defense. Pavements require frequent preventative and corrective maintenance activities that require cost, time, and often destructive physical testing as part of

condition inspections that disrupt airfield operations (Mulry et al. 2015). Decision makers use various data-driven models, such as airport pavement management systems (APMS), to predict pavement condition and better plan investiture and rehabilitation of pavements between physical inspections (Gendreau and Soriano 1998; Shahin 2005). Nearly all state aviation agencies within the US use APMSs to provide a comprehensive, objective, structured approach to improve decision-making efficiency and justify remedial actions necessary to maintain safe and serviceable pavements (Ismail et al. 2009). However, these models are limited by the number and scope of independent variables that drive prediction and are not locally calibrated. Moreover, as climate continues to change, the importance of accuracy, reliability, and sustainability considerations of APMSs as a decision tool for asset and airfield managers will continue to increase.

Research studies investigating life-cycle management of airfield pavements have focused on three main areas: (1) the primary types and causes of pavement deterioration, (2) methods and modeling software used to predict future pavement condition, and (3) pavement sustainability integrating the triad of environment, finance, and values. The first area of studies discusses the most prevalent causes for distress on pavements, including age, environment, traffic, maintenance history, pavement substructure, and construction quality (Haas 2001). Loading (Ameri et al. 2011; Sawant 2009), tire configuration (Shafabakhsh and Kashi 2015; Wang and Al-Qadi 2011), and aircraft frequency (White et al. 1997) contribute to pavement deterioration as well. Pavement age and environmental factors also significantly affect the deterioration rate due to senescence and exposure to weather impacts (Ankit et al. 2011; Chinowsky et al. 2013). The temporal and spatial resolution of condition and distress data is often too coarse to provide reliable predictions for specific locations.

Additionally, efforts to account for climate's role suffer from the reality that models lack the spatial granularity necessary to incorporate high-resolution climate data. Therefore, researchers often conglomerate pavement distress and condition data into spatial and family categories to investigate trends on a larger scale. Bins may be organized as climatic zones defined by temperature and precipitation thresholds (Meihaus 2013; Parsons and Pullen 2016), or geographic boundaries (Sahagun et al. 2017). Other studies determined that age, pavement structure, temperature extremes, and precipitation were commonly significant in retrospective analyses and warranted further research to determine whether changing climate would strengthen the relationships between condition and environmental factors (Ankit et al. 2011; Bennett 2019). Climate change is expected to accelerate pavement degradation with a global temperature change (GTC) of 2.7 °C by the end of the century (Kjellstrom et al. 2018; van Vuuren et al. 2011). Maintenance costs are expected to increase by $2.8 billion annually for the US highway system by 2050 due to rutting and cracking from freeze-thaw and higher temperatures (Chinowsky et al. 2013).

The second area of study investigates modern computerized, reliability-based approaches for effective pavement life-cycle management (Frangopol et al. 2001). Several pavement management systems evaluate highway pavements, but few APMSs have robust databases and prediction capabilities (Ismail et al. 2009). AIRPACS, created by the Air Force Institute of Technology (AFIT), and other prototype tools are knowledge-based and help select rehabilitation alternatives (Seiler et al. 1991). However, PAVER™ is the leading, fully-functional APMS used by state-agencies worldwide, including the US Department of Defense (DoD) and Federal Aviation Administration (FAA), since the 1970s (Federal Aviation Administration 2014; Shahin and Rozanski 1978). PAVER™ is a family-based pavement management system that compares

the current condition of visually inspected, user-defined, pavement families of similar makeup, and develops polynomial-fit degradation approximations from these families (Shahin and Rozanski 1978). Within PAVER™ on airfields, families are determined by three factors: pavement material type, priority, and use (Shahin 1994). APMS's use several factors to establish condition assessment standards for pavements and quantify the need for maintenance and repair, such as the International Roughness Index (IRI) (Taylor and Philp 2015) and the Pavement Condition Index (PCI) (Shahin and Rozanski 1978). PCI is more commonly used throughout private and commercial airport industries and is determined by visual inspection from pavement experts (Shahin 2005; Shahin et al. 1987), considering a holistic set of potential distress sources (Haas 2001). The PCI and IRI provide standardized and accepted metrics to represent an airfield section's current state and model expected changes in condition (Chih-Yuan and Durango-Cohen 2008; Greene et al. 2004). Most pavement management systems use deterministic empirical models with regression equations, but other mechanistic and probabilistic models exist (Sidess et al. 2020). While many highway modeling systems use other variables to estimate future conditions, most APMSs only consider pavement age (Ismail et al. 2009).

The third area of study for pavement life-cycle management considers sustainability and sustainable transportation. Beginning as life-cycle cost analysis research that examines pavement performance and long-term cost over time to optimize financial investment, life-cycle assessment (LCA) considerations have evolved into a holistic sustainability approach to pavement analysis (Allen and Albert 2014). LCA considers economic factors and environmental and social value impacts from original pavement materials through construction and operations to end-of-pavement-life decisions. Pavement sustainability and APMS decisions are combined in life-cycle assessment tools to overtly consider climate change-related variables and impacts on society

based upon balancing the aspects of economy, environment, and social values with a key objective for improved resilience (Harvey et al. 2016).

The research in this paper addresses the remaining research questions in all three of these pavement life cycle areas by exploring a possible framework capable of identifying whether climate plays a role in pavement degradation at airfields and finding which aspects contribute significantly in various climate zones. Despite the significant contributions of previous studies and APMSs, there is little reported research that (1) allows APMS software to adjust assessment predictions due to current and projected future environmental conditions; and (2) accounts for the local climatic effects on airfield pavement degradation. Accordingly, the objectives of this study are to (1) group applicable pavement families for analysis that are expected to degrade similarly, including pavement material structure (type), aircraft traffic priority (rank), and pavement use of the airfield by location (use); and (2) apply a cross-validated, principal component regression (PCR) model to determine the role that many relevant climate factors have played in explaining local condition variability in the pavement families identified in objective 1. A systems framework that accounts for varying potential conditions such as mission change, new aircraft, or climatic change is essential to model and predict life-cycle impacts on pavements in the future. Furthermore, the current spectrum of APMSs and life-cycle assessment techniques may benefit from incorporating climate-influenced degradation predictions into current approaches that are age-centric when the linkage is proven statistically. Ultimately, improved accuracy, fidelity, and granularity in degradation prediction could lead to better-informed pavement planning with climate considerations, design that includes customized agents for sustainability considerations, and refined pavement inspection cycles and criteria to more fully track performance and inform pavement management decisions.

Data

To develop a framework capable of identifying whether climate plays a role in pavement degradation at airfields and find which aspects contribute significantly in various climate zones, it was necessary to obtain several location-matched pavement and climate datasets with sufficient temporal resolution to produce statistically significant results. PAVER™, an APMS program of record for the DOD, contains a condition database for the US Air Force (USAF) and was thus selected as the dataset for this analysis. From the set of 95 global USAF installations present in the PAVER™ summary report, 14 were selected that are representative of (1) all CONUS USAF airfield pavements and predominantly used aircraft types, and (2) several major climate divisions across the continental United States (CONUS). Since this research is performed using local conditions, the quantity of airfield sections at each location is more important than the number of locations considered. While there are many more installations within the identified climate divisions, the purpose of this research is not primarily focused on providing a comprehensive understanding of the dynamics of climate and its precise effects on pavement conditions. Instead, this research targets developing a framework capable of identifying whether climate plays a role in degradation and which aspects of climate contribute to explaining condition variability based on location. Ultimately, the framework is flexible such that it could be applied to any location, pavement type, and using any climate variables, provided sufficient data availability. Figure 6 and Table 2 show the selected installations and their inclusion in the three major Köppen-Geiger climate zones found in the CONUS (Delorit et al. 2020). Only one CONUS installation exists within the tropical and polar zones, Homestead AFB in southern Florida, so these regions were not considered further in this analysis.

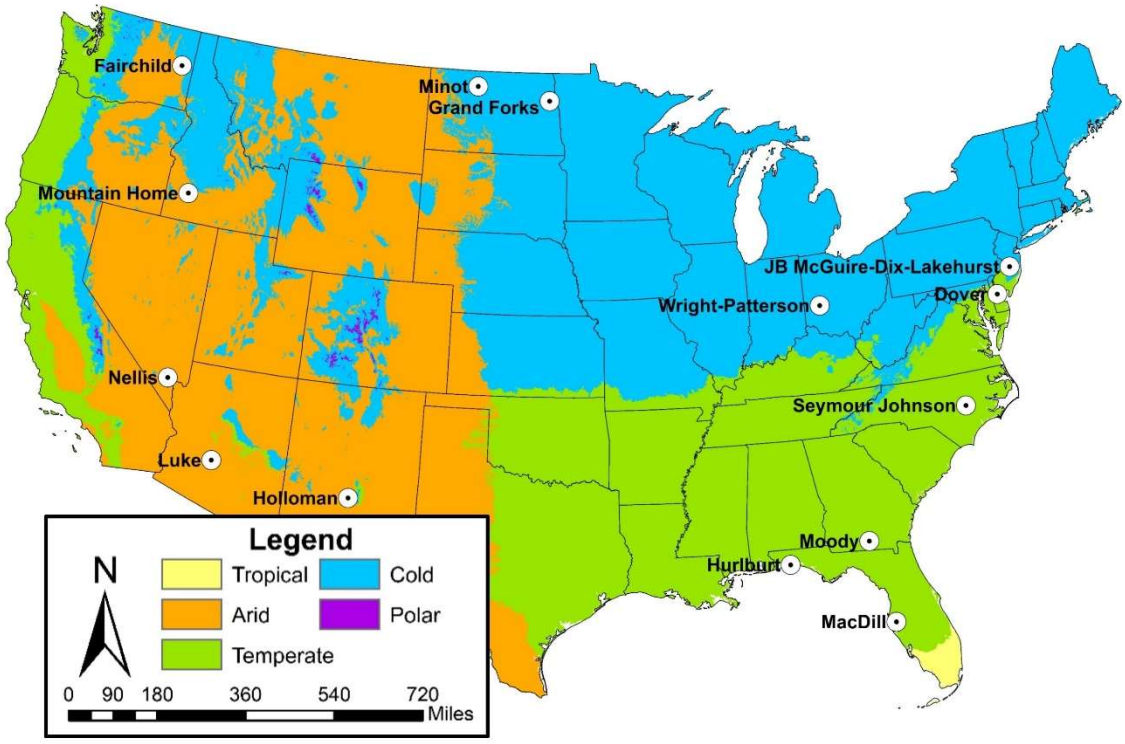

Figure 6. A representative sample of CONUS AF installations included in this analysis within Köppen-Geiger climatic zones.

Table 2. Abbreviations, nearest city, state, and asset count (number of individual pavement sections) of USAF installation locations for this analysis.

Installation	Abbreviation	Nearest City	State	Asset Count
Dover Air Force Base	Dover	Dover	DE	330
Fairchild Air Force Base	Fairchild	Spokane	WA	207
Grand Forks Air Force Base	GrandForks	Grand Forks	ND	73
Holloman Air Force Base	Holloman	Alamogordo	NM	130
Hurlburt Field	Hurlburt	Fort Walton Beach	FL	128
Luke Air Force Base	Luke	Phoenix	AZ	93
MacDill Air Force Base	MacDill	Tampa	FL	105
McGuire-Dix-Lakehurst, Joint Base	McGuire	Trenton	NJ	64
Minot Air Force Base	Minot	Minot	ND	78
Moody Air Force Base	Moody	Valdosta	GA	247
Mountain Home Air Force Base	MtHome	Mountain Home	ID	50
Nellis Air Force Base	Nellis	Las Vegas	NV	258
Seymour Johnson Air Force Base	SeymourJohn	Goldsboro	NC	159
Wright-Patterson Air Force Base	WrightPatt	Dayton	OH	73

The Air Force Civil Engineer Center (AFCEC) provided summaries of PAVER™ data for 2011, 2015, and 2019. Each summary represents rolled up and combined airfield conditions based on the most recent inspection date and data input at that time. AFCEC keeps summary records approximately every four years to account for changes from new airfield evaluations, which occur within five-year intervals (AFI 32-1041 2019). The AFCEC data was sufficient for model significance for many of the locations, but some data gaps exist for older inspections since data from previous year summary reports are stored in incompatible data types at many separate locations; centralized data management has previously been non-uniform, and older files are not supported by PAVER™ 7.0.11, the current version at the time of this research. Although all previous inspections are included in summary report in PAVER™, the predictions are only generated by the most recent inspection for each pavement section in the selected family. Having access to previous snapshots of condition data allowed the authors to create more accurate prediction expectations calibrated by previous condition assessment data.

DOD real property data represented in PAVER™ covers broad uses of any managed pavement, including roads, parking lots, fuel pads, and helipads. To focus the data analysis and framework development on airfield pavements utilized by aircraft, the provided data was filtered and narrowed such that pavement sections were removed if they met several exclusion criteria. Pavement uses of runways, taxiways, aprons, overruns, and shoulders were considered.

Further data sorting and filtering were done to remove expected anomalies and pavement conditions that would most likely not reflect climatic deterioration using the proposed analysis framework. Homogeneous full depth pavements are expected to

degrade similarly. However, composite pavements can confound the data when layers of pavement type are heterogeneous, such as Portland cement concrete (PCC) with an Asphalt concrete (AC) overlay (APC) (Castillo et al. 2019). Therefore, AC, PCC, and Asphalt overlaid on AC (AAC) were included in the final analysis. Despite using USAF inspection and assessment standards from ASTM D5340, some minor, inspection/rater-centric errors are expected (American Society for Testing and Materials 2012). A PCI improvement greater than five is unreasonable unless repair work has been performed on that pavement section, so PCI score improvements greater than five points between inspections were excluded (Knost and Mishalani 2019b).

Pavement condition is expected to be like new, or PCI=100 upon completion of new construction or major reconstruction, so sections were excluded if they had a score less than 100 at age 0. It is otherwise assumed that routine maintenance is performed equally across all airfield pavements, since that fidelity of information is unavailable. Sections were also excluded if they had a failing score within the first ten years after construction, which would suggest another source of deterioration, such as an anomaly event like an earthquake or aircraft crash. Lastly, construction dates earlier than 1985 were excluded since the climatic data was procured from 1985-2019. The summary report from AFCEC provided 2,360 pavement sections (further referred to as 'data points') from the 14 selected USAF installations with construction dates after 1985. After filtering according to these standardized rules, the remaining number of data points used for this research was 1,995, representing 85% of the valid data from the same temporal scale and base selection. For more detailed descriptions of the AFCEC summary reports' data types, see Sahagun et al. 2017.

This analysis seeks to maximize the temporal extent to ensure the statistical significance of predictions. Daily observed data for many climatic variables were procured from AccuWeather's proprietary database, from 1985 through 2019, for the nearest weather station to each selected location. The metrics procured from AccuWeather included temperature, humidity, wind speed, solar irradiance, rainfall, snowfall, and hail accumulation (Ankit et al. 2011; Bennett 2019). The five climatic variables used in this research are provided in Table 3, and while not exhaustive, these variables tend to represent variables known to affect built asset performance. Each of the variables was then compiled annually and normalized using each variable's z-score. Normalization was required since each variable has different units and magnitudes, which would skew the model results.

Table 3. Final climatic variables selected for regression analysis.

Variable	Description	Unit
Freeze-Thaw	Binary, counted when daily maximum and minimum temperature crosses freezing	Days
Precipitation	Cumulative total daily water equivalent precipitation	Inches (in)
Snowfall	Cumulative total snowfall depth	Inches (in)
Sustained Wind Speed	Binary, counted when the daily maximum wind speed exceeds 10 miles per hour	Days
Solar Irradiance	Cumulative total solar irradiance (global), or light intensity observed between sunrise and sunset	Watts per meter squared (W/m^2)

Methodology

The framework follows three necessary steps to meet the outlined objectives: (1) establish families of pavement sections with similar characteristics, (2) create a

continuous degradation function for each family-location pair, and (3) construct a cross-validated, principal component regression (PCR) model to identify whether the selected climate variables contribute to explaining by-family pavement degradation. Each pavement family's PCR model will reveal the significance and strength of relationships between climate and condition by convention. Figure 7 depicts a theoretical diagram for this research methodology.

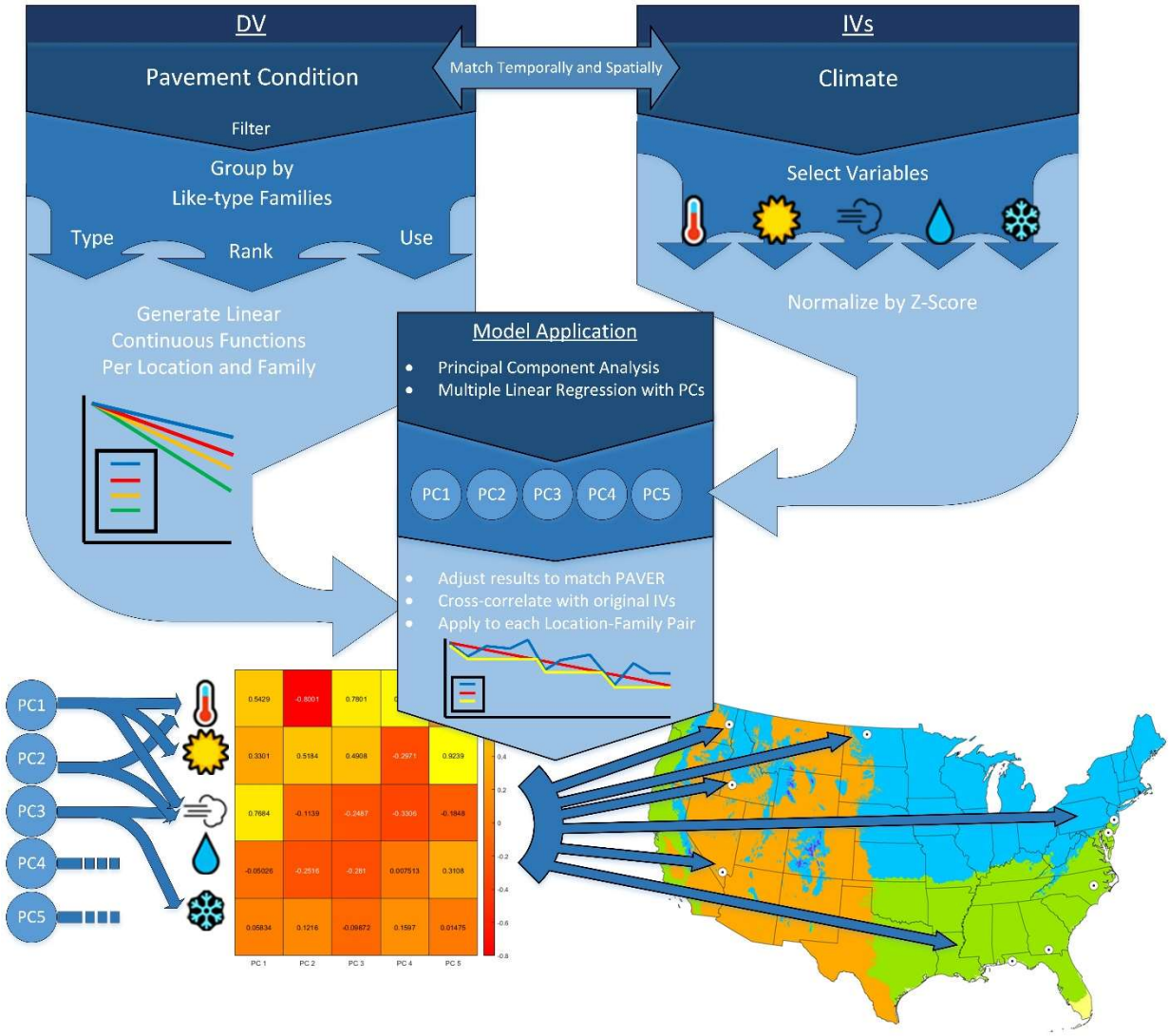

Figure 7. Theoretical diagram outlining the research methodology.

For the first two steps, accepted methodology from PAVER™ was translated into the framework to promote result comparability and validity. Most local pavement asset managers choose primary PCC and primary AC as the two baseline families to plan maintenance at their installation (George VanSteenburg, USACE Transportations Systems Center, Pavement Program Manager, personal communication, Oct 19, 2020). As stated above, these selections lack the specificity desired for analysis, so the pavement sections analyzed were grouped into standardized families of similar type (material), rank (traffic priority), and use (location on the airfield) that are expected to behave similarly, as seen in Table 4.

Table 4. Standardized pavement family selection criteria.

Pavement Type (Material/Structure)	Rank (Traffic Priority)	Use (Location on Airfield)
Rigid	Primary	Runway
Portland Cement Concrete (PCC)	Secondary and Tertiary	Taxiway and Apron
Flexible		Overrun and Shoulder
Asphalt Concrete (AC)		
Asphalt overlaid on AC (AAC)		

The specificity of the family selection is necessary to gain knowledge about the local conditions and determine significant degradation variables; however, this reduces the number of data points per family and decreases model significance. Several assumptions were made to join some pavement sections into the same family for this research, despite differences in some APMS default family assignments. For example, taxiways and aprons were merged into the same category for this analysis, despite one having parked aircraft and the other mobile. However, since another family selection criterion is rank, only primary taxiways and primary aprons, which share similar traffic

conditions, are within the same family. This inclusion of rank as a selection criterion helps increase the similarities in actual condition degradation within each family group. Overall, using three diverse criteria and similar group combinations for family selection ensured more homogeneity within each pavement family and adequate sample population for the analysis.

Of the twelve pavement family groups generated from the three family selection criteria, five do not exist. After sorting and filtering the data, those retained still provide a sufficient spectrum of relevant and diverse pavement sections that are valuable for analysis. All of the primary runway, primary taxiway, and primary apron surfaces were retained and are the most important pavement infrastructure for supporting aircraft operations. Family groups without data availability only include overruns, shoulders, and secondary runways, many of which do not exist. Table 5 displays the valid families and number of pavement sections used in this study.

Table 5. Pavement families and their count of pavement sections available for analysis.

Pavement Family	Abbreviation	Asset Count
Rigid-Primary-Taxiways/Aprons	RPT	588
Rigid-Primary-Runways	RPR	258
Rigid-Secondary/Tertiary-Taxiways/Aprons	RST	455
Flexible-Primary-Taxiways/Aprons	FPT	163
Flexible-Primary-Runways	FPR	115
Flexible-Secondary/Tertiary-Overruns/Shoulders	FSO	211
Flexible-Secondary/Tertiary-Taxiways/Aprons	FST	205

A continuous function is needed to perform regression. PAVER™ creates a by-family degradation function that starts at a condition of 100 and monotonically decreases to failure. The program eliminates erroneous data and then selects the highest-order polynomial fit that maximizes Pearson's coefficient of determination (R^2) with an

acceptable significance ($\rho \leq 0.05$) (Shahin 1994). When data is limited, as is the case with this research, the degradation function can only be linear to satisfy the significance constraint. Linear approximations are inherently inaccurate since actual pavements have an increased deterioration rate near the end of their life cycle (Colorado State University 2019; Parsons and Pullen 2017). Independent of the fit type, these continuous functions act as surrogates for the observed pavement condition and are the baseline against which the climate-based PCR degradation models are compared. Each model's R^2 represents its ability to replicate this linear degradation approximation, which would be the likely output from PAVER™, considering the pavement families assumed in this work.

The third step extends the capability of PAVER™ by including climate variables in the prediction of airfield pavement degradation. A bias-free statistical model was used that employed the tools of principal component regression (PCR) and cross-validation. PCR is commonly used to model the impact of climate on built and natural systems, and it is used when independent variables (IV) are collinear (Delorit et al. 2017). For example, the daily amount of precipitation is collinear with solar irradiance, though inversely. PCR performs a two-step multi-factor linear regression (MLR) that first transforms the original IV's into orthogonal principal components (PC) (Abdi and Williams 2010), and subsequently uses the PCs as IVs in an MLR.

Moreover, rulesets are established that only retain the most significant PCs and those that describe a threshold amount of variation in the model, thereby reducing the risk of overfitting the model by reducing dimensionality. Jolliffe's Rule is a standard ruleset used for this analysis, which retains each PC that explains at least 70% of the mean variance explained by all PCs, thereby eliminating PCs that only contribute less-

significantly to the explained variance (Jolliffe 2002). Eliminating multicollinearity, and resolving the original data into orthogonal signals, means that the new PCs do not directly relate to a single IV. The PCs retained for the MLR are cross-correlated with the IVs to determine which of the IVs explains variability in each PC.

Cross-validation is another statistical method used to remove bias from this deterministic MLR. It absconds, or drops, the dependent variable observation for the time step or time steps surrounding that which is being predicted in the MLR to eliminate a "perfect target" or targets from consideration (Delorit et al. 2017). Here, only the condition value being predicted is dropped, which is referred to as drop-one cross-validation. As expected, adding cross-validation to the MLR process lowers the Pearson's coefficient slightly but produces a bias-reduced set of predictions.

Results

Figure 8 shows the continuous degradation functions (PCI over time) for two families, rigid-primary-taxiway/apron (RPT) and flexible-primary-taxiway/apron (FPT). The lines are color-grouped by Köppen-Geiger zone with green as the temperate zone, orange as arid, and blue as cold. Horizontal dashed lines at PCI = 70 and PCI = 55 represent the family-location pair's life when the average condition drops into the fair and poor ranges, respectively; repair is typically planned for fair sections and replacement for poor (Greene et al. 2004). The solid black line represents the weighted average of all pavement sections from that family and helps highlight the difference in expected life for flexible and rigid pavements; the lifespan for the weighted average of all RPT are beyond 35 years but only approximately 22 years for flexible pavements of the same rank and

location. There are vast differences in actual conditions at each installation, even between those within the same Köppen-Geiger region. For RPT, pavements aged 30 years have variability in condition ranging from 44 to 89, supporting the need for model application at each location.

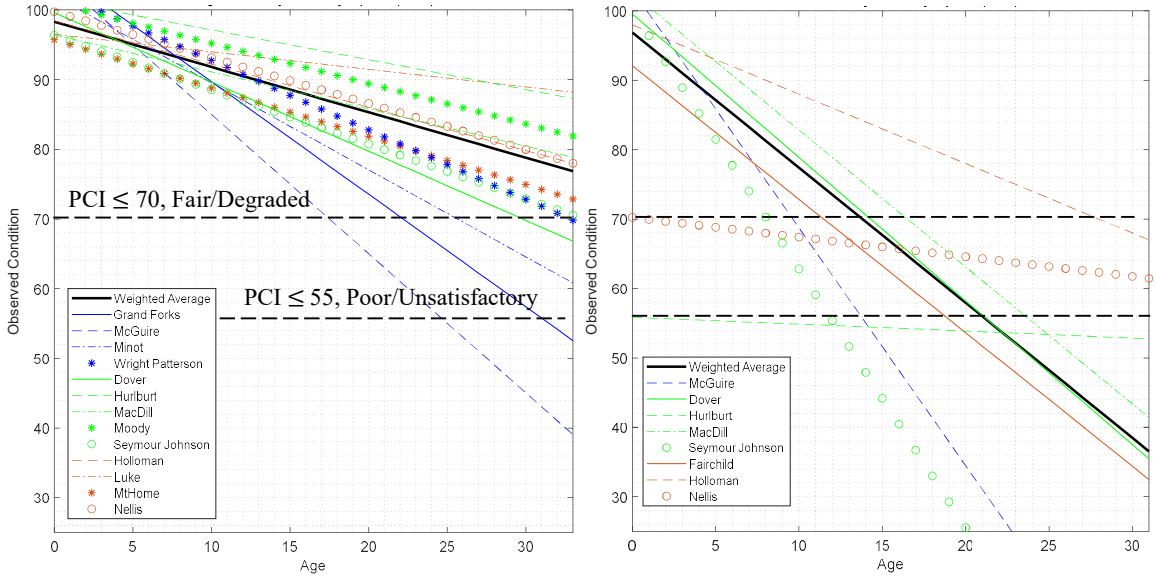

Figure 8. Linear continuous degradation functions for family-location pairs, rigid-primary-taxiway/apron (RPT) and flexible-primary-taxiway/apron (FPT). Coloration is based on the Köppen-Geiger zone: green for temperate, blue for cold, and orange for arid.

The cross-validated PCR method was run for every continuous degradation function, accounting for all pavement types and locations. R^2 and the root mean square error (RMSE) were metrics used to evaluate each climate-driven model's skill in predicting the continuous degradation function. A summary of these results is shown in Table 6. A null means that there was not enough data for that family-location pair to produce significant model results.

Table 6. Summary of raw model results. R^2 labeled by strength (Evans 1996). RMSE error values above 15 are categorized in bold.

Location	R^2	Root Mean Square Error (RMSE)						
		RPT	RPR	RST	FPT	FPR	FSO	FST
Cold								
Grand Forks	0.51[b]	10.7	-	9.03	-	**17.8**	9.1	-
McGuire	0.63[b]	11.9	-	4.91	**20.4**	**16.1**	**39.3**	7.87
Minot	0.63[b]	7.41	2.39	-	-	**25.3**	5.33	**17.8**
Wright-Patterson	0.36	7.48	-	4.71	-	-	**28.3**	-
Mean ± 95% CI	0.53±0.20							
Temperate								
Dover	0.34	7.59	13.7	**16.7**	**15.8**	11.6	**17.9**	**15.9**
Hurlburt	0.46[b]	3.09	1.51	5.74	0.72	-	9.76	9.47
MacDill	0.53[b]	3.36	1.64	1.91	12.4	**26.9**	5.17	2.95
Moody	0.66[a]	3.32	1.79	4.94	-	12.8	10.8	**21.9**
Seymour Johnson	0.56[b]	4.74	8.10	7.43	**22.6**	**30.2**	12.1	11.6
Mean ± 95% CI	0.51±0.15							
Arid								
Fairchild	0.55[a]	-	2.57	5.94	11.9	-	11.6	**20**
Holloman	0.70[a]	3.12	2.27	2.46	5.03	9.23	4.53	2.89
Luke	0.71[a]	1.33	-	4.72	-	-	14.3	11.8
Mountain Home	0.70[a]	3.48	-	4.74	-	-	9.57	6.25
Nellis	0.65[b]	3.84	0.6	3.9	1.65	10.45	14.7	3.11
Mean ± 95% CI	0.66±0.08							

[a]Very strong correlation
[b]Strong correlation

The authors suggest that a square root of residuals variance of 15 is acceptable when the scale of possible CI values is between 0-100. Error values greater than 15 over this 35-year period are in bold and could indicate a predicted healthy assessment when the actual condition was degraded or unsatisfactory. Future research attempts to use this framework as a forecasting tool would need to take extra caution with the families and locations with higher errors, such as flexible-primary-runways (FPR) and other flexible pavements at several cold locations.

Statistical prediction of future condition for real property assets like airfield pavements must account for the reality that assets never improve in condition over time; condition is always steady or declining. In this case, it is possible the model could predict condition increases between time steps, which is impossible without maintenance or repair interventions. Higher skill was reported in nearly every case by adjusting the results to align with the methodology in PAVER™: confining condition to decrease monotonically and setting the initial condition to 100. This increase in accuracy can transform the model into a potential forecasting tool. The new Pearson's coefficient of determination now changes within each location by family and is inversely affected by the error (RMSE). Figure 9 shows the model improvement ($\Delta R^2 = 0.48$) for Dover rigid-primary-runways (RPR).

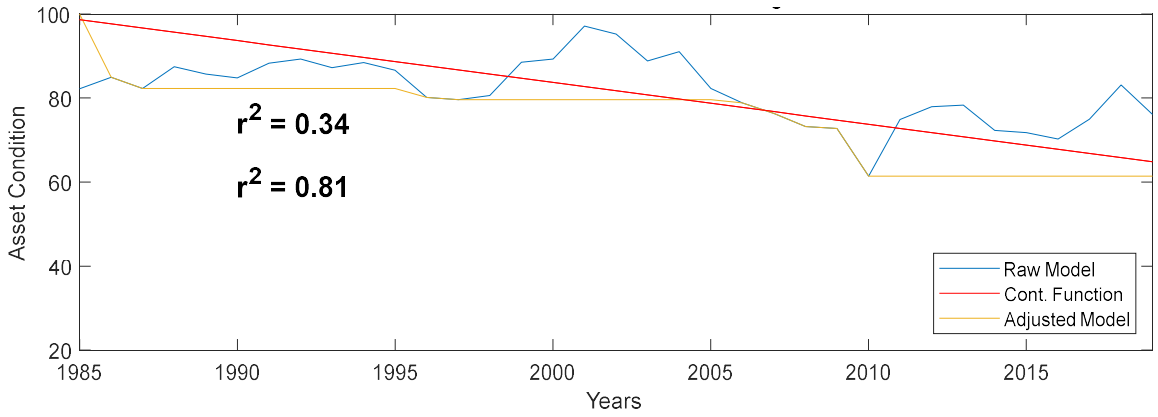

Figure 9. Model improvement by adjusting results to align with accepted methodology for Dover RPR: forcing a zero slope wherever the condition increases and starting at a condition of 100.

The models predominantly have low error values throughout all family-location pairs, with rigid pavement families producing more accurate results than flexible ones.

FPR are not as common as rigid-primary-runways (RPR) for the USAF and could have greater error due to fewer data points. Moreover, flexible pavements performed especially poorly in the temperate and cold zones, suggesting a potential influence from the presence of freeze-thaw that could impact model performance. As is common in these regions, conditions change throughout the year greatly, as is exemplified through the freeze-thaw variable, which represents the daily change in temperature that crosses the freezing point of water. Homogeneity of conditions produces less error, so the arid locations that experienced many common, warmer conditions throughout the year have the lowest error values and the highest average R^2.

Figure 10 illustrates the average coefficient of determination across all pavement families and the most influential climate variables, as determined by the PCs' correlation with the original climate IVs. This figure represents the cumulative effect of climate on that location and does not distinguish changes in climatic effect between families of pavements. The error (RMSE) is a better measurement of how closely the models can describe variation by pavement family: a lower RMSE means this model has more skill and would convey more certainty to which variables are influential.

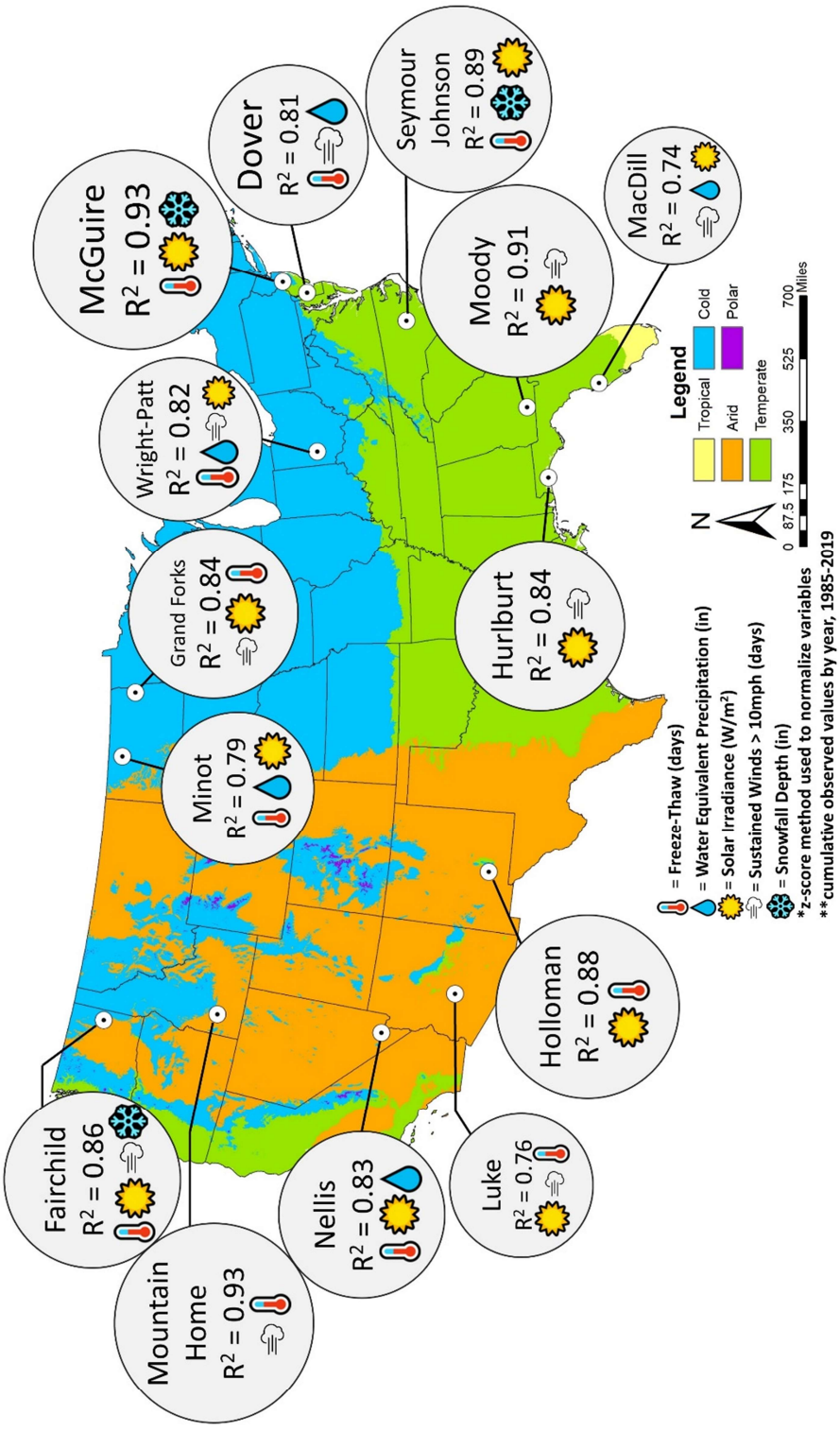

Figure 10. Significant climatic effects on airfield pavement degradation by location in Köppen-Geiger climate zones. Circles are sized by R^2.

Discussion

As shown in Figure 10, several trends were discovered from localized climatic effects by Köppen-Geiger zone. Overall, high correlation values were computed for most locations, varying from 0.74 to 0.93. As expected, freeze-thaw is significant in all zones, though most meaningful in the arid and cold zones and least prevalent in the temperate zone. Pavement in the arid zones is likely designed for less rainfall and could be more susceptible to freeze-thaw effects. The cold zone has a higher magnitude of freeze-thaw days, which likely influences deterioration as pavement expands and contracts. Solar irradiance is significant and strong in nearly every location, and it is the leading climatic influence in five of the installations. Solar irradiance is not typically considered in pavement design, but its existence in the southern temperate and arid locations is logical. Sustained wind and precipitation are also common predictors, but only three installations displayed snowfall as a strong climatic influence: Fairchild, McGuire, and Seymour Johnson. There do not appear to be any trends in the strength of R^2 by Köppen-Geiger zone, suggesting that unknown factors other than climate affect this aspect of the model's performance. However, the arid zone has significantly lower error values than temperate and cold. This suggests that clearly defined climate shifts throughout the year reduce model skill while consistent weather in the arid zones produces better results from the models. Many installations do not have various families due to historical design choices or construction material limitations. The family with the most represented data between all installations was flexible-secondary/tertiary-overruns/shoulders (FSO), followed by rigid-primary-taxiways/aprons (RPT) and rigid-secondary/tertiary-taxiways/aprons (RST). Every location had enough FSO sections for significant model results, while 13 of

the 14 locations have enough for both RPT and RST. FSO only had a total of 211 sections, while RPT had 588. This finding is substantiated by the fact that shoulders made from flexible pavement are typically used throughout airfields. In contrast, airfields have more taxiways and aprons to hold and accommodate aircraft movement around fewer select runway surfaces.

The model results by family-location pairs are shown in Table 7. Several interesting families and installations were selected for further discussion due to their importance and relative differences. The families RPR and FPR will be compared because they are the critical pavements that support aircraft operations and missions. FSO will be analyzed because it is the most complete family between bases. FSO will also show deterioration with little-to-no aircraft traffic and could represent the true climate-related deterioration without aircraft traffic factors. The models should theoretically describe more variation in the FSO family since environmental effects account for the primary deterioration.

Table 7. Model results after adjusting to a non-increasing slope that starts at condition 100. Bold values represent the weakest correlation strengths (Evans 1996).

	Pearson's Coefficient of Determination (R^2)						
Location	RPT	RPR	RST	FPT	FPR	FSO	FST
Cold							
GrandForks	0.85	-	0.85	-	0.85	0.82	-
McGuire	0.94	-	0.91	0.94	0.94	0.94	0.91
Minot	0.86	0.80	-	-	0.84	**0.62**	0.85
WrightPatt	0.81	-	0.87	-	-	0.78	-
Temperate							
Dover	0.81	0.81	0.81	0.81	0.80	0.81	0.81
Hurlburt	0.87	0.76	0.87	-	-	0.83	0.84
MacDill	0.75	0.83	0.69	0.81	0.82	0.81	**0.46**
Moody	0.91	0.91	0.91	-	0.90	0.90	0.91
SeymourJohn	0.88	0.90	0.90	0.90	0.90	0.90	0.88
Arid							
Fairchild	-	0.87	0.86	0.85	-	0.87	0.87
Holloman	0.89	0.93	0.89	0.89	0.93	0.83	0.79
Luke	0.71	-	0.79	-	-	0.78	0.79
MtHome	0.92	-	0.95	-	-	0.93	0.94
Nellis	0.89	-	0.89	-	0.88	0.89	**0.58**
Mean	0.85	0.85	0.86	0.86	0.87	0.84	0.80
±95% C.I.	0.04	0.03	0.04	0.03	0.03	0.05	0.08

Most families within the same location have similar coefficient of determination values. This is because the same climatic conditions were experienced across the entire installation, so differences between families are associated with the RMSE and the model's ability to adjust to a non-increasing slope that starts at condition 100. Contrary to the author's hypothesis, the FSO family did not account for a larger percentage of the variance than the other families, and none of the families had a higher value than the others. This may be because routine maintenance activities are focused on the primary surfaces and might neglect unused portions of the airfield. Some aspects of climate might also have more detrimental effects on FSO pavements, meaning that the variability in

location would increase the diversity of effects and lower the model's overall average skill. For example, several locations with higher freeze-thaw days have lower correlation skills, such as Minot and Wright-Patterson. Figure 11 calls out the coefficient of determination, error, and count of assets for selected, climate-diverse locations.

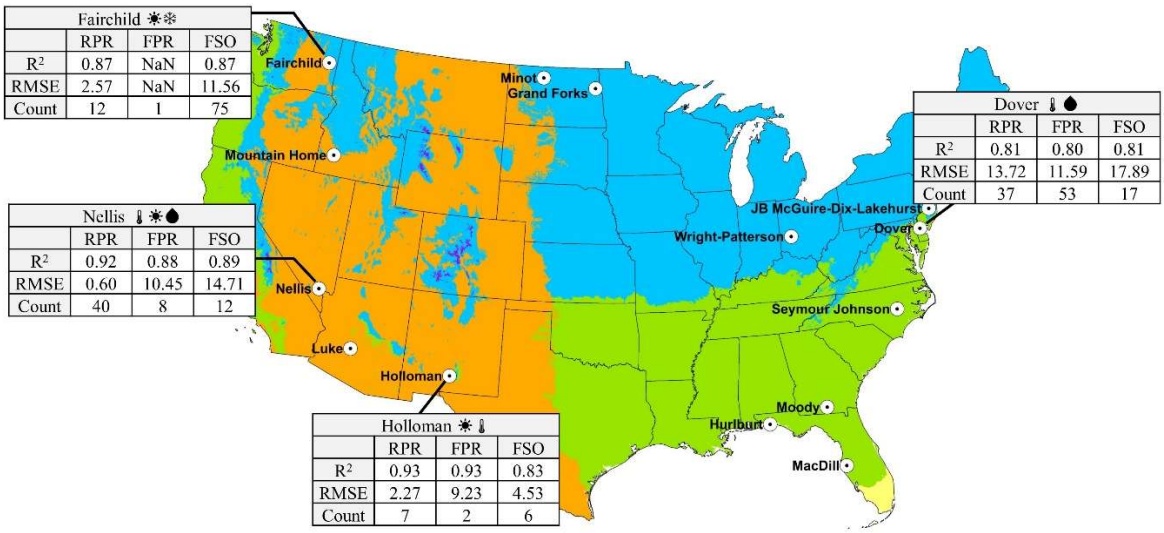

Figure 11. Comparison of selected locations and families.

Fairchild lies in the arid climate zone and primarily flies cargo aircraft like the KC-135, similar to the Boeing 717, with a gross takeoff weight of 146,510 kg. Dover also flies mostly cargo aircraft such as the C-5 and C-17 (maximum takeoff weight of 265,352 kg, civilian counterpart Boeing 777) and lies in the temperate climate zone's northern edge. Nellis is in the arid zone but flies lighter F-16 fighter aircraft. Lastly, Holloman is in the arid zone and flies light F-16 and F-22 fighter jets (17,010 kg) (US DoD 2001b).

The models can better approximate locations with more homogenous climatic conditions. Nellis and Holloman are entirely within their climate zone, have more similar summer-like conditions year-round, and produce higher correlations, but Dover and Fairchild exist on boundaries of climate regions, have seasonality, and produce slightly

lower correlation scores. The models also have less error in the RPR family. Since this family is often considered the most important, it will assuredly receive the majority of preventative maintenance care. This assumption means that this family's degradation function should maintain the most consistent degradation, as reflected by the model's ability to better replicate this family's continuous function. However, if this assumption is true, then fewer data points exist in the lower PCI ranges for fair and poor RPR pavements, which may limit model effectiveness in this range.

Several limitations, assumptions, and areas of uncertainty were identified for this study. Pavement is typically designed for the expected aircraft and climate in which it is constructed (US DoD 2001a). Pavement design considerations attempt to mitigate the effects of the variables analyzed in this study and could confound the results. This research assumed homogeneity among pavements within each family criterion. It did not consider the specific construction practices, additives, thicknesses, subgrade conditions, or other varied pavement design considerations due to a lack of data. It was assumed that regular maintenance was performed on all pavements and that major rehabilitation of a pavement section would reset the construction date. These assumptions are based on typical USAF airfield assessment, maintenance, and reconstruction practice but were not feasibly validated for each chosen location. More internal uncertainty comes from the model's derivation of the Pearson's coefficient of determination. If the model found perfect correlation, that would still only represent its ability to fit a linear approximation from limited data points. Data limitations forced the functions to be linear, but the true degradation curve is expected to be Gaussian or polynomial, which introduces a source of error. External uncertainty could come from the long temporal gap between the earliest

constructed pavement sections and the first inspection available for the authors. Another source of uncertainty is the actual data input in PAVER™. There were several pavement sections with conflicting entry data that indicated potential human entry or import errors on either the date or PCI information. Another source of external uncertainty is contending priorities between airfield operations managers and pavement asset managers. These professionals have competing metrics of success yet an overall common mission to generate and support combat power: airfield operators desire maximum aircraft output, while pavement managers want to minimize sources of deterioration. However, both desire healthy airfields to generate mission capability and benefit from collaborating on airfield repair needs.

Future Research

Future research opportunities exist in this field that can utilize the established framework and modeling techniques. This study only analyzed five selected climatic variables against pavement type, rank, and location on the airfield. Other variables, including the number of aircraft passes, tire and loading configuration, aircraft weight, subgrade material, construction techniques, and other climatic variables, were neglected and assumed to be included in the remaining percentage of variation explained. Further research could use other or similar independent variables based on data availability and explore interactions between them. The climatic variables used herein could also be studied further at each of the specific family-location pairs to better design pavement for the relevant climatic effects at that location. This paper's framework can be applied to

large civilian airports worldwide to discover strong and significant variables by location to help mitigate pavement degradation and improve APMS in the future.

Future research is needed on sustainable pavements to explicate the life-cycle assessment and life-cycle cost analysis implications of significant climate zone factor considerations that emerge from this research, like solar irradiance and freeze-thaw cycles. Research using climate projections associated with climate change-related independent variables can use this framework as a predictive tool for planning maintenance activities that customize and optimize maintenance policies and practices. The continuous function could be simulated and projected to future years such that the cross-validated, principal component model produces expected results for projected conditions based on the climate for those years. Strictly historical conditions do not limit this framework; a long hindcast can be used to calibrate the model in conjunction with future projections.

Conclusions

This research proposes a framework to predict climate-driven degradation variables for pairings of location and pavement family groups with a dataset of 14 USAF airfields. Three steps are performed to accomplish the objectives: (1) pavement families are identified with similar characteristics, (2) degradation is quantified using a continuous linear function, and (3) this function is simulated from 1985-2019 to perform a bias-free regression model using observed climatic variables across the same temporal scale. Environmental factors contribute significantly to the degradation of airfield pavements. Freeze-thaw, precipitation, solar irradiance, and wind are prevalent throughout the United

States and describe between 74% and 93% of pavement degradation variation. PAVER™ produces reliable results and has proven to be a successful tool for pavement deterioration prediction; however, climatic factors cannot be ignored. Understanding variability of degradation by location could allow prediction software, like PAVER™, to be updated to account for relevant climate variables to predict pavement condition more accurately. The presented framework can be validated and calibrated through more extensive research and utilized on other large airports throughout the world, contingent on data availability, such that pavement design agents can better customize mix designs and enable more effective and sustainable pavement management practices.

IV. Scholarly Article 2: Accounting for the Combined Effects of Local Climate and Traffic on Airfield Pavements Using Principal Component Regression

Evan M. Fortney; Steven J. Schuldt, Ph.D., PE; Sarah L. Brown; James P. Allen, PE, MSS; Justin D. Delorit, Ph.D., PE

Abstract

Healthy airfield pavements support the global economy, passenger travel, and national defense. Accurate pavement degradation predictions are critical to successfully manage maintenance and repair, and they reduce the need for time-intensive, costly physical inspections that disrupt airfield operations. Existing airport pavement management systems (APMS) compute expected degradation as a function of pavement type and age, but existing predictions are not calibrated to local climate and traffic conditions, and they cannot adapt to changing future conditions. This paper implements a bias-reduced statistical model that reveals the effects of local conditions using observed historical climatic and aircraft traffic data from two separate temporal periods. Model performance is evaluated using a diverse dataset of nine Air Force installations representing a wide range of local aircraft sizes and the three major Köppen-Geiger climate zones in the Contiguous United States. Environmental factors are more impactful on pavement degradation than aircraft traffic, with 2-15% increases of accounted degradation variation for the most heavily-trafficked pavement family. Airfield asset managers can use this adaptable framework to more accurately determine sources of local degradation and inform sustainable pavement design and management practices.

Introduction

Healthy airfield pavements support the global economy, passenger travel, and national defense. Since condition assessments disrupt airfield operations, accurate predictions of degradation are essential to successfully manage rehabilitation planning and reduce the need for time-intensive, costly physical inspections (Mulry et al. 2015). Data-driven models, such as airport pavement management systems (APMS), predict future pavement conditions with historical observations and are essential tools to plan rehabilitation of failing pavements between physical inspections (Gendreau and Soriano 1998; Shahin 2005). Despite the successful, widespread use of APMS to maintain safe and serviceable pavements (Ismail et al. 2009), limitations exist due to the selection and scope of variables used to drive predictions that are not locally calibrated and cannot adapt to likely future conditions, such as nonstationary climate or changes in use patterns.

Research studies investigating airfield pavement asset management have focused on two main areas: (1) sources of pavement deterioration and manifestations of damage types, and (2) modeling approaches and methods to predict future pavement conditions and encourage sustainable pavement life-cycle assessment practices. The first area of study discusses the most prevalent causes for distress on rigid and flexible airfield surfaces, such as age, environment, traffic, maintenance history, and construction quality (Haas 2001). Active contributions to pavement deterioration fall broadly into climate exposure and use. Consequently, the unique effects of temperature and precipitation (Chinowsky et al. 2013), soil conditions (Ankit et al. 2011), aircraft loading (Ameri et al. 2011; Sawant 2009), pass frequency (White et al. 1997), and tire configuration (Shafabakhsh and Kashi 2015; Wang and Al-Qadi 2011) introduce complexities to

understanding exactly how pavements degrade. Most approaches are myopic, only considering individual variables and lacking the inclusivity of the spectrum of potential stressors to be independently relevant. Moreover, the resolution of distress data is often too spatially and temporally coarse to provide reliable predictions for specific locations. Accordingly, modeling attempts have failed to account for climate's role due to the lack of spatial granularity necessary to incorporate high-resolution climatic data.

Researchers often conglomerate pavement distress and condition data into familial categories organized by climate zones (Meihaus 2013; Parsons and Pullen 2016) or geographic area (Sahagun et al. 2017) to investigate spatial trends on a larger scale. Age and remaining service life are commonly used modeling variables that attempt to summarize many other effects. Still, pavement structure (Ankit et al. 2011), temperature extremes, and precipitation (Bennett 2019) warrant further research to determine whether changing climate would strengthen the relationship between condition and climate factors. There are many unforeseen costs of climate change-related variables on society, and pavement management needs to take a sustainability-minded approach (Harvey et al. 2016). With expected global temperature changes (GTC) of 2.7 °C due to climate change (Kjellstrom et al. 2018; van Vuuren et al. 2011), pavement degradation may increase due to rutting and cracking from larger temperature fluctuations, which will drive sustainable pavement management practices research (Chinowsky et al. 2013).

The second area of study investigates modeling approaches and methods to predict future pavement conditions. The pavement research community recognizes a universal need for computerized, reliability-based strategies to effectively manage pavement life cycles (Frangopol et al. 2001). However, few APMSs are capable of

generating accurate predictions (Ismail et al. 2009). AIRPACS is a prototype, heuristic tool that recommends rehabilitation options (Seiler et al. 1991) that lacks robustness and commercial implementation. PAVER™ is the leading APMS used by the US Department of Defense (DoD) and Federal Aviation Administration (FAA) (Federal Aviation Administration 2014; Shahin and Rozanski 1978).

PAVER™ is a database, planning tool, and modeling system. It uses a maximum term polynomial regression approach to approximate future pavement conditions for user-defined, like-type pavement families (Shahin 1994; Shahin and Rozanski 1978). Families are typically selected using material type, priority, and use criteria (Shahin 1994). Condition is quantified in PAVER™ by the Pavement Condition Index (PCI), which is determined through visual inspection from pavement experts guided by validated specifications (American Society for Testing and Materials 2012; Shahin 2005; Shahin et al. 1987). Other systems use the International Roughness Index (IRI) (Taylor and Philp 2015) to quantify the need for maintenance and repair. PCI and IRI provide standardized metrics representative of the current health of a pavement section's surface through subgrade and are useful to compare and model future condition changes (Chih-Yuan and Durango-Cohen 2008; Greene et al. 2004).

Pavement design engineers also use tools such as PCASE (US DoD), FAARFIELD (FAA), and Alize-Airfield (French Aviation Authority) to assist in meeting the unique challenge of creating sustainable pavements subjected to dynamic loads (Adolf 2010; Heymsfield and Tingle 2019). Sustainable transportation practices consider various economic factors, community impacts, and environmental burdens from construction, operations, and end-of-life-cycle decisions (Allen and Albert 2014). Most

pavement management systems and design software use deterministic empirical approaches, though other mechanistic and probabilistic models exist (Sidess et al. 2020). Moreover, the selection of independent variables is relatively limited for APMS, which mainly considers pavement age despite success in highway modeling systems' use of other variables (Ismail et al. 2009).

Despite the significant contributions of these studies and modeling systems, there is little reported research that determines the amount of influence from a diverse spectrum of potential localized factors on airfield pavement degradation. Additionally, no existing APMS is capable of adjusting prediction capability using future condition projections. Accordingly, the objectives of this study are to (1) identify significant degradation variables using a framework consisting of bias-reduced, principal component regression (PCR) models, and (2) compare a climate-only set of PCR models with a combined climate and traffic model set to determine any potential differences in model skill that would more accurately attribute the sources of degradation. It is essential for pavement degradation modeling to have a systems framework that accounts for varying potential conditions such as mission change, new aircraft, or climatic change. Furthermore, the current spectrum of APMSs may benefit from understanding how much climate and aircraft traffic contribute individually to pavement degradation. Climate and use-influenced degradation predictions can be incorporated, where skillful, into the current age-based approach for improved and adaptable modeling of pavement deterioration. Ultimately, having improved accuracy in degradation prediction could drive pavement design engineers to create better mix designs that withstand deterioration sources and lead to more thoughtful planning of recurring pavement inspections.

Data

Several location-matched datasets were acquired for pavement, aircraft traffic, and climate data with sufficient temporal resolution to satisfy the research objectives and produce statistically significant results. The US Air Force (USAF) uses PAVER™ as its pavement condition database and condition prediction software. This research analyzed PAVER™ data from nine USAF installations that represent pavements from all major Köppen-Geiger climate zones (Delorit et al. 2020) and active aircraft types in the Contiguous United States, as shown in Figure 12 and Table 8 . This system framework is flexible and can be applied to any combination of location and pavement type using any variables of interest that have matching temporal resonance and data availability.

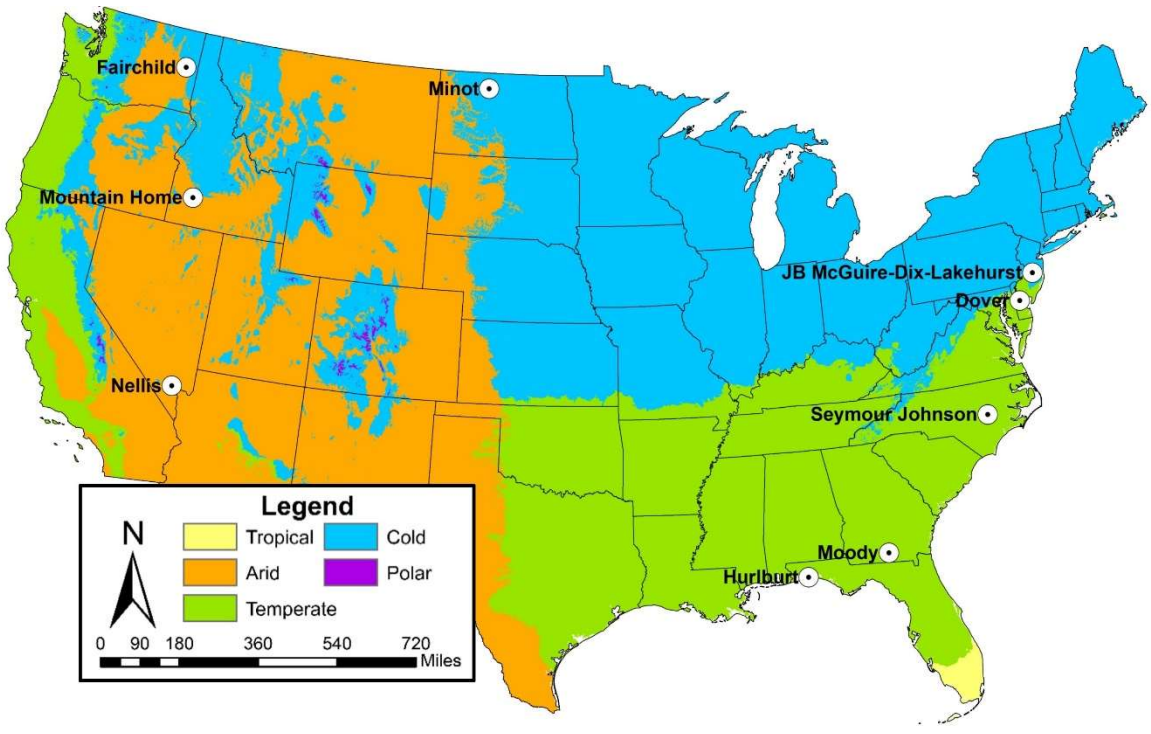

Figure 12. This research analyzed nine USAF installations that represent pavements from all major Köppen-Geiger climate zones and active aircraft types in the CONUS.

Table 8. Abbreviations, nearest city, state, and asset count (pavement sections) of USAF installation locations for this dataset analysis.

Installation	Abbreviation	Nearest City	State	Asset count
Dover Air Force Base	Dover	Dover	DE	60
Fairchild Air Force Base	Fairchild	Spokane	WA	66
Hurlburt Field	Hurlburt	Fort Walton Beach	FL	16
McGuire-Dix-Lakehurst, Joint Base	McGuire	Trenton	NJ	17
Minot Air Force Base	Minot	Minot	ND	35
Moody Air Force Base	Moody	Valdosta	GA	17
Mountain Home Air Force Base	MtHome	Mountain Home	ID	11
Nellis Air Force Base	Nellis	Las Vegas	NV	11
Seymour Johnson Air Force Base	SeymourJohn	Goldsboro	NC	33

The Air Force Civil Engineer Center (AFCEC) provided PAVER™ data summary reports from 2011, 2015, and 2019. The data were filtered to include only viable pavement sections with homogenous construction that did not receive significant rehabilitation during the reporting periods. It is assumed that routine maintenance is performed equally across all airfield pavements, since that fidelity of information is unavailable. Sahagun et al. (2017) provide a full description of all available data from the AFCEC summary reports to include branch use, section ID, true area, surface type, years since major work, distress description, and condition (PCI).

Aircraft traffic data is recorded by each installation's control tower and compiled for an annual, encompassing Air Traffic Activity Report (ATAR) by the Air Force Flight Standards Agency (AFFSA). The ATAR displays the number of passes per installation, where one pass is counted when an aircraft crosses an imaginary transverse line within 152m (500ft) of the end of the runway, excluding "touch-and-go" operations where the aircraft never applies its full weight on the pavement surface (US DoD 2001b). Accordingly, each selected location has one attributed value of total passes per year of

analysis. This research converted the aircraft pass data into equivalent passes that account for aircraft type and loading to compare locations, as explained further in the Methodology section.

Climatic data were procured from AccuWeather's proprietary database for 2010-2019 from the nearest weather station to each location. The five climatic variables used in this research are annual, normalized values for the total count of freeze-thaw (days), sum of daily water equivalent precipitation (inches), sum of daily snowfall depth (inches), count of days with sustained wind speed above 4.7m/s (10mph) (days), and sum of daily solar irradiance (W/m^2). These metrics are not exhaustive, but they are representative of variables known to affect built asset performance. They include previously studied weather variables, such as freeze-thaw and precipitation, and variables that require further analysis but are expected to contribute to pavement deterioration, such as solar irradiance and sustained wind. Pass data was available for the years 2010-2019, which, based on the frequency of condition assessments, constrained the analysis to 266 sections between the nine chosen locations.

Methodology

The framework applied to these datasets follows three necessary steps that mimic part of the prediction processes from PAVER™ to meet the outlined objectives: (1) group families of standardized, like-type pavement sections that share similarities in type and use, (2) produce continuous functions describing degradation for each family-location pair, and (3) execute a cross-validated, principal component regression (PCR) model to predict the continuous function using a time series of selected climatic and traffic-based

independent variables. The framework is run in two modes – climate only, and a combined climate and traffic model (climate-passes) – to create a comparison which will enable an analysis of the value of collecting pass data. Figure 13 is a theoretical framework for this methodology portraying how the data combines into the model application.

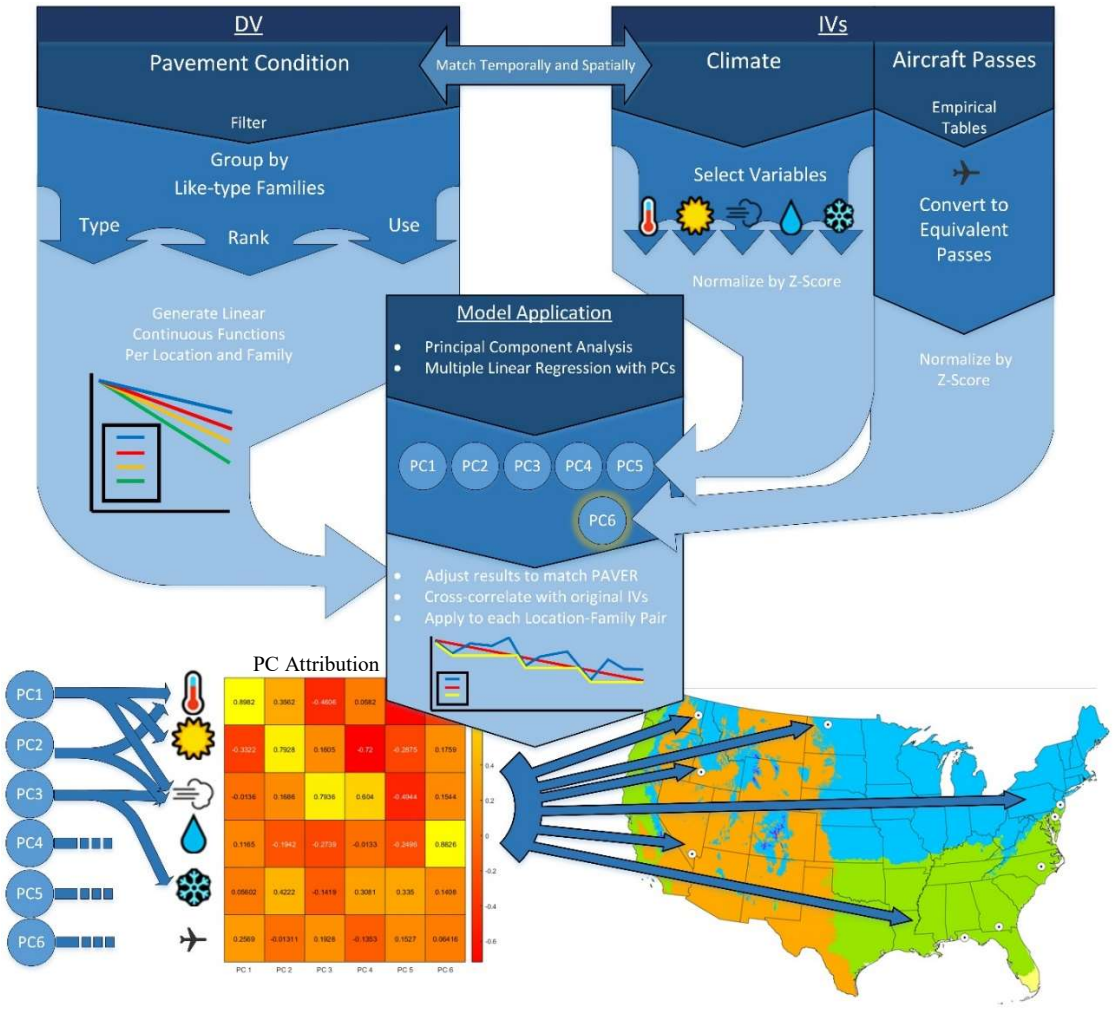

Figure 13. Theoretical diagram of the research methodology for this systems framework.

The first step of this methodology follows the standard practice for pavement analysis by creating families of like-type pavements. Common criteria used for analysis are pavement type (material/ structure), rank (priority), and location on the airfield (use)

(Shahin 1994). Table **9** describes the PCASE traffic type designators A through D, which are similar criteria used in pavement design (US DoD 2001a). This analysis takes the unique approach of combining the traffic type designators with pavement type. Eight potential families were created, of which Rig D and Flex B did not exist or did not have enough data to perform analysis. One example family is Rig A, meaning all surfaces comprised of Portland cement concrete (PCC) within the first 304.8m (1000ft) of a runway and primary taxiway surfaces.

Table 9. Standardized pavement family selection criteria including traffic designator

Pavement Type (Material/Structure)	PCASE Traffic Type Designator
Rigid	A
Portland Cement Concrete (PCC)	First 304.8m (1000ft) of rwys and primary txys Designed for full load, 100% passes, and channelized traffic
Flexible	
Asphalt Concrete (AC) Asphalt overlaid on AC (AAC)	B All aprons Designed for full load, 100% passes, and unchannelized traffic
	C Runway interiors and secondary taxiways Designed for 75% load, 100% passes, and unchannelized traffic
	D Runway edges (overruns and shoulders) Designed for 75% load, 1% passes, unchannelized traffic

The traffic type designators are a more thoughtful descriptor for how aircraft traffic applies to each specific part of the airfield that encompasses rank, whereas only using rank simply describes how vital a pavement section is to support the primary mission with the terms primary, secondary, and tertiary (US DoD 2001a). Traffic types A and B experience full weighted loading, while C and D expect only 75% of the weight

due to lower traffic. Moreover, traffic type A experiences channelized traffic with a narrower wander width than types B, C, and D. Lastly, traffic type D is only expected to receive 1% of the total passes. These traffic types presented issues that required mitigation when performing regression at the installation level using annual time steps since the aircraft traffic data presents only one cumulative, annual value for each installation that is ignorant of aircraft characteristics such as weight or tire configuration. Therefore, the pass number between installations is not comparable and needs to be converted to equivalent passes based on a standard aircraft and pass limit.

PCASE has internal calculations based on empirically derived tables that calculate equivalent passes for any combination of location, pavement type, traffic area, and controlling aircraft. This analysis used the design standard for allowable passes of 50,000 passes of a C-17 aircraft (US DoD 2001b). The heaviest, permanently stationed aircraft from each location were compiled and paired with the pass data in the PCASE software to determine equivalent pass factors for each pavement family by aircraft. This technique provided factors that were multiplied by the actual pass data from the ATAR to create a time series necessary for further analysis stages. Figure 3 is an example empirical table used by PCASE's internal software to determine the equivalent passes, and Table 10 shows the equivalent pass factors produced by PCASE for this research. The PCASE traffic types were explicitly chosen as criteria for family selection since they are also the design expectations that determine equivalent passes. Aligning pavement families with equivalent passes maximizes the percent of useful data from the available dataset rather than using rank or airfield location.

Table 10. Factors used to determine equivalent passes by family and location.

Location	Heaviest Permanently Stationed Airframe	Aircraft Weight (kg)	Pavement Families							
			Rig A	Rig B	Rig C	Rig D[a]	Flex A	Flex B[a]	Flex C	Flex D
Dover	C-5	348813	8.96	7.64	13.7	-	486.3	-	411.3	17.4
Fairchild	KC-135	146510	18.2	23.6	39.3	-	9.73	-	11.3	3.22
Hurlburt	C-130	70307	65.7	89.9	136	-	114	-	87.2	15.3
McGuire	C-17	265352	1	1	1	-	1	-	1	1
Minot	B-52	221353	0.0061	0.0062	0.0082	-	0.015	-	0.014	0.064
Moody	C-130	70307	65.7	89.9	135.9	-	113.9	-	87.2	15.3
MtHome	F-15E	36741	1.8	1.97	2.64	-	50.7	-	27.7	4.69
Nellis	F-16	17010	43023	31973	66105	-	-[b]	-	-[b]	78564
SeymourJohnson	F-15E	36741	1.8	1.97	2.64	-	50.7	-	27.7	4.69

[a]These families do not exist or do not have enough data for analysis

[b]Error values produced in PCASE, likely due to very high values that exceeded the character limit

The second necessary step for this research is to build a continuous function through least-squares regression over the historical condition assessments. PAVER™ uses by-family degradation functions to fit the highest-order polynomial curves that maximize Pearson's coefficient of determination (R^2), start at a perfect condition of 100, monotonically decrease to failure, and is produced with an acceptable confidence level (typically $\rho \leq 0.05$) (Shahin 1994). When data is limited, as is the case with this research, and the confidence level constraint is not met with a higher-order polynomial fit, the degradation function must be linear. The pavement families described in this work output linear approximations in PAVER™ due to the short temporal scale and data limitation (Fortney et al. 2021). Inherent inaccuracies exist in all predictions since pavement surfaces have an increased deterioration rate near the end of their life cycle (Colorado State University 2019; Parsons and Pullen 2017). Regardless of fit type, the continuous function only acts as an approximation for the observed pavement condition. Discrete outcomes from the continuous degradation functions are treated as the dependent variable in the prediction model.

The novel, final step of this research involves the treatment of climate and equivalent passes as determinants in the degradation model that can be locally calibrated through principal component regression (PCR). Selected climatic variables and aircraft passes are input to a cross-validated PCR model. This bias-reduced statistical model was used because of its proven capabilities in modeling the impact of climate on the built and natural environment since the independent variables (IV) are often collinear (Delorit et al. 2017). Rather than remove an IV that is suspected to be collinear, or keep all IVs and admit to the collinearity, PCR enables the retention of unique, orthogonal signals without

the loss of information. For example, the daily snowfall depth is collinear with temperature, though inversely. PCR transforms those original IVs into orthogonal principal components (PC) (Abdi and Williams 2010) by performing a two-step multi-factor linear regression (MLR). Subsequently, the newly formed, independent PCs are used in place of the IVs in this MLR. This research employed Jolliffe's Rule to retain only the PCs that describe a threshold amount of variation in the model and reduce the risk from overfitting. Jolliffe's Rule retains each PC that explains at least 70% of the mean variance explained by all PCs, thereby eliminating PCs with less contribution to the explained variability (Jolliffe 2002). For this research, the mean variance with five climate-based PCs is 0.2, representing a 14% PC retention threshold. Six PCs, including traffic passes, results in a threshold of 11.6%. Figure 14 compares Dover and Hurlburt, which retained different PCs when using the thresholds from Jolliffe's Rule.

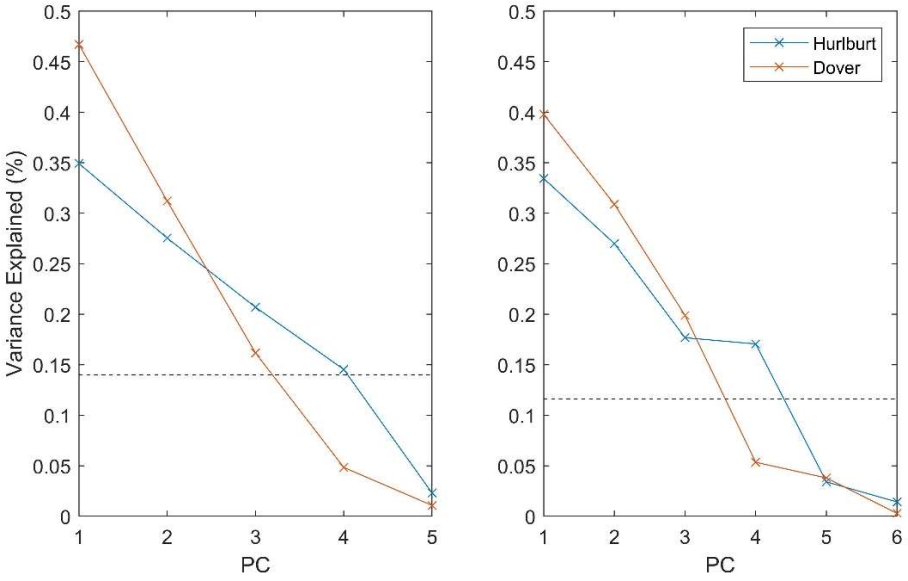

Figure 14. Example scree plot displaying the percent variance explained by each principal component for Dover and Hurlburt.

Applying PCR eliminates multicollinearity by resolving the original IV data into orthogonal signals. The newly created PCs do not relate directly to any single IV. They must be cross-correlated with the IVs to determine which amount of the original IVs explains variability in each PC. The absolute strength of the correlation was considered since climatic effects may be positively or negatively correlated. For example, with Fairchild AFB, the first PC has a correlation of 0.89 for freeze-thaw, -0.33 for solar irradiance, and 0.26 for equivalent passes, meaning that PC 1 is primarily freeze-thaw with a strong influence of solar irradiance. The rest of the IVs within PC 1 are negligible. This research employed a holistic mindset to compare the number of retained PCs with the correlation to each IV to determine which IVs were significant and important.

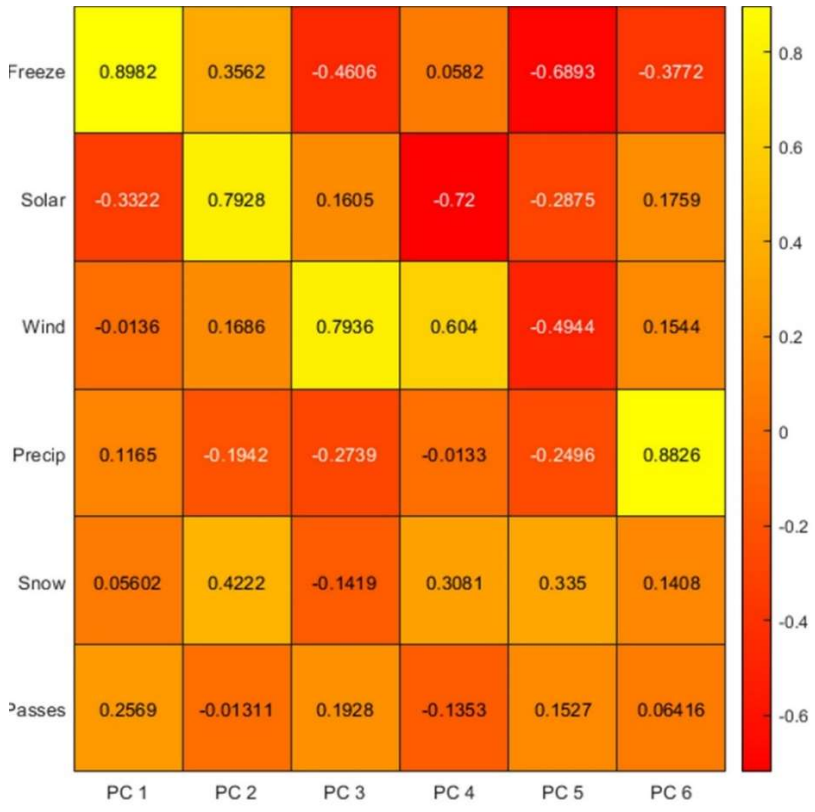

Figure 15. Example heat map showing correlation between each PC and IV for Fairchild.

To assist in the selection process, thresholds were set to determine when an IV should be counted toward a PC: PC 1 > 0.3, PC 2 > 0.4, and PC 3 > 0.5. Also, the model significance and each PC significance were determined, and all were significant at a 74% confidence interval (CI) except Minot AFB, with a 50% CI. With this example, the model retained freeze-thaw and solar because they are both above 0.4. Moreover, the highest correlation values for PC 2 and 3 were considered since 3 PCs were retained for this location. Fairchild's heat map displaying the correlation of PC to IVs is shown in Figure 15, and Fairchild's degradation variability is described in order by freeze-thaw, solar, wind, and snow. The equivalent passes IV is notable in the first PC but still insignificant.

Cross-validation was also used as a statistical method to abscond, or drop, the dependent variable observation for the time step or time steps surrounding the MLR prediction such that "perfect targets" are eliminated from consideration (Delorit et al. 2017). Since only the first predicted condition value is dropped, the form used herein is referred to as drop-one cross-validation. Adding cross-validation to the MLR process is expected to lower the Pearson's correlation (R^2) slightly because the model makes predictions whereas it otherwise had deterministic points to guide the predictions. This minor reduction in model skill is necessary to produce a set of predictions with minimal bias.

This research also duplicated step three with two model sets: one that only included climate and another that included both climate and traffic passes. Differences between the two model sets will reveal the individual impacts that climate and traffic passes have on pavement degradation for the short timescale of 2010-2019.

Results

Examples of the linear approximations for the continuous degradation functions are shown in Figure **16**, comparing Rig A with Flex A, the most important and heavily trafficked parts of the airfield with juxtaposed material type. The lines for each location's degradation rate are colored according to Köppen-Geiger zone, with green as the temperate zone, orange as arid, and blue as cold (Delorit et al. 2020). The solid black line is the weighted average of all locations within that family. A condition of 70 is the threshold for when a pavement section is considered degraded and could receive some rehabilitative care. A condition of 55 represents failing sections that should be replaced (Greene et al. 2004). Dashed lines have been added at 70 and 55 to display the difference in the expected life cycle between rigid and flexible pavements. Over this timespan, flexible pavements are more variable and have a sharper degradation line. Fairchild Air Force Base (AFB) Flex A pavement sections fall within the degraded category within the first 5 years of the pavement life. Both Rig A and Flex A for Fairchild are below the weighted average of locations for these respective families. These findings suggest some abnormality with the conditions at Fairchild. For example, there could be extremely degradative environmental factors, high traffic volumes, aircraft conditions that are especially harmful to the airfield surfaces, or a statistical error. A statistical error could arise from the short temporal scale of analysis and limited data points (only five pavement sections remained for Fairchild Flex A pavements that met the inclusion

criteria and were constructed on or after 2010 due to aircraft pass data constraints).

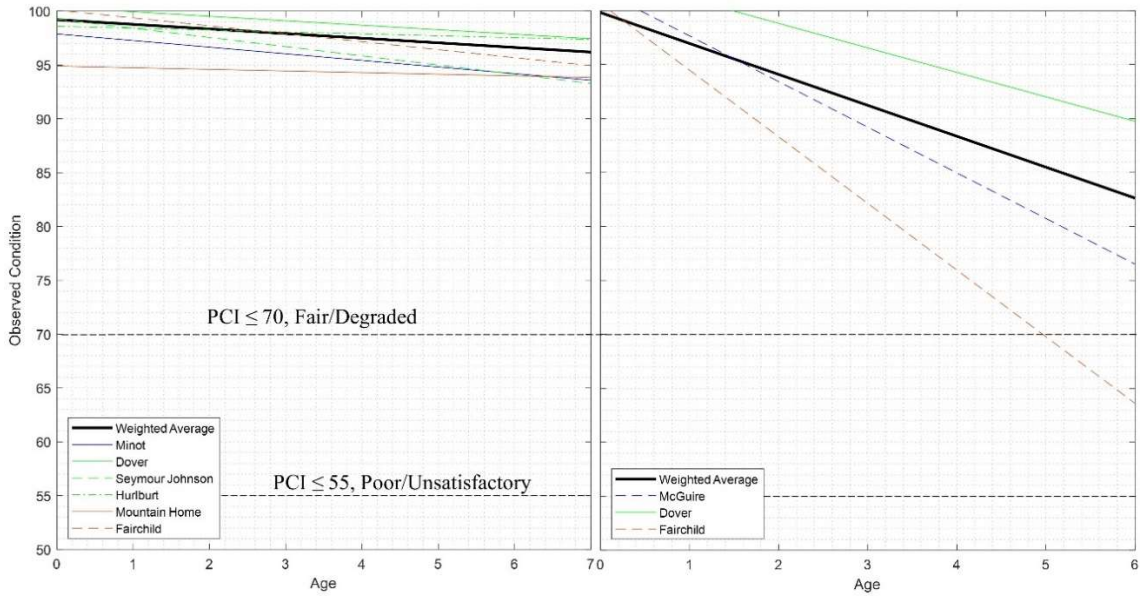

Figure 16. Linear continuous degradation functions for family-location pairs, Rigid A and Flexible A. Coloration is based on the Köppen-Geiger zones: green for temperate, blue for cold, and orange for arid.

Each continuous degradation function was used as the dependent variable in the cross-validated PCR model. R^2 and the root mean square error (RMSE) are used as deterministic skill metrics. The statistical model outputs are post-processed to ensure a decreasing, monotonic relationship between time and degradation. Only predictions of degradation between time steps were accounted for. In cases where the model suggested pavement condition improvement between years, the condition value was held constant for that time step. This post-processing aligns with PAVER™ and better matches actual condition limitations.

The PCR model was first applied to all family-location pairs using only the five selected climatic IVs. Table 11 displays the R^2 and significance (p-values) for all models when only considering climate. The significance was found before adjusting to the methodology in PAVER™, so all families have the same value within each location since climatic conditions are experienced across the entire location equally. A blank field represents cases where pavement data was insufficient to issue statistically significant predictions. Given the reliability and longevity of pavements, the authors hypothesized that the effects of environmental influences would be minimal across 10 years; however, the models described between 30-84% of the variation in degradation, meaning that climate has a significant and powerful role in degradation even over short time spans. Too many data gaps exist to make conclusions about differences between model skill for families Rig C, Flex A, and Flex D. However, pavements within PCASE traffic designator A, the first 304.8m (1000ft) of runways and all primary taxiways, are typically made from rigid pavements. Family Rig A has fewer limitations in data. Rig A will be further analyzed in the Discussion section because it has the most expected aircraft traffic, contains the most primary-designation sections, and may be considered the most important surface that supports aircraft operations. According to this analysis, traffic designator C, runway interiors, and secondary/tertiary taxiways are the most common flexible surfaces.

Table 11. Summary of climate-only Pearson's coefficient of determination and p-value after adjusting to mimic PAVER: non-increasing slope that starts at a condition 100.

Location	Significance (p-value)	Pearson's Coefficient of Determination (R^2)					
		Rig A	Rig B	Rig C	Flex A	Flex C	Flex D
Cold							
McGuire	0.50	-	-	-	0.40	0.39	-
Minot	0.78	0.36	0.32	0.35	-	0.40	0.30
Temperate							
Dover	0.14	0.80	0.81	-	0.81	0.80	-
Hurlburt	0.16	0.51	-	-	-	-	-
Moody	0.11	-	0.58	-	-	-	-
SeymourJohn	0.42	0.38	0.34	0.40	-	0.45	-
Arid							
Fairchild	0.12	0.72	0.71	0.71	0.72	0.73	0.71
MtHome	0.23	0.36	-	-	-	-	-
Nellis	0.013	-	-	-	-	0.84	0.65

Note: a hyphen represents insufficient data for model application

The same PCR model was run a second time, now inclusive of equivalent passes as an IV. The authors hypothesized that the model skill would increase as they accounted for more sources of variation. Almost every model application displayed increased skill with an average change of $R^2 = 0.04$. The R^2 values from the climate-only model set were divided by the results of the climate and passes model set ($R^2_{Climate} / R^2_{Climate+Passes}$) × 100% to reveal the percentage of model skill attributed to climate. Table 12 displays this percentage and the difference in R^2 between the two model sets. Analysis of the model set comparison continues in the Discussion section.

Table 12. The difference in R^2 after adding traffic passes and percent R^2 contribution by climate.

	Rig A		Rig B		Rig C		Flex A		Flex C		Flex D	
Location	ΔR^2	%	ΔR^2	%	ΔR^2	%	ΔR^2	%	ΔR^2	%	ΔR^2	%
Cold												
McGuire	-	-	-	-	-	-	0.105	*79*	0.095	*81*	-	-
Minot	0.023	*94*	0.016	*95*	0.022	*94*	-	-	0.024	*94*	0.009	*97*
Temperate												
Dover	0.114	*88*	0.113	*88*	-	-	0.111	*88*	0.113	*88*	-	-
Hurlburt	0.011	*98*	-	-	-	-	-	-	-	-	-	-
Moody	-	-	0.089	*87*	-	-	-	-	-	-	-	-
SeymourJohn	0.068	*85*	0.039	*90*	0.083	*83*	-	-	0.126	*78*	-	-
Arid												
Fairchild	-0.012	*102*	-0.013	*102*	-0.013	*102*	-0.012	*102*	-0.011	*102*	-0.013	*102*
MtHome	0.014	*96*	-	-	-	-	-	-	-	-	-	-
Nellis	-	-	-	-	-	-	-	-	-0.087	*112*	0.016	*98*

Note: Percent values greater than 100 signify a case where adding traffic data reduced model performance

Table 13 gives the error (RMSE) values produced by the model set that had both climate and pass data. RMSE is especially important when creating expectations that are used to schedule maintenance activities. Although the model used in this research is useful for understanding sources of degradation, this research is not concerned with having low error values since validation and further research are required to transform this model or merge its applications with PAVER™ to create a useful condition prediction tool. Still, low error values were found for most family-location pairs. The RMSE values for this final model set are less than 10 with few exceptions: Fairchild Flex A and most Flex C.

Table 13. Summary of error for the climate-passes model set.

	Root Mean Square Error (RMSE, PCI Value)					
Location	Rig A	Rig B	Rig C	Flex A	Flex C	Flex D
Cold						
McGuire	-	-	-	9.37	6.80	-
Minot	1.86	0.45	1.46	-	12.92	2.72
Temperate						
Dover	0.81	1.69	0.00	4.39	12.58	-
Hurlburt	0.41	-	-	-	-	-
Moody	-	1.04	-	-	-	-
SeymourJohn	2.09	1.49	5.18	-	15.90	-
Arid						
Fairchild	1.79	8.74	0.61	14.99	3.64	4.55
MtHome	0.41	-	-	-	-	-
Nellis	-	-	-	-	3.76	0.93
Mean ± 95% C.I.	1.23±0.54	2.68±2.35	2.41±1.53	7.19±4.30	9.27±3.66	2.73±1.14

Discussion

The climate-passes model set reveals several interesting conclusions when compared to the climate-only model set. Dover had the largest increase in skill when adding passes, followed by Seymour Johnson. Including pass data increased model skill by as much as 22% across all family-location pairs. This improvement suggests that aircraft passes describe a meaningful amount of degradation. However, the observed model improvement was less than what the authors hypothesized, likely because climatic factors are more harmful to the pavements analyzed. Another explanation is that pavements are designed for the expected aircraft traffic at each location, and those design choices are performing well, thereby minimizing the model's ability to detect trends in aircraft passes and pavement degradation. Climatic design considerations are not as advanced or tailored.

One notable conclusion from Table 11 is that the model R^2 values do not differ significantly between families within an installation because the climatic conditions are experienced across the entire installation; the model skill was fairly consistent when considering each location independently. However, the root mean square error (RMSE) is a better indicator of how well the model was able to replicate the continuous function for each family. As seen in Table 13 rigid families had significantly lower error values than Flex A and Flex C pavements, displaying the model's ability to more accurately predict the continuous function. This suggests that rigid pavements degrade more predictably than flexible when subjected to the same climatic influences, potentially due to better performance as shown by the low-sloped continuous functions.

Pavement family Rig A is the most important to mission support, and most locations had enough data from this family to perform the model. Rig A's RMSE values are all excellent and less than three. The scale of potential values for RMSE is the same as PCI (0-100), and across a 10-year window, the authors suggest that an error of less than 10 is acceptable. Also, the model R^2 without aircraft passes ranged from 0.36 to 0.80 and only increased by 2-15% when including passes. Families with traffic type A are expected to receive the most aircraft traffic and experience the highest percent improvement in model skill. Still, the results from this research suggest that climate is a more meaningful contributor to pavement degradation than aircraft passes.

Even though the percent of degradation variation is mostly described by climate, Fairchild families surprisingly had slight decreases in R^2, and Nellis Flex C decreased by 0.087. Both locations are in the arid zones, but Fairchild had the largest number of pavement sections with 67 while Nellis had the least, 11. Fairchild is further juxtaposed since that location also primarily flies large KC-135 aircraft (civilian aircraft equivalency to the Boeing 717 with a gross takeoff weight of 146,510 kg). In comparison, Nellis operates light F-16 fighter aircraft (17,010 kg), which are a full-scale magnitude lighter than Fairchild's aircraft (US DoD 2001b). Higher or lower R^2 values correspond with the model's amount of certainty in its ability to understand degradation effects, not with the strength of those effects. Nellis' lack of data hinders model performance. Acquiring additional normally distributed pavement condition data would allow the model to perform more skillfully. Fairchild, however, has enough data points to avoid these issues. Figure 17 displays one possible explanation: Fairchild has strong degradative effects from many climatic sources with the second-highest coefficient of determination (R^2 =

0.71). This suggests that the trends inherent in the climatic effects are strongly correlated with Fairchild's continuous degradation function, but the correlation between passes and degradation is weaker.

Using linear approximations for the continuous functions creates the potential for inflated model results; PCR implements MLR with PCs, so by design, MLR will have the best results when applied to linear functions. The theoretical true nature of pavement condition depreciation is nonlinear, so the results from these models may lose some significance. This limitation mainly applies when considering this model framework as a raw prediction tool. PAVER™ successfully creates accurate condition predictions, and the purpose of this model framework is to enhance existing capabilities by incorporating local condition variables and providing the capability to utilize future projections of climatic conditions to combat temporal uncertainty. The benefits provided through this model framework overcome any potential result inflation due to the linear approximations from the continuous functions.

Since the PCR model set retains the PCs that are the most meaningful in describing variation in pavement degradation, this process shows the specific variables that have had the most significant impact on each location. Figure 17 displays the important and significant climatic variables by location using cross-correlation of the retained principal components with the independent variables. With further research, this knowledge could be compiled and recorded for use in current APMS as a module that creates more accurate predictions influenced by climate and use.

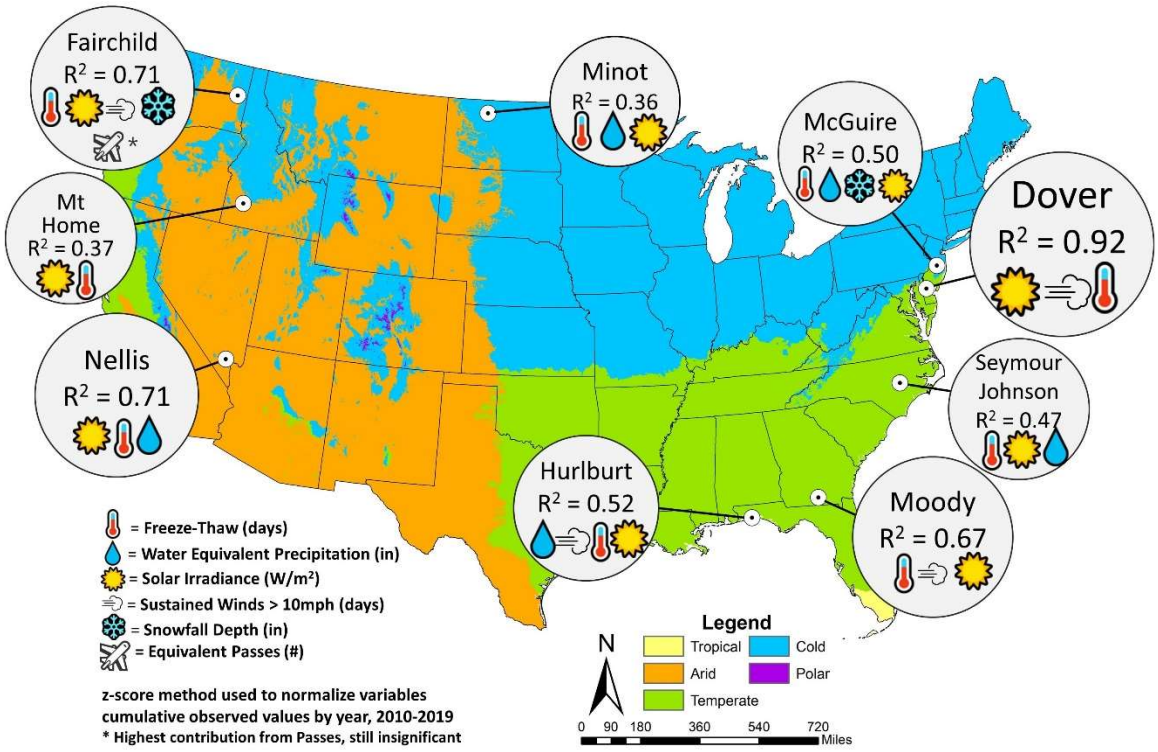

Figure 17. Location-specific, significant variables on pavement degradation with Köppen-Geiger climate divisions. Circles are sized by R2.

Aircraft passes were present in only one location, Fairchild, where passes described 26% of the first PC. Even at this location, which had the largest presence of aircraft passes, this variable was still insignificant. Furthermore, the model R^2 dropped by 1-2% for Fairchild when considering passes, despite almost all other locations increasing in skill. The detrimental effects of freeze-thaw are significant at every location, being the leading source of deterioration in five locations, with a higher leading presence in the cold and temperate zones. Freeze-thaw is a known degradative factor and validates the model's ability to recognize significant and relevant environmental factors by location. Moreover, the frequency of freeze-thaw days is higher in the cold and temperate zones. The presence of freeze-thaw in the arid zone and southwestern US locations with

typically dry or warm conditions, respectively, can be attributed to several factors: pavement design in arid locations may not use additives or construction techniques to combat the effects of freeze-thaw, and fewer freeze-thaw days means that annual differences of freeze-thaw recurrence would make up a larger percentage of change and be more heavily accounted for by the models.

Solar irradiance is present at every location. It is the leading degradation source in three locations, and it has the strongest presence in the arid zone. The pervasive appearance of solar irradiance implies a strong effect on pavement degradation. Irradiance levels remain relatively constant between years, by location, which could confound the model results. The regression model gives consistent, zero-sloped trends more weight due to similarities with the linear, low-sloped continuous functions. Regardless, solar irradiance is rarely accounted for in pavement design or pavement life-cycle rehabilitation; therefore, novel discovery can motivate research into the sun's effect on pavement surfaces.

Snowfall depth was only significant at two locations, Fairchild and McGuire. Many locations that receive snow have extensive snow-removal programs to ensure steady aircraft operations. By removing snowfall, any potential detrimental effects of snowfall may be mitigated and therefore absent in Minot and Dover, which received large amounts of snow throughout the observed period.

Limitations

Several assumptions were made to address identified limitations and uncertainty. The first main limitation is the amount of aircraft pass data since ATAR records have only been compiled since 2010 and are the limiting factor on data acquisition for the modeling analysis performed herein. Due to the short temporal scale of the aircraft traffic data, the results had less significance; however, the results still revealed the leading variables of interest with a lower level of significance. The initial analysis intended to include 1,995 pavement sections from 14 locations across 1985-2019, but only 266 pavement sections remained that were constructed after 2010 between nine remaining locations; five locations from the original data had so few data points with this constrained timeframe that they were removed from the analysis. The number of data points per location varied from 11 to 67, creating many gaps where pavement families could not be analyzed, and the significance of the models ranged from 51-99% ($0.007 \leq \rho \leq 0.49$). However, high confidence intervals may not be necessary for pavement deterioration analysis. The data's fidelity and consistency allow for lower CI that still discovers the importance of model contributors, the largest sources of deterioration among the included variables. Pavement design engineers and asset managers understand that there are many degradation sources, so identifying specific threats, as is accomplished with this research, is beneficial regardless of confidence level. Moreover, multiple threats were identified per location, such that low confidence on the first would still allow one to three other significant sources of degradation.

Another source of uncertainty surrounds the creation of the equivalent passes variable. The internal, empirically based calculations in PCASE were trusted to

determine equivalent passes through a module that is not the primary function of this design software. Rounding errors may also be an issue since the number of acceptable passes used to determine equivalent passes was 50K from a C-17, resulting in very high pass values for smaller fighter aircraft. Several conditions were assumed to be static between airfield since the data was unavailable, such as subgrade condition strength and failure criteria. PCASE's standard values were used, although the authors recognize that differences in construction standards and materials will affect these variables. Aircraft operation uncertainty also influenced the creation of the equivalent passes variable, which assumed a single, leading aircraft as the cause of deterioration at an installation.

Real-world aircraft operations are unpredictable. The heaviest, permanently stationed aircraft is likely the leading contributor to pavement damage. However, many other aircraft of varying weights and wheel configurations regularly operate stochastically between airfields depending on mission requirements. The aircraft pass data represents all passes without distinguishing aircraft, introducing even more uncertainty. Several assumptions were made such that design criteria match the experienced conditions, but this cannot always be accurate. For example, pavement is designed such that certain traffic types share common loading and wander widths. However, the travel paths of aircraft on the airfield will not precisely represent the designed percentages. Critical overloading of pavement is another source of uncertainty that significantly increases pavement damage. This overloading can be caused by aircraft that are heavier than the design conditions or aircraft mishaps (e.g., no landing gear, fire on the airfield, aircraft crash).

Conclusions

This research used an adaptable framework on a dataset of nine USAF airfields to discover the variables that most accurately describe pavement deterioration variability by location. The applied framework also compared the effects that aircraft passes have on pavement condition performance with climatic influences. Three steps are performed to accomplish the research objectives that amplify capability from PAVER™: (1) pavement families with similar qualities were grouped using standardized criteria, (2) degradation functions were generated as a target for modeling, and (3) a bias-reduced, principal component regression model was applied to each family-location pair across a temporal scale of 10 years, from 2010-2019, such that cross-correlation of the PCs to the IVs revealed the significance and strength of variable impact. The models described between 36-92% of the variation in degradation, meaning that climate and aircraft passes have a significant and influential role in degradation even over short time frames. A comparison of model sets revealed that climate describes a far larger percentage of variation than aircraft passes, with passes increasing model skill by only 14% on average. The small increased benefit of including passes suggests that climatic conditions have a larger degradative effect or that pavements are successfully designed according to the expected aircraft travel and not climate. Freeze-thaw and solar irradiance are commonly significant degradative sources and were prevalent throughout the contiguous United States. Although aircraft passes were shown to be more detrimental to flexible pavements than rigid, aircraft passes were not among the leading influences at any installation considered in this analysis. Pavement design engineers can create more sustainable pavements by

understanding how climate and aircraft passes affect pavement performance and tailoring design to the local causes of pavement damage.

VI. Conclusions and Recommendations – Creating Condition Aware Pavement Predictions

Evan M. Fortney; Justin D. Delorit, Ph.D., PE; Steven J. Schuldt, Ph.D., PE

Intended for Publication: *The Military Engineer:* Asset Management,
Society of American Military Engineers (September-October 2021)

Article Summary

AFIT researchers created a statistical framework that determines impacts of local climate and traffic on airfield pavement degradation. The framework analyzed data for nine USAF installations with different aircraft and in different climate zones. Results show that climate accounts for the majority of degradation and passes are much less influential.

Creating Condition Aware Pavement Condition Predictions

Airfield pavements are a critical component of the global transportation network, and they provide a platform for national defense. Healthy airfield pavements are essential to ensuring the ability to project power worldwide. With over 2 billion square feet of airfield pavement in its inventory and the centrality of sortie generation to the Air Force's core mission, the Air Force invests heavily in recurring maintenance and periodic rehabilitation projects. However, proactive planning of repair activities is difficult because pavement degradation rates are uncertain and dynamic. Asset managers use degradation models in the absence of a recent physical evaluation to plan maintenance

and repair activities. PAVER™ is the Department of Defense's (DoD) tool of choice for all pavement life-cycle management.

PAVER™ was created in the 1970s and is used worldwide by the USAF, US Navy, US Army, the Federal Aviation Authority, and many other state agencies. PAVER™ is a database and model-based software that pavement asset managers use to maintain records of all inspection data and make predictions about pavement degradation in order to manage roadway and airfield pavements as they slowly break down over their life cycles. With this capability, a Civil Engineer Squadron's Requirements and Optimization or Engineering Flight can make decisions between physical inspections, which are required every five years by Air Force Instruction. One of the main limitations of PAVER™ is that it only bases predictions on section age, neglecting potential degradative effects of exposure to known, local aircraft loading and climate effects, such as freeze-thaw, solar irradiance, wind, and precipitation.

A collaborative effort between the Air Force Institute of Technology's (AFIT) Graduate Engineering Management Masters students and the US Army Corps of Engineers' Construction Engineering Research Lab (CERL) endeavored to understand how long-term pavement condition correlates with actual climate trends and mission intensity. They used local, historical climate, pavement condition, and aircraft pass data from a spread of selected Air Force installations to inform statistical model sets that hold the potential to increase the accuracy of existing prediction models. The research team created a statistical, regression-based framework that can be applied to any large airport. This framework and statistical process were performed on three datasets that span major climate zones and house varying airframes. Testing multiple datasets with different

timeframes and variables shows the wide range of applicability for the created framework, and it provides insight into how time and conditions interact. The first framework application establishes whether climatic influences are significant and which specific types of weather effects contribute to poor pavement condition at select locations. It evaluated a dataset with five climatic variables from 1985 to 2019 at 14 CONUS installations and had the longest available temporal scale. The second model set sought to determine if climatic influences remain the same across time by comparing the first, 35-year dataset to a 10-year dataset at nine CONUS installations from 2010-2019. The final set of models included both climatic and aircraft pass data from 2010-2019 to investigate the influence of aircraft on pavement degradation.

The climatic variables used in this study were freeze-thaw (days), water equivalent precipitation (inches), snowfall depth (inches), sustained wind speeds above 10 miles per hour (days), and solar irradiance (W/m^2). These variables have very different values with equally varying units. They were normalized so that they could be compared regardless of units or magnitude, then summed by year. Lastly, each annual value was compiled throughout time so that the cumulative effects could be discovered at each location.

The first data set had 1,995 pavement sections over 35 years, and the results were significant across most pavement families and locations. When applied to each pavement family at each installation, the regression model revealed which climatic variables significantly impacted each location. Solar irradiance was commonly significant in the southern states. High-level sustained wind was significant in many locations ranging from Grand Forks to MacDill to Mountain Home, and freeze-thaw had a large effect in

10 of the 14 locations studied. Freeze-thaw is expected to influence pavement performance, but understanding the impact of some other, lesser-studied climate variables is exciting. The results from the first dataset highlight that pavement design should be focused at the installation level using localized climate conditions to best meet their needs and fight the local sources of deterioration.

The purpose of model sets 2 and 3 was two-fold: (1) to test whether the importance of climate variables and model skill were sensitive to time and (2) to determine whether traffic data meaningfully impacted model skill. As shown in Figure 18, many of the influences were similar when applied to different time spans. Minot notably had the same effects between the two model sets; however, the significant climatic variables changed in every other location, displaying how weather trends change over time. Moreover, climate plays a much larger role in pavement deterioration than passes. When only considering the most important pavement family (the first 1000 feet of runways and primary taxiways) made from rigid materials (Portland cement concrete), the model could account for 36-80% of the pavement degradation (R^2) without including aircraft passes. By including passes as an independent variable alongside climate inputs, the resulting skill improvement for this family is expected to increase since more known degradation sources are being included for the model. However, the improvement was minimal (ΔR^2 = 2-15%), with one location decreasing in skill by 2%. This result is somewhat shocking, especially considering that traditional wisdom suggests that condition is primarily a function of use. However, the authors postulate this could indicate that pavement design efforts are successfully accounting for expected aircraft loads: we are doing a good job designing long-lasting airfield pavements! Regardless,

this revelation justifies renewed efforts to make pavement design more robust by considering local climatic elements when creating mix designs. Exposure to the elements is the most impactful source of deterioration.

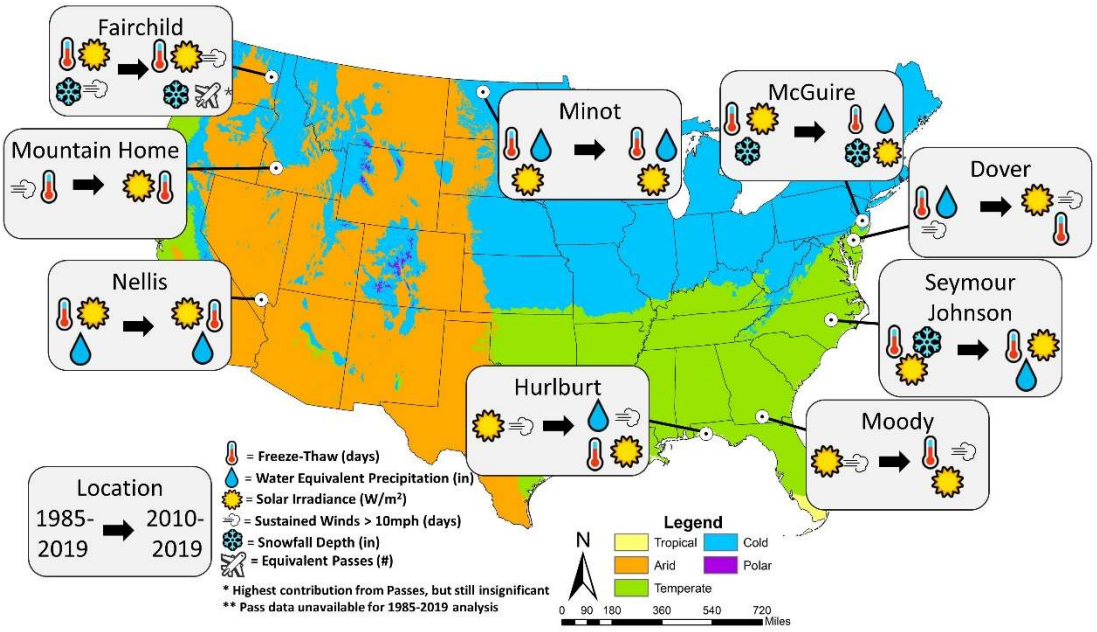

Figure 18. Comparison of climatic effects from varying temporal ranges on airfield pavements.

A major challenge for asset managers is how to handle changing future conditions. Nonstationary projections of climate require modeling software to be adaptive if it is to be trustworthy. Climate change projections or future mission requirements introduce risk to which the current systems cannot adapt. Moreover, the system framework created through this collaboration directly challenges the concept of static climatic conditions, and it can be adapted for projected conditions, helping asset managers mitigate the effects of an uncertain future.

The discoveries made through this research collaboration align with DoD goals to use data-driven, deliberate, and systematic approaches to life-cycle management of our pavements. We're collecting a lot of data that AF researchers are beginning to use to discover trends. Still, we also need to continually ask ourselves whether current data collection helps decision-makers. The research team easily found location-matched data types for historical climate and pavement conditions partly thanks to the Air Force Civil Engineer Center's successes with centralized data collection efforts over the last decade. It was surprising, though, that the Air Force only kept centralized aircraft pass data since 2010. This was the main limitation to the second and third framework applications with less than 300 pavement sections between 9 locations, creating gaps and reducing the research team's confidence in some of the model results. We should collect more and different data if we hope to keep making sustainable pavement investment decisions.

Now imagine the number of assets that are environmentally exposed worldwide: roads, chillers, roofs, windows, GOVs, construction equipment, swimming pools, tracks, etc. Accounting for exposure at their specific locations and adapting to changing future conditions could improve the predictive strength of not just PAVER™, but BUILDER too!

Research Significance

Climate non-stationarity means that different climatic factors are significant and important between the analysis from 1985 and 2010. This finding validates the need to include adaptable features in prediction generation software. Efforts could be improved on collecting important climatic effects for each location to give options for how the

degradation function might be affected by including those climatic variables. Similarly, this research justifies incorporating actual passes by location into APMS software to allow future, expected values to account for new mission bed down or significant temperature increase.

Since climatic factors describe a much larger percentage of the variance in pavement degradation than equivalent passes, this research creates a compelling argument to renew efforts into life-cycle care for airfield pavements tailored around mitigating climatic effects.

This research also allows for more thoughtful consideration of the frequency of airfield inspections and better choice management. Whereas the current regulation for USAF airfields is for a physical inspection every 5 years, that timeline could be challenged for specific locations if their conditions are predictable or well understood (AFI 32-1041 2019). Money and time that would have been spent on an airfield inspection could be reprioritized to finance more recurring crack repairs and everyday maintenance or allow for more frequent inspections on an airfield with less certain or more harmful conditions. The potential option value added to decision makers from the framework created in this research provides previously unavailable opportunities.

Research Contributions

The primary research contributions of this thesis include:

1. The development of a systems framework capable of utilizing historical observational data or projected future condition data with application on any large airport with enough pavement sections for model significance;

2. Discovering that the selected climatic variables of freeze-thaw, precipitation, snowfall, sustained wind, and solar irradiance accounted for 74-93% of the variation in pavement degradation across all pavement families of the 14 locations representative of USAF airports in the contiguous United States between 1985 and 2019;
3. Displaying the non-stationarity of climatic effects temporally; and
4. Characterizing the percent improvement in model performance by comparing model sets including aircraft passes, which confirmed that climatic factors are more significant in describing degradation.

Recommendations for Future Research

Several areas of this research could be extended through further research. First, the framework presented herein could be applied using projections of future climate values corresponding with climate change predictions in conjunction with a set of calibrating historical observations. Similarly, projections of aircraft use or type can be used to simulate degradation under new loading or frequency. This gives adaptability to current prediction capabilities and allows decision makers to understand the possible effects of changing conditions.

Secondly, this framework could be systematically applied to every location of interest and the records compiled in PCASE so that design engineers know the leading causes of deterioration for their design location. Centralized data maintenance has improved research capability, and design standards can equivalently improve through the centralized collection of localized deterioration sources so that mix designs and other

pavement design considerations can be tailored more effectively for their destined location.

Thirdly, more and different variables of many types could be used to understand more minute or uncommon influences if there is a suspected influence, so long as the data is formatted into an annual time series. The five climatic variables used in this research cover a broad range of typical environmental conditions that are both likely to occur and likely to cause some harm to pavements over time. Still, the current variable selection certainly does not cover every possible variable and conscientiously ignores latent contributors to deterioration such as subgrade strength, construction history, and maintenance programs' effectiveness. The dependent variable could also be changed from PCI to a metric of social or economic impact, opening the possibility to study the effects of airfield noise, aircraft frequency, CO2 emissions, construction delays, and other independent variables on the whole spectrum of sustainability considerations. Social impacts could be measured across time to see the effects of aircraft operations or airfield construction practices. Financial trends could be discovered and correlated with previous construction decisions, provided the availability of meaningful data.

Lastly, this research was impacted by a lack of data such that the effects of condition on portions of airfield pavement sections had to be neglected for analysis. As data is consistently and accurately accumulated over time, more can be used to fill the model output gaps and create a more confident and complete product for asset managers and pavement designers. Potential improvement for data collection exists with aircraft passes. The data for this research was only kept since 2010 and was an annual value

representing passes from all aircraft that did not distinguish aircraft types or travel paths on the airfield.

Appendix

Heat Plot Outputs

1985-2019 Analysis (14 locations)

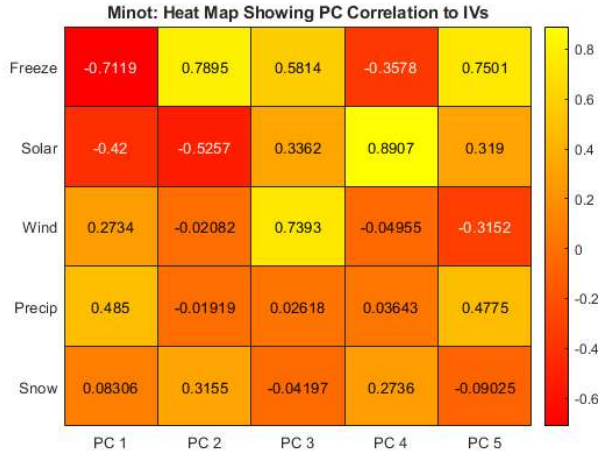

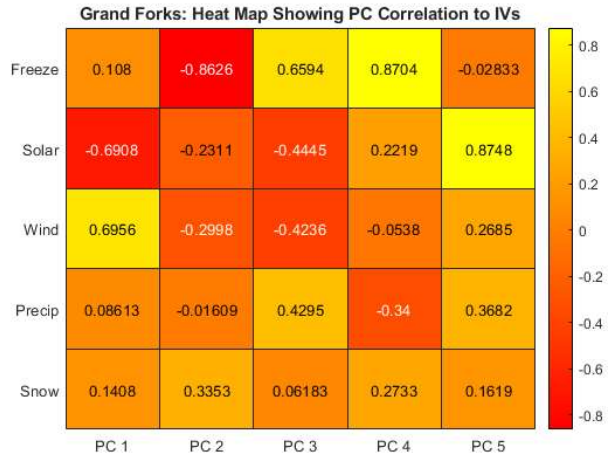

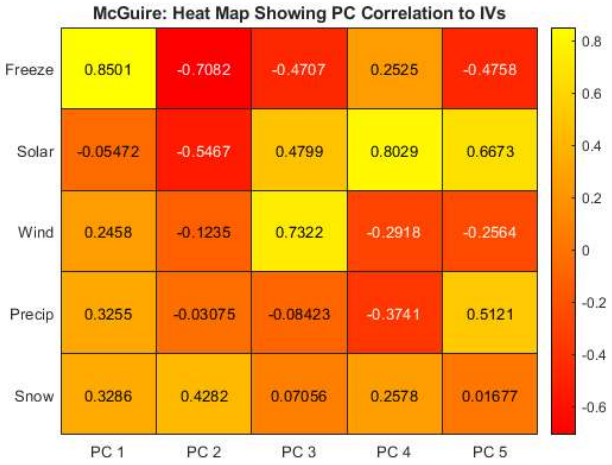

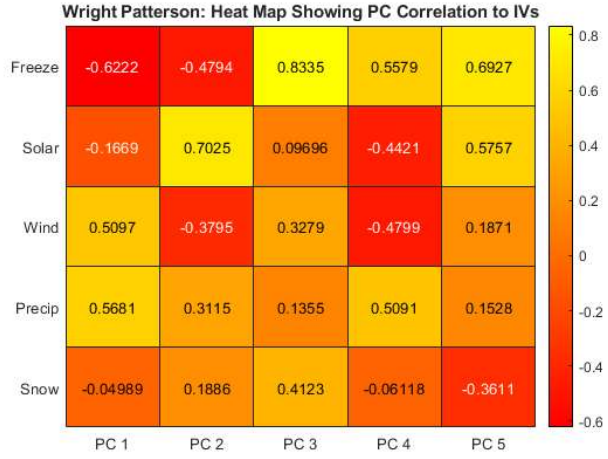

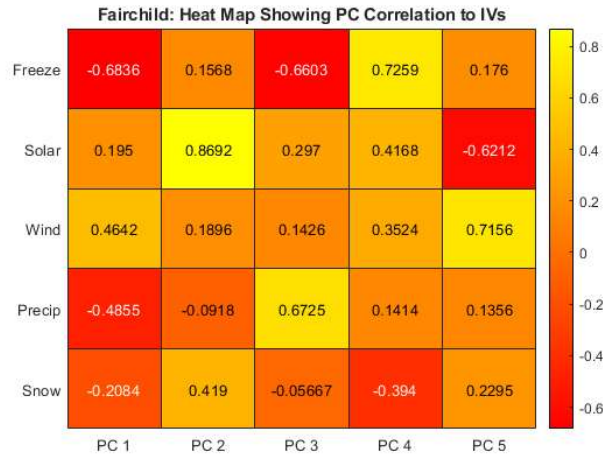

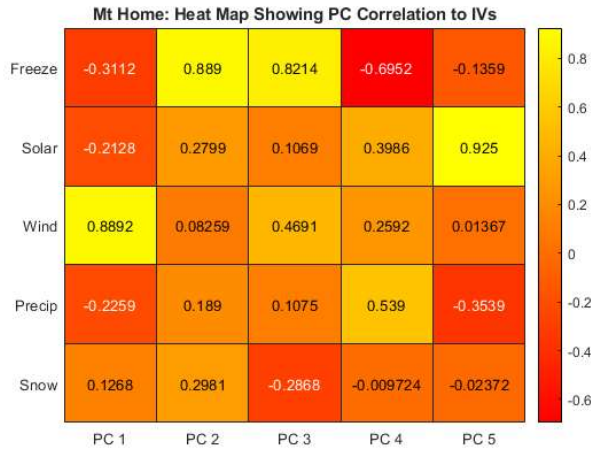

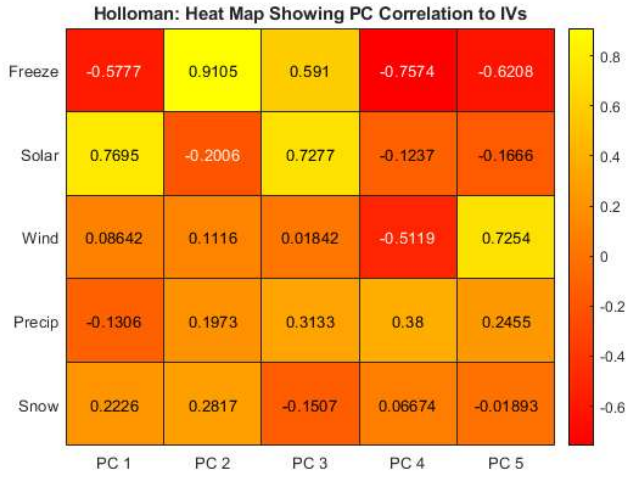
Holloman: Heat Map Showing PC Correlation to IVs
Freeze -0.5777 0.9105 0.591 -0.7574 -0.6208
Solar 0.7695 -0.2006 0.7277 -0.1237 -0.1666
Wind 0.08642 0.1116 0.01842 -0.5119 0.7254
Precip -0.1306 0.1973 0.3133 0.38 0.2455
Snow 0.2226 0.2817 -0.1507 0.06674 -0.01893
PC 1 PC 2 PC 3 PC 4 PC 5
0.8 0.6 0.4 0.2 0 -0.2 -0.4 -0.6

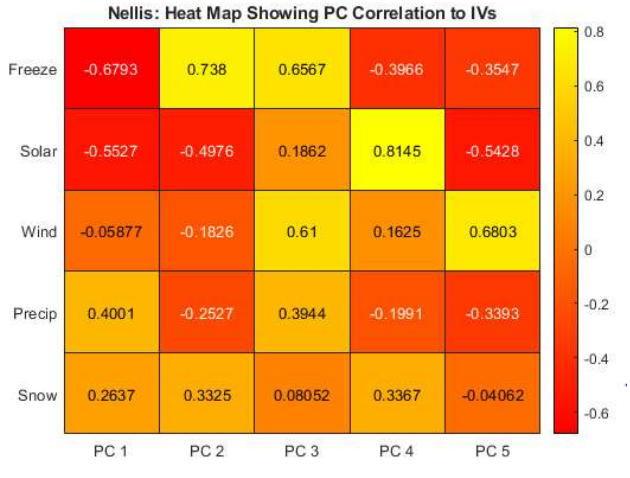
Nellis: Heat Map Showing PC Correlation to IVs
Freeze -0.6793 0.738 0.6567 -0.3966 -0.3547
Solar -0.5527 -0.4976 0.1862 0.8145 -0.5428
Wind -0.05877 -0.1826 0.61 0.1625 0.6803
Precip 0.4001 -0.2527 0.3944 -0.1991 -0.3393
Snow 0.2637 0.3325 0.08052 0.3367 -0.04062
PC 1 PC 2 PC 3 PC 4 PC 5
0.8 0.6 0.4 0.2 0 -0.2 -0.4 -0.6

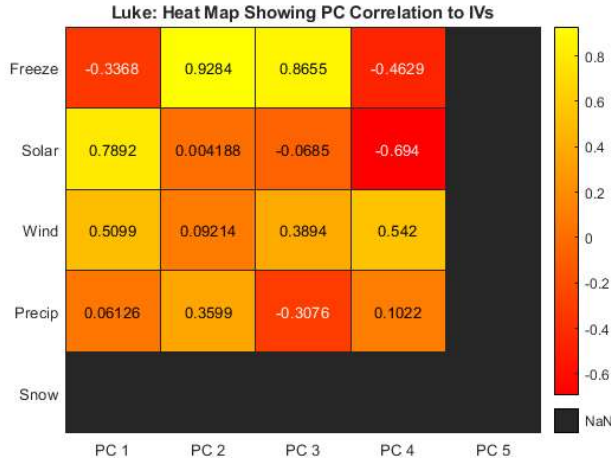
Luke: Heat Map Showing PC Correlation to IVs
Freeze -0.3368 0.9284 0.8655 -0.4629
Solar 0.7892 0.004188 -0.0685 -0.694
Wind 0.5099 0.09214 0.3894 0.542
Precip 0.06126 0.3599 -0.3076 0.1022
Snow
PC 1 PC 2 PC 3 PC 4 PC 5
0.8 0.6 0.4 0.2 0 -0.2 -0.4 -0.6
NaN

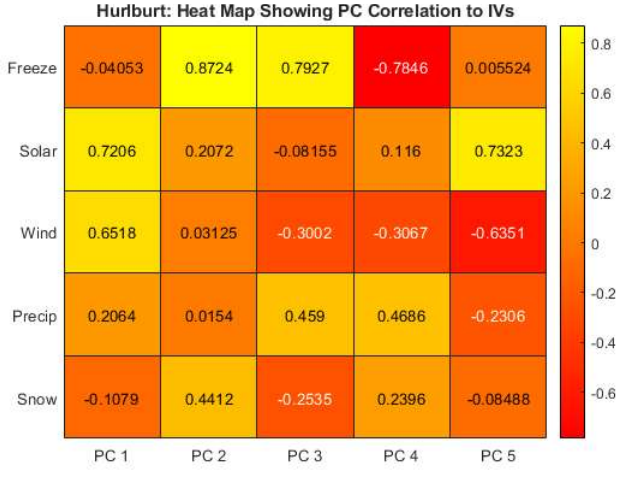
Hurlburt: Heat Map Showing PC Correlation to IVs
Freeze -0.04053 0.8724 0.7927 -0.7846 0.005524
Solar 0.7206 0.2072 -0.08155 0.116 0.7323
Wind 0.6518 0.03125 -0.3002 -0.3067 -0.6351
Precip 0.2064 0.0154 0.459 0.4686 -0.2306
Snow -0.1079 0.4412 -0.2535 0.2396 -0.08488
PC 1 PC 2 PC 3 PC 4 PC 5
0.8 0.6 0.4 0.2 0 -0.2 -0.4 -0.6

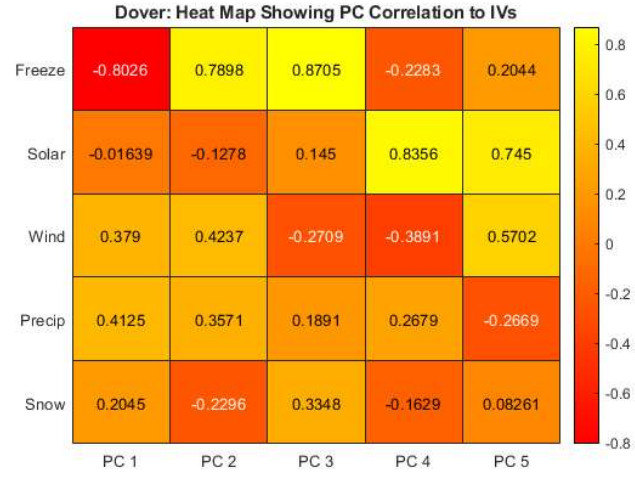
Dover: Heat Map Showing PC Correlation to IVs
Freeze -0.8026 0.7898 0.8705 -0.2283 0.2044
Solar -0.01639 -0.1278 0.145 0.8356 0.745
Wind 0.379 0.4237 -0.2709 -0.3891 0.5702
Precip 0.4125 0.3571 0.1891 0.2679 -0.2669
Snow 0.2045 -0.2296 0.3348 -0.1629 0.08261
PC 1 PC 2 PC 3 PC 4 PC 5
0.8 0.6 0.4 0.2 0 -0.2 -0.4 -0.6 -0.8

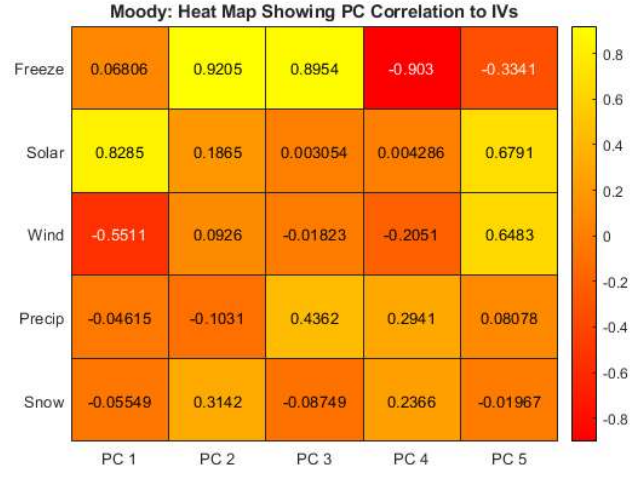
Moody: Heat Map Showing PC Correlation to IVs
Freeze 0.06806 0.9205 0.8954 -0.903 -0.3341
Solar 0.8285 0.1865 0.003054 0.004286 0.6791
Wind -0.5511 0.0926 -0.01823 -0.2051 0.6483
Precip -0.04615 -0.1031 0.4362 0.2941 0.08078
Snow -0.05549 0.3142 -0.08749 0.2366 -0.01967
PC 1 PC 2 PC 3 PC 4 PC 5
0.8 0.6 0.4 0.2 0 -0.2 -0.4 -0.6 -0.8

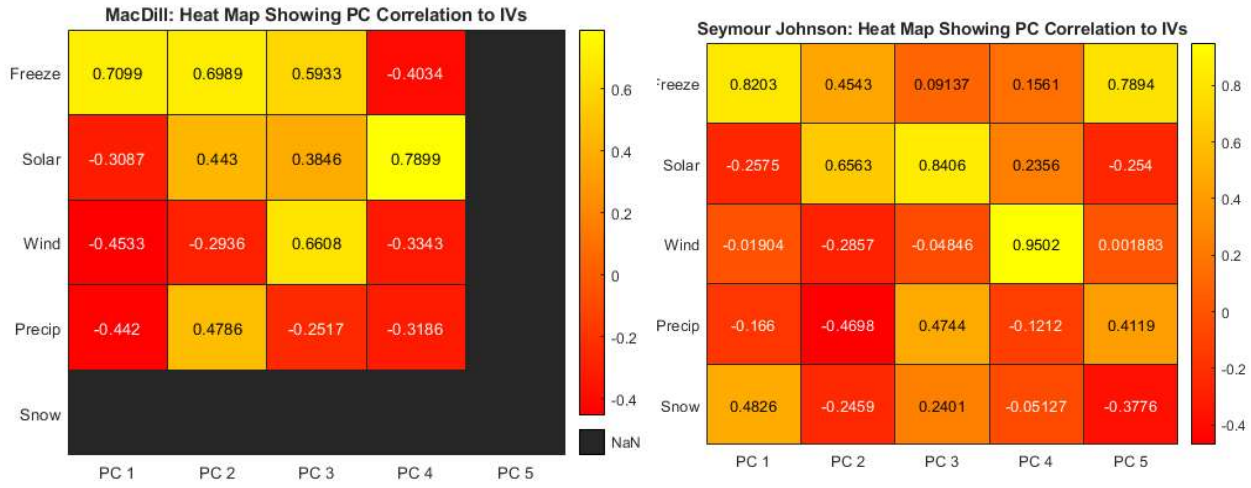

2010-2019 Analysis (9 locations)

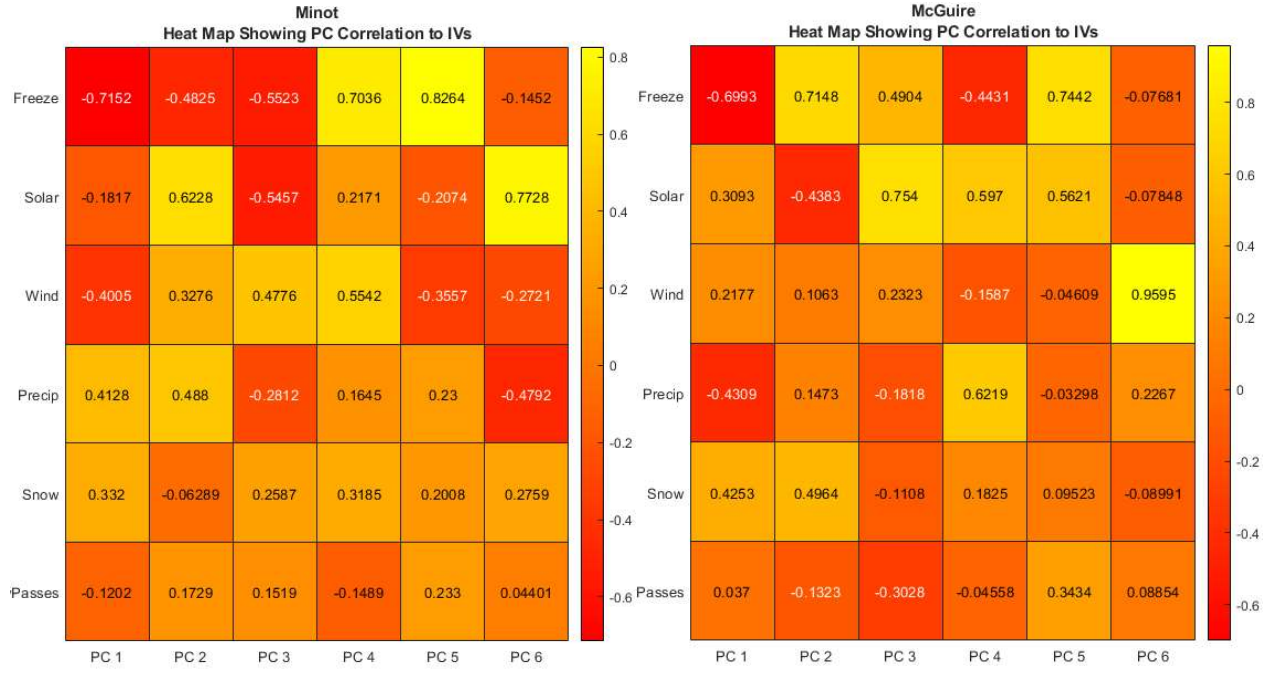

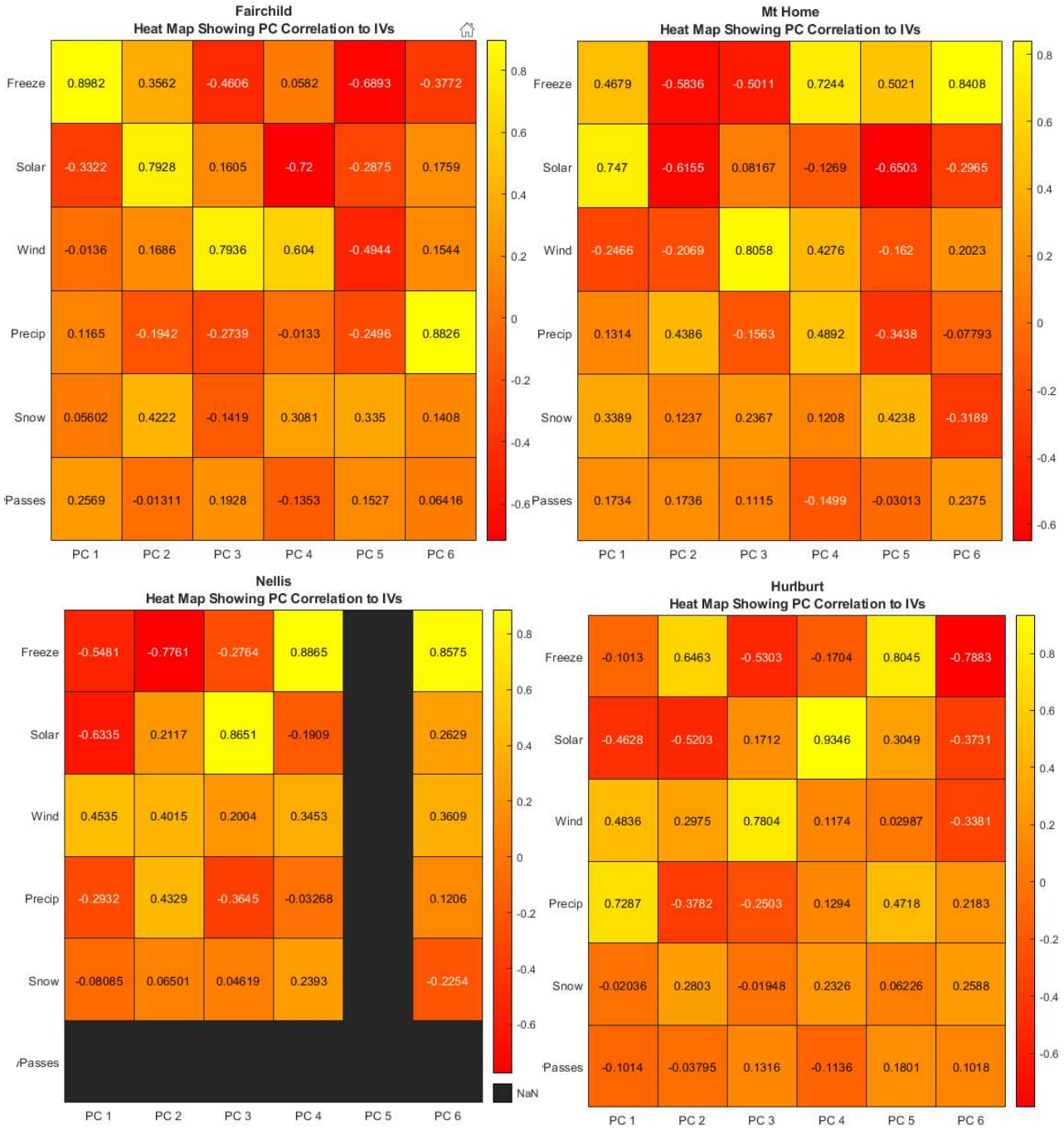
Fairchild
Heat Map Showing PC Correlation to IVs
Freeze 0.8982 0.3562 -0.4606 0.0582 -0.6893 -0.3772
Solar -0.3322 0.7928 0.1605 -0.72 -0.2875 0.1759
Wind -0.0136 0.1686 0.7936 0.604 -0.4944 0.1544
Precip 0.1165 -0.1942 -0.2739 -0.0133 -0.2496 0.8826
Snow 0.05602 0.4222 -0.1419 0.3081 0.335 0.1408
Passes 0.2569 -0.01311 0.1928 -0.1353 0.1527 0.06416
PC 1 PC 2 PC 3 PC 4 PC 5 PC 6
0.8 0.6 0.4 0.2 0 -0.2 -0.4 -0.6
Mt Home
Heat Map Showing PC Correlation to IVs
Freeze 0.4679 -0.5836 -0.5011 0.7244 0.5021 0.8408
Solar 0.747 -0.6155 0.08167 -0.1269 -0.6503 -0.2965
Wind -0.2466 -0.2069 0.8058 0.4276 -0.162 0.2023
Precip 0.1314 0.4386 -0.1563 0.4892 -0.3438 -0.07793
Snow 0.3389 0.1237 0.2367 0.1208 0.4238 -0.3189
Passes 0.1734 0.1736 0.1115 -0.1499 -0.03013 0.2375
PC 1 PC 2 PC 3 PC 4 PC 5 PC 6
0.8 0.6 0.4 0.2 0 -0.2 -0.4 -0.6
Nellis
Heat Map Showing PC Correlation to IVs
Freeze -0.5481 -0.7761 -0.2764 0.8865 0.8575
Solar -0.6335 0.2117 0.8651 -0.1909 0.2629
Wind 0.4535 0.4015 0.2004 0.3453 0.3609
Precip -0.2932 0.4329 -0.3645 -0.03268 0.1206
Snow -0.08085 0.06501 0.04619 0.2393 -0.2254
Passes
PC 1 PC 2 PC 3 PC 4 PC 5 PC 6
0.8 0.6 0.4 0.2 0 -0.2 -0.4 -0.6
NaN
Hurlburt
Heat Map Showing PC Correlation to IVs
Freeze -0.1013 0.6463 -0.5303 -0.1704 0.8045 -0.7883
Solar -0.4628 -0.5203 0.1712 0.9346 0.3049 -0.3731
Wind 0.4836 0.2975 0.7804 0.1174 0.02987 -0.3381
Precip 0.7287 -0.3782 -0.2503 0.1294 0.4718 0.2183
Snow -0.02036 0.2803 -0.01948 0.2326 0.06226 0.2588
Passes -0.1014 -0.03795 0.1316 -0.1136 0.1801 0.1018
PC 1 PC 2 PC 3 PC 4 PC 5 PC 6
0.8 0.6 0.4 0.2 0 -0.2 -0.4 -0.6

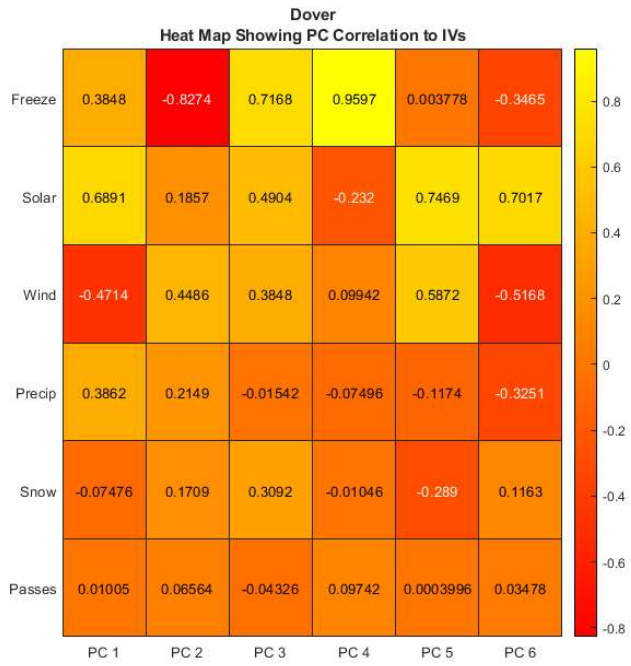
Dover
Heat Map Showing PC Correlation to IVs
Freeze 0.3848 -0.8274 0.7168 0.9597 0.003778 -0.3465
Solar 0.6891 0.1857 0.4904 -0.232 0.7469 0.7017
Wind -0.4714 0.4486 0.3848 0.09942 0.5872 -0.5168
Precip 0.3862 0.2149 -0.01542 -0.07496 -0.1174 -0.3251
Snow -0.07476 0.1709 0.3092 -0.01046 -0.289 0.1163
Passes 0.01005 0.06564 -0.04326 0.09742 0.0003996 0.03478
PC 1 PC 2 PC 3 PC 4 PC 5 PC 6
0.8 0.6 0.4 0.2 0 -0.2 -0.4 -0.6 -0.8

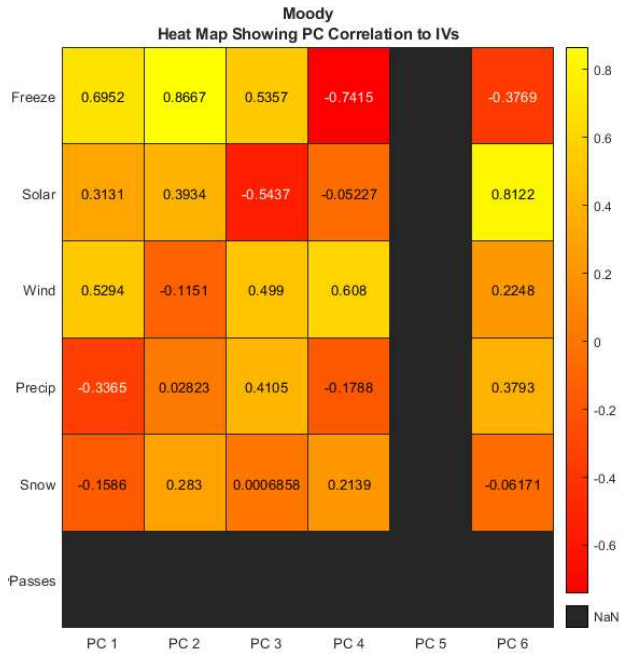
Moody
Heat Map Showing PC Correlation to IVs
Freeze 0.6952 0.8667 0.5357 -0.7415 -0.3769
Solar 0.3131 0.3934 -0.5437 -0.05227 0.8122
Wind 0.5294 -0.1151 0.499 0.608 0.2248
Precip -0.3365 0.02823 0.4105 -0.1788 0.3793
Snow -0.1586 0.283 0.0006858 0.2139 -0.06171
Passes
PC 1 PC 2 PC 3 PC 4 PC 5 PC 6
0.8 0.6 0.4 0.2 0 -0.2 -0.4 -0.6
NaN

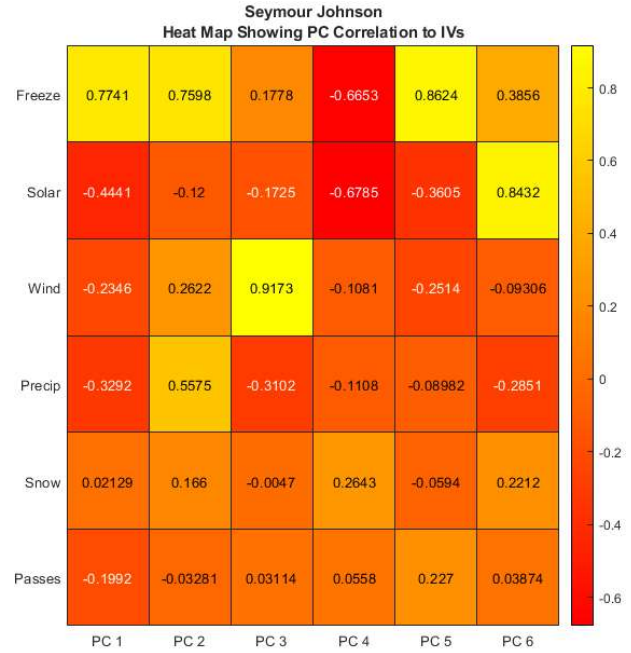
Seymour Johnson
Heat Map Showing PC Correlation to IVs
Freeze 0.7741 0.7598 0.1778 -0.6653 0.8624 0.3856
Solar -0.4441 -0.12 -0.1725 -0.6785 -0.3605 0.8432
Wind -0.2346 0.2622 0.9173 -0.1081 -0.2514 -0.09306
Precip -0.3292 0.5575 -0.3102 -0.1108 -0.08982 -0.2851
Snow 0.02129 0.166 -0.0047 0.2643 -0.0594 0.2212
Passes -0.1992 -0.03281 0.03114 0.0558 0.227 0.03874
PC 1 PC 2 PC 3 PC 4 PC 5 PC 6
0.8 0.6 0.4 0.2 0 -0.2 -0.4 -0.6

Excel Formatting for MATLAB Data Processing

One .csv file for each installation. Columns represent different variables. Rows represent the cumulative values of each variable by year. Normalizing of variables is performed within MATLAB.

1985-2019 Analysis Example .csv, Climate Only: all columns, top 5 rows

Year	Number of Freeze-Thaw Days	Annual Solar Irradiance	Number of Days with Sustained Winds (above 10 mph)	Annual Water Equivalent Precipitation (inches)	Annual Snowfall (inches)
1985	54	1603281	18	31.87	1
1986	44	1587465	17	39.8	0.2
1987	43	1551564	21	42.79	1
1988	55	1611981	10	40.85	8.1

2010-2019 Analysis Example .csv, Climate and Passes: all columns, top 5 rows

Yr	Freeze	Solar	Wind	Precip	Snow	EqPass Rig_A	EqPass Flex_A	EqPass Rig_B	EqPass Flex_B	EqPass Rig_C	EqPass Flex_C	EqPass Rig_D	EqPass Flex_D	Raw
2010	76	1897295	57	37.5	16.9	1876948	1003445	2433844	1167420	4052970	11674.2	1869729	3320754	103129
2011	45	1856837	57	45.7	0.1	1932094	1032927	2505352	1201720	4172049	12017.2	1924663	3418342	106159
2012	33	1823192	46	35.2	0	2192936	1172377	2843588	1363958	4735296	13639.58	2184502	3879801	120491
2013	54	1748364	51	56.5	1.2	1828663	977631.5	2371234	1137388	3948707	11373.88	1821630	3235327	100476

MATLAB Code, using version R2020a

```
%TITLE: STEP 1: Continuous Function for Pavement Age & PCI
%INPUT: Combined Pavement_Only.csv file (Pavement_Only2)
%OUTPUT: Plots showing continous functions by Pavement Family Type
%Captain Sarah Brown and Captain Evan Fortney
%Date: 25 Feb 2021
%Version 5: REMOVE APC, Climate Only 1985-2019
clear, clc, close all

%% Instructions

%1. Look at the actual csv to determine which base/family pairs are lacking data
%2. If missing data, comment the corresponding base/family scatterplot
%3. Ensure both Legends match the existing data by deleting
  % the corresponding plots (f2 or f6, whatever)
  % AND the labels ('Nellis' or'Fairchild')
%4. Next, change the continuous function for each missing base/family pair
  % ensure that a previous family exists already...
    %4.1 For example, if the FIRST family for Fairchild does not exist, use this syntax:
        % Fairchild_Total = [];
```

```
        % Fairchild_Total = horzcat(X',Fairchild_Total,zeroTemp);
    %4.2 For every other family after the first one, if missing data, use the following syntax:
        % Fairchild_Total = horzcat(Fairchild_Total,zeroTemp);

%% FAMILIES, 1985 analysis

%Select The Variables for Which Pavement Type:
% DV = 22;  %Family #1: RIGID - PRIMARY - TAXIWAYS/APRONS
% DV = 23;  %Family #2: RIGID - PRIMARY - RUNWAYS
% DV = 24;  %Family #3: RIGID - SEC/TER - TAXIWAYS/APRONS
% DV = 25;  %Family #4: FLEXI - PRIMARY - TAXIWAYS/APRONS
% DV = 26;  %Family #5: FLEXI - PRIMARY - RUNWAYS
% DV = 27;  %Family #6: FLEXI - SEC/TER - OVERRUNS/SHOULDERS
% DV = 28;  %Family #7: FLEXI - SEC/TER - TAXIWAYS/APRONS


%% 1. Import Data

Data = readtable('Pavement_Only2.csv', 'HeaderLines',0);     %Import Line for Pavement Data File
nrow = size(Data,1);
Type = unique(Data.Base)
Type = unique(Data.AC_Type);
yMax = max(Data.Age);
Data.Plane = zeros(nrow,1);
nrow = size(Data,1);
Data.Output = zeros(nrow, 1);  %adding blank column to the end of the table (will store the outputs of for
loops later on)

nAssets = height(Data); %finds the number of unique Asset ID's
for i=1:nAssets
    if Data.Age(i) == 0
        if Data.PCI(i) < 100
            Data.Output(i) = 1;
        else
            Data.Output(i) = 0;
        end
    end
end
Data(Data.Output == 1, :) = [];

Data_Rigid = Data((Data.Surf2 == "Rigid"),:);
Data_Flex = Data((Data.Surf2 == "Flexible"),:);

Data_Rigid_Pri = Data_Rigid((Data_Rigid.Rank2 == "Pri"),:);
Data_Rigid_S_T = Data_Rigid((Data_Rigid.Rank2 == "Sec and Tert"),:);
Data_Flex_Pri = Data_Flex((Data_Flex.Rank2 == "Pri"),:);
Data_Flex_S_T = Data_Flex((Data_Flex.Rank2 == "Sec and Tert"),:);

Rigid_Pri_Taxiway = Data_Rigid_Pri((Data_Rigid_Pri.Use == "TAXIWAY" | Data_Rigid_Pri.Use ==
"APRON"),:);
Rigid_Pri_Runway = Data_Rigid_Pri((Data_Rigid_Pri.Use == "RUNWAY"),:);
```

```
Rigid_SecTer_Taxiway = Data_Rigid_S_T((Data_Rigid_S_T.Use == "TAXIWAY" | Data_Rigid_S_T.Use
== "APRON"),:);

Flex_Pri_Taxiway = Data_Flex_Pri((Data_Flex_Pri.Use == "TAXIWAY" | Data_Flex_Pri.Use ==
"APRON"),:);
Flex_Pri_Runway = Data_Flex_Pri((Data_Flex_Pri.Use == "RUNWAY"),:);

Flex_SecTer_Overrun = Data_Flex_S_T((Data_Flex_S_T.Use == "OVERRUN" | Data_Flex_S_T.Use ==
"SHOULDER"),:);
Flex_SecTer_Taxiway = Data_Flex_S_T((Data_Flex_S_T.Use == "TAXIWAY" | Data_Flex_S_T.Use ==
"APRON"),:);

zeroTemp = zeros(35,1);

X = 0:1:34;         %Create Simulation 'Ages'

%% SECTION 1 = Rigid - Primary - Taxiways & Aprons
xAge_Rigid_Pri_Taxiway = Rigid_Pri_Taxiway.Age;
yCI_Rigid_Pri_Taxiway = Rigid_Pri_Taxiway.PCI;

GrandForks_R_P_T = Rigid_Pri_Taxiway((Rigid_Pri_Taxiway.Base == "GrandForks"),:);
Minot_R_P_T = Rigid_Pri_Taxiway((Rigid_Pri_Taxiway.Base == "Minot"),:);
MtHome_R_P_T = Rigid_Pri_Taxiway((Rigid_Pri_Taxiway.Base == "MtHome"),:);
Fairchild_R_P_T = Rigid_Pri_Taxiway((Rigid_Pri_Taxiway.Base == "Fairchild"),:);

WrightPatt_R_P_T = Rigid_Pri_Taxiway((Rigid_Pri_Taxiway.Base == "WrightPatterson"),:);
McGuire_R_P_T = Rigid_Pri_Taxiway((Rigid_Pri_Taxiway.Base == "McGuire"),:);
Dover_R_P_T = Rigid_Pri_Taxiway((Rigid_Pri_Taxiway.Base == "Dover"),:);

Luke_R_P_T = Rigid_Pri_Taxiway((Rigid_Pri_Taxiway.Base == "Luke"),:);
Nellis_R_P_T = Rigid_Pri_Taxiway((Rigid_Pri_Taxiway.Base == "Nellis"),:);
Holloman_R_P_T = Rigid_Pri_Taxiway((Rigid_Pri_Taxiway.Base == "Holloman"),:);

MacDill_R_P_T = Rigid_Pri_Taxiway((Rigid_Pri_Taxiway.Base == "MacDill"),:);
Hurlburt_R_P_T = Rigid_Pri_Taxiway((Rigid_Pri_Taxiway.Base == "Hurlburt"),:);
Moody_R_P_T = Rigid_Pri_Taxiway((Rigid_Pri_Taxiway.Base == "Moody"),:);
SeymourJohn_R_P_T = Rigid_Pri_Taxiway((Rigid_Pri_Taxiway.Base == "SeymourJohnson"),:);


figure(1)

xInput = [xAge_Rigid_Pri_Taxiway];
yInput = [yCI_Rigid_Pri_Taxiway];

fit_Rigid_Pri_Tax = fit(xInput, yInput,'poly1')
fit_Ca = coeffvalues(fit_Rigid_Pri_Tax);

m1a = fit_Ca(1); intercept1 = fit_Ca(2);
yMa = intercept1 + m1a*X;                   %CONTINOUS FUNCTION OF PCIs
```

```
fit_C_con = confint(fit_Rigid_Pri_Tax,0.90);     %NUMBER SETS CONFIDENCE INTERVAL -
CURRENTLY AT 90% Confidence Interval
mcon1 = fit_C_con(1,1); mcon2 = fit_C_con(2,1);
intcon1 = fit_C_con(1,2); intcon2 = fit_C_con(2,2);

y5 = mcon1*X + intcon1;
y95 = mcon2*X + intcon2;

yline(0,'b-','LineWidth',5); hold on;  %add a thick horizontal line at y=0
X2 = [X,fliplr(X)];
inBetween = [y5, fliplr(y95)];
con = fill(X2, inBetween, [0.50 0.50 0.50]); hold on;
set(con,'facealpha',0.2,'EdgeColor', 'none')

plot(X,y5,'b--'); hold on;
plot(X,y95,'b--'); hold on;

f1 = plot(X,yMa,'k-'); hold on;
f2 = scatter(GrandForks_R_P_T.Age,
GrandForks_R_P_T.PCI,30,'d','MarkerFaceColor','b','MarkerEdgeColor','b','MarkerFaceAlpha',
0.2,'MarkerEdgeAlpha', 0.2); hold on;
f3 = scatter(Minot_R_P_T.Age,
Minot_R_P_T.PCI,30,'MarkerFaceColor','b','MarkerEdgeColor','b','MarkerFaceAlpha',
0.2,'MarkerEdgeAlpha', 0.2); hold on;
f4 = scatter(MtHome_R_P_T.Age,
MtHome_R_P_T.PCI,30,'s','MarkerFaceColor','b','MarkerEdgeColor','b','MarkerFaceAlpha',
0.2,'MarkerEdgeAlpha', 0.2); hold on;
% f5 = scatter(Fairchild_R_P_T.Age,
Fairchild_R_P_T.PCI,30,'^','MarkerFaceColor','b','MarkerEdgeColor','b','MarkerFaceAlpha',
0.2,'MarkerEdgeAlpha', 0.2); hold on;

f6 = scatter(WrightPatt_R_P_T.Age,
WrightPatt_R_P_T.PCI,30,'d','MarkerFaceColor','m','MarkerEdgeColor','m','MarkerFaceAlpha',
0.2,'MarkerEdgeAlpha', 0.2);
f7 = scatter(McGuire_R_P_T.Age,
McGuire_R_P_T.PCI,30,'MarkerFaceColor','m','MarkerEdgeColor','m','MarkerFaceAlpha',
0.2,'MarkerEdgeAlpha', 0.2);
f8 = scatter(Dover_R_P_T.Age,
Dover_R_P_T.PCI,30,'s','MarkerFaceColor','m','MarkerEdgeColor','m','MarkerFaceAlpha',
0.2,'MarkerEdgeAlpha', 0.2); hold on;

f9 = scatter(Luke_R_P_T.Age,
Luke_R_P_T.PCI,30,'d','MarkerFaceColor','r','MarkerEdgeColor','r','MarkerFaceAlpha',
0.2,'MarkerEdgeAlpha', 0.2); hold on;
f10 = scatter(Nellis_R_P_T.Age,
Nellis_R_P_T.PCI,30,'MarkerFaceColor','r','MarkerEdgeColor','r','MarkerFaceAlpha',
0.2,'MarkerEdgeAlpha', 0.2); hold on;
f11 = scatter(Holloman_R_P_T.Age,
Holloman_R_P_T.PCI,30,'s','MarkerFaceColor','r','MarkerEdgeColor','r','MarkerFaceAlpha',
0.2,'MarkerEdgeAlpha', 0.2); hold on;
```

```
f12 = scatter(MacDill_R_P_T.Age,
MacDill_R_P_T.PCI,30,'d','MarkerFaceColor','g','MarkerEdgeColor','g','MarkerFaceAlpha',
0.2,'MarkerEdgeAlpha', 0.2); hold on;
f13 = scatter(Hurlburt_R_P_T.Age,
Hurlburt_R_P_T.PCI,30,'MarkerFaceColor','g','MarkerEdgeColor','g','MarkerFaceAlpha',
0.2,'MarkerEdgeAlpha', 0.2); hold on;
f14 = scatter(Moody_R_P_T.Age,
Moody_R_P_T.PCI,30,'s','MarkerFaceColor','g','MarkerEdgeColor','g','MarkerFaceAlpha',
0.2,'MarkerEdgeAlpha', 0.2); hold on;
f15 = scatter(SeymourJohn_R_P_T.Age,
SeymourJohn_R_P_T.PCI,30,'^','MarkerFaceColor','g','MarkerEdgeColor','g','MarkerFaceAlpha',
0.2,'MarkerEdgeAlpha', 0.2); hold on;

title('Primary Rigid Pavements - TAXIWAYS & APRONS');
xlabel('Age'); ylabel('Observed Condition'); grid minor;
legend([f1,f2,f3,f4,f6,f7,f8,f9,f10,f11,f12,f13,f14,f15],'Linear Fit','Grand Forks','Minot','Mt Home','Wright
Patterson','McGuire','Dover','Luke','Nellis','Holloman','MacDill','Hurlburt','Moody','Seymour Johnson');
axis([0 (max(Rigid_Pri_Taxiway.Age)) 25 100]);

xt = 8;  %x-axis starting point for equation caption
yt = 30; %y-axis starting point for equation caption
caption = sprintf('y = %f * x + %f',m1a,intercept1);
text(xt, yt, caption, 'FontSize', 14, 'Color', 'k', 'FontWeight', 'bold');

figure(2) %FIGURE SHOWING COMBINED LINE WITH 1 LINE PER BASE
f1 = plot(X,yMa,'k-','LineWidth',2); hold on;

%Base #1 - Grand Forks
xInput = [GrandForks_R_P_T.Age];
yInput = [GrandForks_R_P_T.PCI];
fit_R_P_T_GrandForks = fit(xInput, yInput,'poly1')
fit_Ca = coeffvalues(fit_R_P_T_GrandForks);
m1a = fit_Ca(1); intercept1 = fit_Ca(2);
GrandForks_R_P_T_fit = intercept1 + m1a*X;
f2 = plot(X,GrandForks_R_P_T_fit,'b-'); hold on;
GrandForks_Total = horzcat(X',GrandForks_R_P_T_fit');

%Base #2 - Minot
xInput = [Minot_R_P_T.Age];
yInput = [Minot_R_P_T.PCI];
fit_R_P_T_Minot = fit(xInput, yInput,'poly1')
fit_Ca = coeffvalues(fit_R_P_T_Minot);
m1a = fit_Ca(1); intercept1 = fit_Ca(2);
Minot_R_P_T_fit = intercept1 + m1a*X;
f3 = plot(X,Minot_R_P_T_fit,'b--'); hold on;
Minot_Total = horzcat(X',Minot_R_P_T_fit');

%Base #3 - Mountain Home
xInput = [MtHome_R_P_T.Age];
yInput = [MtHome_R_P_T.PCI];
fit_R_P_T_MtHome = fit(xInput, yInput,'poly1')
fit_Ca = coeffvalues(fit_R_P_T_MtHome);
m1a = fit_Ca(1); intercept1 = fit_Ca(2);
```

```
MtHome_R_P_T_fit = intercept1 + m1a*X;
f4 = plot(X,MtHome_R_P_T_fit,'b-.'); hold on;
MtHome_Total = horzcat(X',MtHome_R_P_T_fit');

%Base #4 - Fairchild - NO DATA: EXLUDING
Fairchild_Total = [];
Fairchild_Total = horzcat(X',Fairchild_Total,zeroTemp);

%Base #5 - Wright Patterson
xInput = [WrightPatt_R_P_T.Age];
yInput = [WrightPatt_R_P_T.PCI];
fit_R_P_T_WrightPatt = fit(xInput, yInput,'poly1')
fit_Ca = coeffvalues(fit_R_P_T_WrightPatt);
m1a = fit_Ca(1); intercept1 = fit_Ca(2);
WrightPatt_R_P_T_fit = intercept1 + m1a*X;
f6 = plot(X,WrightPatt_R_P_T_fit,'m-'); hold on;
WrightPatt_Total = horzcat(X',WrightPatt_R_P_T_fit');

%Base #6 - McGuire
xInput = [McGuire_R_P_T.Age];
yInput = [McGuire_R_P_T.PCI];
fit_R_P_T_McGuire = fit(xInput, yInput,'poly1')
fit_Ca = coeffvalues(fit_R_P_T_McGuire);
m1a = fit_Ca(1); intercept1 = fit_Ca(2);
McGuire_R_P_T_fit = intercept1 + m1a*X;
f7 = plot(X,McGuire_R_P_T_fit,'m--'); hold on;
McGuire_Total = horzcat(X',McGuire_R_P_T_fit');

%Base #7 - Dover
xInput = [Dover_R_P_T.Age];
yInput = [Dover_R_P_T.PCI];
fit_R_P_T_Dover = fit(xInput, yInput,'poly1')
fit_Ca = coeffvalues(fit_R_P_T_Dover);
m1a = fit_Ca(1); intercept1 = fit_Ca(2);
Dover_R_P_T_fit = intercept1 + m1a*X;
f8 = plot(X,Dover_R_P_T_fit,'m-.'); hold on;
Dover_Total = horzcat(X',Dover_R_P_T_fit');

%Base #8 - Luke
xInput = [Luke_R_P_T.Age];
yInput = [Luke_R_P_T.PCI];
fit_R_P_T_Luke = fit(xInput, yInput,'poly1')
fit_Ca = coeffvalues(fit_R_P_T_Luke);
m1a = fit_Ca(1); intercept1 = fit_Ca(2);
Luke_R_P_T_fit = intercept1 + m1a*X;
f9 = plot(X,Luke_R_P_T_fit,'r-'); hold on;
Luke_Total = horzcat(X',Luke_R_P_T_fit');

%Base #9 - Nellis
xInput = [Nellis_R_P_T.Age];
yInput = [Nellis_R_P_T.PCI];
fit_R_P_T_Nellis = fit(xInput, yInput,'poly1')
fit_Ca = coeffvalues(fit_R_P_T_Nellis);
```

```
m1a = fit_Ca(1); intercept1 = fit_Ca(2);
Nellis_R_P_T_fit = intercept1 + m1a*X;
f10 = plot(X,Nellis_R_P_T_fit,'r--'); hold on;
Nellis_Total = horzcat(X',Nellis_R_P_T_fit');

%Base #10 - Holloman
xInput = [Holloman_R_P_T.Age];
yInput = [Holloman_R_P_T.PCI];
fit_R_P_T_Holloman = fit(xInput, yInput,'poly1')
fit_Ca = coeffvalues(fit_R_P_T_Holloman);
m1a = fit_Ca(1); intercept1 = fit_Ca(2);
Holloman_R_P_T_fit = intercept1 + m1a*X;
f11 = plot(X,Holloman_R_P_T_fit,'r-.'); hold on;
Holloman_Total = horzcat(X',Holloman_R_P_T_fit');

%Base #11 - MacDill
xInput = [MacDill_R_P_T.Age];
yInput = [MacDill_R_P_T.PCI];
fit_R_P_T_MacDill = fit(xInput, yInput,'poly1')
fit_Ca = coeffvalues(fit_R_P_T_MacDill);
m1a = fit_Ca(1); intercept1 = fit_Ca(2);
MacDill_R_P_T_fit = intercept1 + m1a*X;
f12 = plot(X,MacDill_R_P_T_fit,'g-'); hold on;
MacDill_Total = horzcat(X',MacDill_R_P_T_fit');

%Base #12 - Hurlburt
xInput = [Hurlburt_R_P_T.Age];
yInput = [Hurlburt_R_P_T.PCI];
fit_R_P_T_Hurlburt = fit(xInput, yInput,'poly1')
fit_Ca = coeffvalues(fit_R_P_T_Hurlburt);
m1a = fit_Ca(1); intercept1 = fit_Ca(2);
Hurlburt_R_P_T_fit = intercept1 + m1a*X;
f13 = plot(X,Hurlburt_R_P_T_fit,'g--'); hold on;
Hurlburt_Total = horzcat(X',Hurlburt_R_P_T_fit');

%Base #13 - Moody
xInput = [Moody_R_P_T.Age];
yInput = [Moody_R_P_T.PCI];
fit_R_P_T_Moody = fit(xInput, yInput,'poly1')
fit_Ca = coeffvalues(fit_R_P_T_Moody);
m1a = fit_Ca(1); intercept1 = fit_Ca(2);
Moody_R_P_T_fit = intercept1 + m1a*X;
f14 = plot(X,Moody_R_P_T_fit,'g-.'); hold on;
Moody_Total = horzcat(X',Moody_R_P_T_fit');

%Base #14 - Seymour Johnson
xInput = [SeymourJohn_R_P_T.Age];
yInput = [SeymourJohn_R_P_T.PCI];
fit_R_P_T_SeymourJohn = fit(xInput, yInput,'poly1')
fit_Ca = coeffvalues(fit_R_P_T_SeymourJohn);
m1a = fit_Ca(1); intercept1 = fit_Ca(2);
SeymourJohn_R_P_T_fit = intercept1 + m1a*X;
f15 = plot(X,SeymourJohn_R_P_T_fit,'g:'); hold on;
```

```
SeymourJohn_Total = horzcat(X',SeymourJohn_R_P_T_fit');

axis([0 (max(Rigid_Pri_Taxiway.Age)) 25 100]);
title('Rigid Primary Taxiway/Apron (RPT)');
xlabel('Age'); ylabel('Observed Condition'); grid minor;
legend([f1,f2,f3,f4,f6,f7,f8,f9,f10,f11,f12,f13,f14,f15],'Linear Fit','Grand Forks','Minot','Mt Home','Wright
Patterson','McGuire','Dover','Luke','Nellis','Holloman','MacDill','Hurlburt','Moody','Seymour Johnson');

%% SECTION 2 = Rigid - Primary - Runways
xAge_Rigid_Pri_Runway = Rigid_Pri_Runway.Age;
yCI_Rigid_Pri_Runway = Rigid_Pri_Runway.PCI;

GrandForks_R_P_R = Rigid_Pri_Runway((Rigid_Pri_Runway.Base == "GrandForks"),:);
Minot_R_P_R = Rigid_Pri_Runway((Rigid_Pri_Runway.Base == "Minot"),:);
MtHome_R_P_R = Rigid_Pri_Runway((Rigid_Pri_Runway.Base == "MtHome"),:);
Fairchild_R_P_R = Rigid_Pri_Runway((Rigid_Pri_Runway.Base == "Fairchild"),:);

WrightPatt_R_P_R = Rigid_Pri_Runway((Rigid_Pri_Runway.Base == "WrightPatterson"),:);
McGuire_R_P_R = Rigid_Pri_Runway((Rigid_Pri_Runway.Base == "McGuire"),:);
Dover_R_P_R = Rigid_Pri_Runway((Rigid_Pri_Runway.Base == "Dover"),:);

Luke_R_P_R = Rigid_Pri_Runway((Rigid_Pri_Runway.Base == "Luke"),:);
Nellis_R_P_R = Rigid_Pri_Runway((Rigid_Pri_Runway.Base == "Nellis"),:);
Holloman_R_P_R = Rigid_Pri_Runway((Rigid_Pri_Runway.Base == "Holloman"),:);

MacDill_R_P_R = Rigid_Pri_Runway((Rigid_Pri_Runway.Base == "MacDill"),:);
Hurlburt_R_P_R = Rigid_Pri_Runway((Rigid_Pri_Runway.Base == "Hurlburt"),:);
Moody_R_P_R = Rigid_Pri_Runway((Rigid_Pri_Runway.Base == "Moody"),:);
SeymourJohn_R_P_R = Rigid_Pri_Runway((Rigid_Pri_Runway.Base == "SeymourJohnson"),:);



figure(3)

xInput = [xAge_Rigid_Pri_Runway];
yInput = [yCI_Rigid_Pri_Runway];

fit_Rigid_Pri_Run = fit(xInput, yInput,'poly1')
fit_Cb = coeffvalues(fit_Rigid_Pri_Run);

m1b = fit_Cb(1); intercept2 = fit_Cb(2);
yMb = intercept2 + m1b*X;                    %CONTINOUS FUNCTION OF PCIs

fit_C_con2 = confint(fit_Rigid_Pri_Run,0.90);     %NUMBER SETS CONFIDENCE INTERVAL -
CURRENTLY AT 90% Confidence Interval
mcon1 = fit_C_con2(1,1); mcon2 = fit_C_con2(2,1);
intcon1 = fit_C_con2(1,2); intcon2 = fit_C_con2(2,2);

y5 = mcon1*X + intcon1;
y95 = mcon2*X + intcon2;

yline(0,'b-','LineWidth',5); hold on;  %add a thick horizontal line at y=0
```

```
X2 = [X,fliplr(X)];
inBetween = [y5, fliplr(y95)];
con = fill(X2, inBetween, [0.50 0.50 0.50]); hold on;
set(con,'facealpha',0.2,'EdgeColor', 'none')

plot(X,y5,'b--'); hold on;
plot(X,y95,'b--'); hold on;

f1 = plot(X,yMb,'k-'); hold on;
% f2 = scatter(GrandForks_R_P_R.Age,
GrandForks_R_P_R.PCI,30,'d','MarkerFaceColor','b','MarkerEdgeColor','b','MarkerFaceAlpha',
0.2,'MarkerEdgeAlpha', 0.2); hold on;
f3 = scatter(Minot_R_P_R.Age,
Minot_R_P_R.PCI,30,'MarkerFaceColor','b','MarkerEdgeColor','b','MarkerFaceAlpha',
0.2,'MarkerEdgeAlpha', 0.2); hold on;
% f4 = scatter(MtHome_R_P_R.Age,
MtHome_R_P_R.PCI,30,'s','MarkerFaceColor','b','MarkerEdgeColor','b','MarkerFaceAlpha',
0.2,'MarkerEdgeAlpha', 0.2); hold on;
f5 = scatter(Fairchild_R_P_R.Age,
Fairchild_R_P_R.PCI,30,'^','MarkerFaceColor','b','MarkerEdgeColor','b','MarkerFaceAlpha',
0.2,'MarkerEdgeAlpha', 0.2); hold on;

% f6 = scatter(WrightPatt_R_P_R.Age,
WrightPatt_R_P_R.PCI,30,'d','MarkerFaceColor','m','MarkerEdgeColor','m','MarkerFaceAlpha',
0.2,'MarkerEdgeAlpha', 0.2);
% f7 = scatter(McGuire_R_P_R.Age,
McGuire_R_P_R.PCI,30,'MarkerFaceColor','m','MarkerEdgeColor','m','MarkerFaceAlpha',
0.2,'MarkerEdgeAlpha', 0.2);
f8 = scatter(Dover_R_P_R.Age,
Dover_R_P_R.PCI,30,'s','MarkerFaceColor','m','MarkerEdgeColor','m','MarkerFaceAlpha',
0.2,'MarkerEdgeAlpha', 0.2);

% f9 = scatter(Luke_R_P_R.Age,
Luke_R_P_R.PCI,30,'d','MarkerFaceColor','r','MarkerEdgeColor','r','MarkerFaceAlpha',
0.2,'MarkerEdgeAlpha', 0.2); hold on;
f10 = scatter(Nellis_R_P_R.Age,
Nellis_R_P_R.PCI,30,'MarkerFaceColor','r','MarkerEdgeColor','r','MarkerFaceAlpha',
0.2,'MarkerEdgeAlpha', 0.2); hold on;
f11 = scatter(Holloman_R_P_R.Age,
Holloman_R_P_R.PCI,30,'s','MarkerFaceColor','r','MarkerEdgeColor','r','MarkerFaceAlpha',
0.2,'MarkerEdgeAlpha', 0.2); hold on;

f12 = scatter(MacDill_R_P_R.Age,
MacDill_R_P_R.PCI,30,'d','MarkerFaceColor','g','MarkerEdgeColor','g','MarkerFaceAlpha',
0.2,'MarkerEdgeAlpha', 0.2); hold on;
f13 = scatter(Hurlburt_R_P_R.Age,
Hurlburt_R_P_R.PCI,30,'MarkerFaceColor','g','MarkerEdgeColor','g','MarkerFaceAlpha',
0.2,'MarkerEdgeAlpha', 0.2); hold on;
f14 = scatter(Moody_R_P_R.Age,
Moody_R_P_R.PCI,30,'s','MarkerFaceColor','g','MarkerEdgeColor','g','MarkerFaceAlpha',
0.2,'MarkerEdgeAlpha', 0.2); hold on;
```

```
f15 = scatter(SeymourJohn_R_P_R.Age,
SeymourJohn_R_P_R.PCI,30,'^','MarkerFaceColor','g','MarkerEdgeColor','g','MarkerFaceAlpha',
0.2,'MarkerEdgeAlpha', 0.2); hold on;

title('Primary Rigid Pavements - RUNWAYS');
xlabel('Age'); ylabel('Observed Condition'); grid minor;
legend([f1,f3,f5,f8,f10,f11,f12,f13,f14,f15],'Linear
Fit','Minot','Fairchild','Dover','Nellis','Holloman','MacDill','Hurlburt','Moody','Seymour Johnson');
axis([0 (max(Rigid_Pri_Runway.Age)) 25 100]);

xt = 8;  %x-axis starting point for equation caption
yt = 30; %y-axis starting point for equation caption
caption = sprintf('y = %f * x + %f',m1b,intercept2);
text(xt, yt, caption, 'FontSize', 14, 'Color', 'k', 'FontWeight', 'bold');

figure(4) %FIGURE SHOWING COMBINED LINE WITH 1 LINE PER BASE
f1 = plot(X,yMb,'k-','LineWidth',2); hold on;

%Base #1 - Grand Forks

% xInput = [GrandForks_R_P_R.Age];
% yInput = [GrandForks_R_P_R.PCI];
% fit_R_P_R_GrandForks = fit(xInput, yInput,'poly1')
% fit_Ca = coeffvalues(fit_R_P_R_GrandForks);
% m1a = fit_Ca(1); intercept1 = fit_Ca(2);
% GrandForks_R_P_R_fit = intercept1 + m1a*X;
% f2 = plot(X,GrandForks_R_P_R_fit,'b-'); hold on;
% GrandForks_Total = horzcat(GrandForks_Total,GrandForks_R_P_R_fit');
GrandForks_Total = horzcat(GrandForks_Total,zeroTemp);

%Base #2 - Minot
xInput = [Minot_R_P_R.Age];
yInput = [Minot_R_P_R.PCI];
fit_R_P_R_Minot = fit(xInput, yInput,'poly1')
fit_Ca = coeffvalues(fit_R_P_R_Minot);
m1a = fit_Ca(1); intercept1 = fit_Ca(2);
Minot_R_P_R_fit = intercept1 + m1a*X;
f3 = plot(X,Minot_R_P_R_fit,'b--'); hold on;
Minot_Total = horzcat(Minot_Total,Minot_R_P_R_fit');

%Base #3 - Mountain Home - NO DATA: EXLUDING
MtHome_Total = horzcat(MtHome_Total,zeroTemp);

%Base #4 - Fairchild
xInput = [Fairchild_R_P_R.Age];
yInput = [Fairchild_R_P_R.PCI];
fit_R_P_R_Fairchild = fit(xInput, yInput,'poly1')
fit_Ca = coeffvalues(fit_R_P_R_Fairchild);
m1a = fit_Ca(1); intercept1 = fit_Ca(2);
Fairchild_R_P_R_fit = intercept1 + m1a*X;
f5 = plot(X,Fairchild_R_P_R_fit,'b:'); hold on;
Fairchild_Total = horzcat(Fairchild_Total,Fairchild_R_P_R_fit');
```

```
%Base #5 - Wright Patterson
% xInput = [WrightPatt_R_P_R.Age];
% yInput = [WrightPatt_R_P_R.PCI];
% fit_R_P_R_WrightPatt = fit(xInput, yInput,'poly1');
% fit_Ca = coeffvalues(fit_R_P_R_WrightPatt);
% m1a = fit_Ca(1); intercept1 = fit_Ca(2);
% WrightPatt_R_P_R_fit = intercept1 + m1a*X;
% f6 = plot(X,WrightPatt_R_P_R_fit,'m-'); hold on;
% WrightPatt_Total = horzcat(WrightPatt_Total,WrightPatt_R_P_R_fit');
WrightPatt_Total = horzcat(WrightPatt_Total,zeroTemp);

%Base #6 - McGuire - NO DATA: EXLUDING
McGuire_Total = horzcat(McGuire_Total,zeroTemp);

%Base #7 - Dover
xInput = [Dover_R_P_R.Age];
yInput = [Dover_R_P_R.PCI];
fit_R_P_R_Dover = fit(xInput, yInput,'poly1')
fit_Ca = coeffvalues(fit_R_P_R_Dover);
m1a = fit_Ca(1); intercept1 = fit_Ca(2);
Dover_R_P_R_fit = intercept1 + m1a*X;
f8 = plot(X,Dover_R_P_R_fit,'m-.'); hold on;
Dover_Total = horzcat(Dover_Total,Dover_R_P_R_fit');

%Base #8 - Luke - NO DATA: EXLUDING
Luke_Total = horzcat(Luke_Total,zeroTemp);

%Base #9 - Nellis
xInput = [Nellis_R_P_R.Age];
yInput = [Nellis_R_P_R.PCI];
fit_R_P_R_Nellis = fit(xInput, yInput,'poly1')
fit_Ca = coeffvalues(fit_R_P_R_Nellis);
m1a = fit_Ca(1); intercept1 = fit_Ca(2);
Nellis_R_P_R_fit = intercept1 + m1a*X;
f10 = plot(X,Nellis_R_P_R_fit,'r--'); hold on;
Nellis_Total = horzcat(Nellis_Total,Nellis_R_P_R_fit');

%Base #10 - Holloman
xInput = [Holloman_R_P_R.Age];
yInput = [Holloman_R_P_R.PCI];
fit_R_P_R_Holloman = fit(xInput, yInput,'poly1')
fit_Ca = coeffvalues(fit_R_P_R_Holloman);
m1a = fit_Ca(1); intercept1 = fit_Ca(2);
Holloman_R_P_R_fit = intercept1 + m1a*X;
f11 = plot(X,Holloman_R_P_R_fit,'r-.'); hold on;
Holloman_Total = horzcat(Holloman_Total,Holloman_R_P_R_fit');

%Base #11 - MacDill
xInput = [MacDill_R_P_R.Age];
yInput = [MacDill_R_P_R.PCI];
fit_R_P_R_MacDill = fit(xInput, yInput,'poly1')
fit_Ca = coeffvalues(fit_R_P_R_MacDill);
```

```
m1a = fit_Ca(1); intercept1 = fit_Ca(2);
MacDill_R_P_R_fit = intercept1 + m1a*X;
f12 = plot(X,MacDill_R_P_R_fit,'g-'); hold on;
MacDill_Total = horzcat(MacDill_Total,MacDill_R_P_R_fit');

%Base #12 - Hurlburt
xInput = [Hurlburt_R_P_R.Age];
yInput = [Hurlburt_R_P_R.PCI];
fit_R_P_R_Hurlburt = fit(xInput, yInput,'poly1')
fit_Ca = coeffvalues(fit_R_P_R_Hurlburt);
m1a = fit_Ca(1); intercept1 = fit_Ca(2);
Hurlburt_R_P_R_fit = intercept1 + m1a*X;
f13 = plot(X,Hurlburt_R_P_R_fit,'g--'); hold on;
Hurlburt_Total = horzcat(Hurlburt_Total,Hurlburt_R_P_R_fit');

%Base #13 - Moody
xInput = [Moody_R_P_R.Age];
yInput = [Moody_R_P_R.PCI];
fit_R_P_R_Moody = fit(xInput, yInput,'poly1')
fit_Ca = coeffvalues(fit_R_P_R_Moody);
m1a = fit_Ca(1); intercept1 = fit_Ca(2);
Moody_R_P_R_fit = intercept1 + m1a*X;
f14 = plot(X,Moody_R_P_R_fit,'g-.'); hold on;
Moody_Total = horzcat(Moody_Total,Moody_R_P_R_fit');

%Base #14 - Seymour Johnson
xInput = [SeymourJohn_R_P_R.Age];
yInput = [SeymourJohn_R_P_R.PCI];
fit_R_P_R_SeymourJohn = fit(xInput, yInput,'poly1')
fit_Ca = coeffvalues(fit_R_P_R_SeymourJohn);
m1a = fit_Ca(1); intercept1 = fit_Ca(2);
SeymourJohn_R_P_R_fit = intercept1 + m1a*X;
f15 = plot(X,SeymourJohn_R_P_R_fit,'g:'); hold on;
SeymourJohn_Total = horzcat(SeymourJohn_Total,SeymourJohn_R_P_R_fit');

axis([0 (max(Rigid_Pri_Runway.Age)) 25 100]);
title('Primary Rigid Pavements - RUNWAYS');
xlabel('Age'); ylabel('Observed Condition'); grid minor;
legend([f1,f3,f5,f8,f10,f11,f12,f13,f14,f15],'Linear
Fit','Minot','Fairchild','Dover','Nellis','Holloman','MacDill','Hurlburt','Moody','Seymour Johnson');

%% CONTINUE using correct syntax for each family
%and methodology outlined in the notes at the beginning of this script
%repeat for all 7 families (1985). The first two are copied above.

%% Save matricies of Age vs. CI

save('GrandForks_Total','GrandForks_Total');
save('Minot_Total','Minot_Total');
save('MtHome_Total','MtHome_Total');
save('Fairchild_Total','Fairchild_Total');
save('WrightPatt_Total','WrightPatt_Total');
save('McGuire_Total','McGuire_Total');
```

```
save('Dover_Total','Dover_Total');
save('Luke_Total','Luke_Total');
save('Nellis_Total','Nellis_Total');
save('Holloman_Total','Holloman_Total');
save('MacDill_Total','MacDill_Total');
save('Hurlburt_Total','Hurlburt_Total');
save('Moody_Total','Moody_Total');
save('SeymourJohn_Total','SeymourJohn_Total');
```

```
%TITLE: STEP 1: Continuous Function for Pavement Age & PCI
%INPUT: Combined Pavement_Only2010_3.csv file
%OUTPUT: Plots showing continous functions by Pavement Family Type
%Captain Sarah Brown & Capt Evan Fortney
%Date: 25 Feb 2021
%Version 4.3 CHANGED pavement families to RigA-D and FlexA-D
clear, clc, close all

%% Instructions

%1. Look at the actual csv to determine which base/family pairs are lacking data
%2. If missing data, comment the corresponding base/family scatterplot
%3. Ensure both Legends match the existing data by deleting
 % the corresponding plots (f2 or f6, whatever)
 % AND the labels ('Nellis' or'Fairchild')
%4. Next, change the continuous function for each missing base/family pair
 % ensure that a previous family exists already...
  %4.1 For example, if the FIRST family for Fairchild does not exist, use this syntax:
      % Fairchild_Total3 = [];
      % Fairchild_Total3 = horzcat(X',zeroTemp);
  %4.2 For every other family after the first one, if missing data, use the following syntax:
      % Fairchild_Total3 = horzcat(Fairchild_Total3,zeroTemp);

%% FAMILIES, 2010 analysis
%Rigid Alpha, Primary Taxiways and Runway Ends
%Rigid Bravo, Aprons
%Rigid Charlie, Secondary Taxiways and Runway Interiors
%DOES NOT EXIST: Rigid Delta, Overruns/Shoulders
%Flexible Alpha, Primary Taxiways and Runway Ends
%DOES NOT EXIST: Flexible Bravo, Aprons
%Flexible Charlie, Secondary Taxiways and Runway Interiors
%Flexible Delta, Overruns/Shoulders

%% 1. Import Data

Data = readtable('Pavement_Only2010_3.csv', 'HeaderLines',0);     %Import Line for Pavement Data File
nrow = size(Data,1);
Type = unique(Data.Base)
Type = unique(Data.AC_Type);
yMax = max(Data.Age);
Data.Plane = zeros(nrow,1);
 nrow = size(Data,1);
Data.Output = zeros(nrow, 1);  %adding blank column to the end of the table (will store the outputs of for
loops later on)

nAssets = height(Data); %finds the number of unique Asset ID's
for i=1:nAssets
   if Data.Age(i) == 0
      if Data.PCI(i) < 100
         Data.Output(i) = 1;
      else
         Data.Output(i) = 0;
      end
```

```
    end
end
Data(Data.Output == 1, :) = [];

Data_Rig = Data((Data.Surf2 == "Rig"),:);
Data_Flex = Data((Data.Surf2 == "Flex"),:);

Data_Rig_A = Data_Rig((Data_Rig.PCASE == "A"),:);
Data_Rig_B = Data_Rig((Data_Rig.PCASE == "B"),:);
Data_Rig_C = Data_Rig((Data_Rig.PCASE == "C"),:);
Data_Rig_D = Data_Rig((Data_Rig.PCASE == "D"),:);

Data_Flex_A = Data_Flex((Data_Flex.PCASE == "A"),:);
Data_Flex_B = Data_Flex((Data_Flex.PCASE == "B"),:);
Data_Flex_C = Data_Flex((Data_Flex.PCASE == "C"),:);
Data_Flex_D = Data_Flex((Data_Flex.PCASE == "D"),:);

zeroTemp = zeros(10,1);

X = 0:1:9;          %Create Simulation 'Ages'

%% SECTION 1, RIGID A
xAge_Rig_A = Data_Rig_A.Age;
yCI_Rig_A = Data_Rig_A.PCI;

Minot_Rig_A = Data_Rig_A((Data_Rig_A.Base == "Minot"),:);
McGuire_Rig_A = Data_Rig_A((Data_Rig_A.Base == "McGuire"),:);

Dover_Rig_A = Data_Rig_A((Data_Rig_A.Base == "Dover"),:);
SeymourJohn_Rig_A = Data_Rig_A((Data_Rig_A.Base == "SeymourJohnson"),:);
Hurlburt_Rig_A = Data_Rig_A((Data_Rig_A.Base == "Hurlburt"),:);
Moody_Rig_A = Data_Rig_A((Data_Rig_A.Base == "Moody"),:);

MtHome_Rig_A = Data_Rig_A((Data_Rig_A.Base == "MtHome"),:);
Fairchild_Rig_A = Data_Rig_A((Data_Rig_A.Base == "Fairchild"),:);
Nellis_Rig_A = Data_Rig_A((Data_Rig_A.Base == "Nellis"),:);


figure(1)

xInput = [xAge_Rig_A];
yInput = [yCI_Rig_A];

fit_Data_Rig_A = fit(xInput, yInput,'poly1')
fit_Ca = coeffvalues(fit_Data_Rig_A);

m1a = fit_Ca(1); intercept1 = fit_Ca(2);
yMa = intercept1 + m1a*X;                   %CONTINOUS FUNCTION OF PCIs

fit_C_con = confint(fit_Data_Rig_A,0.90);     %NUMBER SETS CONFIDENCE INTERVAL -
CURRENTLY AT 90% Confidence Interval
```

```
mcon1 = fit_C_con(1,1); mcon2 = fit_C_con(2,1);
intcon1 = fit_C_con(1,2); intcon2 = fit_C_con(2,2);

y5 = mcon1*X + intcon1;
y95 = mcon2*X + intcon2;

yline(0,'b-','LineWidth',5); hold on;  %add a thick horizontal line at y=0
X2 = [X,fliplr(X)];
inBetween = [y5, fliplr(y95)];
con = fill(X2, inBetween, [0.50 0.50 0.50]); hold on;
set(con,'facealpha',0.2,'EdgeColor', 'none')

plot(X,y5,'b--'); hold on;
plot(X,y95,'b--'); hold on;

f1 = plot(X,yMa,'k-'); hold on;
f2 = scatter(Minot_Rig_A.Age,
Minot_Rig_A.PCI,30,'MarkerFaceColor','b','MarkerEdgeColor','b','MarkerFaceAlpha',
0.5,'MarkerEdgeAlpha', 0.5); hold on;
% f3 = scatter(McGuire_Rig_A.Age,
McGuire_Rig_A.PCI,30,'s','MarkerFaceColor','b','MarkerEdgeColor','b','MarkerFaceAlpha',
0.5,'MarkerEdgeAlpha', 0.5);

f4 = scatter(Dover_Rig_A.Age,
Dover_Rig_A.PCI,30,'MarkerFaceColor','g','MarkerEdgeColor','g','MarkerFaceAlpha',
0.5,'MarkerEdgeAlpha', 0.5); hold on;
f5 = scatter(SeymourJohn_Rig_A.Age,
SeymourJohn_Rig_A.PCI,30,'s','MarkerFaceColor','g','MarkerEdgeColor','g','MarkerFaceAlpha',
0.5,'MarkerEdgeAlpha', 0.5); hold on;
f6 = scatter(Hurlburt_Rig_A.Age,
Hurlburt_Rig_A.PCI,30,'d','MarkerFaceColor','g','MarkerEdgeColor','g','MarkerFaceAlpha',
0.5,'MarkerEdgeAlpha', 0.5); hold on;
% f7 = scatter(Moody_Rig_A.Age,
Moody_Rig_A.PCI,30,'^','MarkerFaceColor','g','MarkerEdgeColor','g','MarkerFaceAlpha',
0.5,'MarkerEdgeAlpha', 0.5); hold on;

f8 = scatter(MtHome_Rig_A.Age, MtHome_Rig_A.PCI,30,'MarkerFaceColor',[0.8500 0.3250
0.0980],'MarkerEdgeColor',[0.8500 0.3250 0.0980],'MarkerFaceAlpha', 0.5,'MarkerEdgeAlpha', 0.5); hold
on;
f9 = scatter(Fairchild_Rig_A.Age, Fairchild_Rig_A.PCI,30,'s','MarkerFaceColor',[0.8500 0.3250
0.0980],'MarkerEdgeColor',[0.8500 0.3250 0.0980],'MarkerFaceAlpha', 0.5,'MarkerEdgeAlpha', 0.5); hold
on;
% f10 = scatter(Nellis_Rig_A.Age, Nellis_Rig_A.PCI,30,'d','MarkerFaceColor',[0.8500 0.3250
0.0980],'MarkerEdgeColor',[0.8500 0.3250 0.0980],'MarkerFaceAlpha', 0.5,'MarkerEdgeAlpha', 0.5); hold
on;


title('Rigid Alpha, Primary Txwys & Rwy Ends');
xlabel('Age'); ylabel('Observed Condition'); grid minor;
% legend([f1,f2,f3,f4,f5,f6,f7,f8,f9,f10],{'Weighted Average','Minot','McGuire','Dover','Seymour
Johnson','Hurlburt','Moody','Mountain Home','Fairchild','Nellis'},'Location','southwest');
legend([f1,f2,f4,f5,f6,f8,f9],{'Weighted Average','Minot','Dover','Seymour Johnson','Hurlburt','Mountain
Home','Fairchild'},'Location','southwest');
```

```
axis([0 (max(Data_Rig_A.Age)) 50 100]);

xt = 2.5;  %x-axis starting point for equation caption
yt = 55; %y-axis starting point for equation caption
caption = sprintf('y = %f * x + %f',m1a,intercept1);
text(xt, yt, caption, 'FontSize', 14, 'Color', 'k', 'FontWeight', 'bold');

figure(2) %FIGURE SHOWING COMBINED LINE WITH 1 LINE PER BASE
f1 = plot(X,yMa,'k-','LineWidth',2); hold on;

%Base #1 - Minot
xInput = [Minot_Rig_A.Age];
yInput = [Minot_Rig_A.PCI];
fit_Rig_A_Minot = fit(xInput, yInput,'poly1')
fit_Ca = coeffvalues(fit_Rig_A_Minot);
m1a = fit_Ca(1); intercept1 = fit_Ca(2);
Minot_Rig_A_fit = intercept1 + m1a*X;
f2 = plot(X,Minot_Rig_A_fit,'b'); hold on;
Minot_Total3 = horzcat(X',Minot_Rig_A_fit');
% Minot_Total3 = [];
% Minot_Total3 = horzcat(X',zeroTemp);

%Base #2 - McGuire
% xInput = [McGuire_Rig_A.Age];
% yInput = [McGuire_Rig_A.PCI];
% fit_Rig_A_McGuire = fit(xInput, yInput,'poly1')
% fit_Ca = coeffvalues(fit_Rig_A_McGuire);
% m1a = fit_Ca(1); intercept1 = fit_Ca(2);
% McGuire_Rig_A_fit = intercept1 + m1a*X;
% f3 = plot(X,McGuire_Rig_A_fit,'b--'); hold on;
% McGuire_Total3 = horzcat(X',McGuire_Rig_A_fit');
McGuire_Total3 = [];
McGuire_Total3 = horzcat(X',zeroTemp);

%Base #3 - Dover
xInput = [Dover_Rig_A.Age];
yInput = [Dover_Rig_A.PCI];
fit_Rig_A_Dover = fit(xInput, yInput,'poly1')
fit_Ca = coeffvalues(fit_Rig_A_Dover);
m1a = fit_Ca(1); intercept1 = fit_Ca(2);
Dover_Rig_A_fit = intercept1 + m1a*X;
f4 = plot(X,Dover_Rig_A_fit,'g'); hold on;
Dover_Total3 = horzcat(X',Dover_Rig_A_fit');
% Dover_Total3 = [];
% Dover_Total3 = horzcat(X',zeroTemp);

%Base #4 - Seymour Johnson
xInput = [SeymourJohn_Rig_A.Age];
yInput = [SeymourJohn_Rig_A.PCI];
fit_Rig_A_SeymourJohn = fit(xInput, yInput,'poly1')
fit_Ca = coeffvalues(fit_Rig_A_SeymourJohn);
m1a = fit_Ca(1); intercept1 = fit_Ca(2);
SeymourJohn_Rig_A_fit = intercept1 + m1a*X;
```

```
f5 = plot(X,SeymourJohn_Rig_A_fit,'g--'); hold on;
SeymourJohn_Total3 = horzcat(X',SeymourJohn_Rig_A_fit');
% SeymourJohn_Total3 = [];
% SeymourJohn_Total3 = horzcat(X',zeroTemp);

%Base #5 - Hurlburt
xInput = [Hurlburt_Rig_A.Age];
yInput = [Hurlburt_Rig_A.PCI];
fit_Rig_A_Hurlburt = fit(xInput, yInput,'poly1')
fit_Ca = coeffvalues(fit_Rig_A_Hurlburt);
m1a = fit_Ca(1); intercept1 = fit_Ca(2);
Hurlburt_Rig_A_fit = intercept1 + m1a*X;
f6 = plot(X,Hurlburt_Rig_A_fit,'g-.'); hold on;
Hurlburt_Total3 = horzcat(X',Hurlburt_Rig_A_fit');
% Hurlburt_Total3 = [];
% Hurlburt_Total3 = horzcat(X',zeroTemp);

%Base #6 - Moody
% xInput = [Moody_Rig_A.Age];
% yInput = [Moody_Rig_A.PCI];
% fit_Rig_A_Moody = fit(xInput, yInput,'poly1')
% fit_Ca = coeffvalues(fit_Rig_A_Moody);
% m1a = fit_Ca(1); intercept1 = fit_Ca(2);
% Moody_Rig_A_fit = intercept1 + m1a*X;
% f7 = plot(X,Moody_Rig_A_fit,'g:'); hold on;
% Moody_Total3 = horzcat(X',Moody_Rig_A_fit');
Moody_Total3 = [];
Moody_Total3 = horzcat(X',zeroTemp);

%Base #7 - Mountain Home
xInput = [MtHome_Rig_A.Age];
yInput = [MtHome_Rig_A.PCI];
fit_Rig_A_MtHome = fit(xInput, yInput,'poly1')
fit_Ca = coeffvalues(fit_Rig_A_MtHome);
m1a = fit_Ca(1); intercept1 = fit_Ca(2);
MtHome_Rig_A_fit = intercept1 + m1a*X;
f8 = plot(X,MtHome_Rig_A_fit,'color',[0.8500 0.3250 0.0980],'color',[0.8500 0.3250 0.0980]); hold on;
MtHome_Total3 = horzcat(X',MtHome_Rig_A_fit');
% MtHome_Total3 = [];
% MtHome_Total3 = horzcat(X',zeroTemp);

%Base #8 - Fairchild
xInput = [Fairchild_Rig_A.Age];
yInput = [Fairchild_Rig_A.PCI];
fit_Rig_A_Fairchild = fit(xInput, yInput,'poly1')
fit_Ca = coeffvalues(fit_Rig_A_Fairchild);
m1a = fit_Ca(1); intercept1 = fit_Ca(2);
Fairchild_Rig_A_fit = intercept1 + m1a*X;
f9 = plot(X,Fairchild_Rig_A_fit,'--','color',[0.8500 0.3250 0.0980],'color',[0.8500 0.3250 0.0980]); hold on;
Fairchild_Total3 = horzcat(X',Fairchild_Rig_A_fit');
% Fairchild_Total3 = [];
% Fairchild_Total3 = horzcat(X',zeroTemp);
```

```
%Base #9 - Nellis
% xInput = [Nellis_Rig_A.Age];
% yInput = [Nellis_Rig_A.PCI];
% fit_Rig_A_Nellis = fit(xInput, yInput,'poly1')
% fit_Ca = coeffvalues(fit_Rig_A_Nellis);
% m1a = fit_Ca(1); intercept1 = fit_Ca(2);
% Nellis_Rig_A_fit = intercept1 + m1a*X;
% f10 = plot(X,Nellis_Rig_A_fit,'-.','color',[0.8500 0.3250 0.0980],'color',[0.8500 0.3250 0.0980]); hold
on;
% Nellis_Total3 = horzcat(X',Nellis_Rig_A_fit');
Nellis_Total3 = [];
Nellis_Total3 = horzcat(X',zeroTemp);

axis([0 (max(Data_Rig_A.Age)) 50 100]);
title('Rigid Alpha, Primary Txwys & Rwy Ends');
xlabel('Age'); ylabel('Observed Condition'); grid minor;
% legend([f1,f2,f3,f4,f5,f6,f7,f8,f9,f10],{'Weighted Average','Minot','McGuire','Dover','Seymour
Johnson','Hurlburt','Moody','Mountain Home','Fairchild','Nellis'},'Location','southwest');
legend([f1,f2,f4,f5,f6,f8,f9],{'Weighted Average','Minot','Dover','Seymour Johnson','Hurlburt','Mountain
Home','Fairchild'},'Location','southwest');


%% SECTION 2 = Rigid B

xAge_Rig_B = Data_Rig_B.Age;
yCI_Rig_B = Data_Rig_B.PCI;

Minot_Rig_B = Data_Rig_B((Data_Rig_B.Base == "Minot"),:);
McGuire_Rig_B = Data_Rig_B((Data_Rig_B.Base == "McGuire"),:);

Dover_Rig_B = Data_Rig_B((Data_Rig_B.Base == "Dover"),:);
SeymourJohn_Rig_B = Data_Rig_B((Data_Rig_B.Base == "SeymourJohnson"),:);
Hurlburt_Rig_B = Data_Rig_B((Data_Rig_B.Base == "Hurlburt"),:);
Moody_Rig_B = Data_Rig_B((Data_Rig_B.Base == "Moody"),:);

MtHome_Rig_B = Data_Rig_B((Data_Rig_B.Base == "MtHome"),:);
Fairchild_Rig_B = Data_Rig_B((Data_Rig_B.Base == "Fairchild"),:);
Nellis_Rig_B = Data_Rig_B((Data_Rig_B.Base == "Nellis"),:);


figure(3)

xInput = [xAge_Rig_B];
yInput = [yCI_Rig_B];

fit_Data_Rig_B = fit(xInput, yInput,'poly1')
fit_Ca = coeffvalues(fit_Data_Rig_B);

m1a = fit_Ca(1); intercept1 = fit_Ca(2);
yMa = intercept1 + m1a*X;                    %CONTINOUS FUNCTION OF PCIs
```

```
fit_C_con = confint(fit_Data_Rig_B,0.90);     %NUMBER SETS CONFIDENCE INTERVAL -
CURRENTLY AT 90% Confidence Interval
mcon1 = fit_C_con(1,1); mcon2 = fit_C_con(2,1);
intcon1 = fit_C_con(1,2); intcon2 = fit_C_con(2,2);

y5 = mcon1*X + intcon1;
y95 = mcon2*X + intcon2;

yline(0,'b-','LineWidth',5); hold on;  %add a thick horizontal line at y=0
X2 = [X,fliplr(X)];
inBetween = [y5, fliplr(y95)];
con = fill(X2, inBetween, [0.50 0.50 0.50]); hold on;
set(con,'facealpha',0.2,'EdgeColor', 'none')

plot(X,y5,'b--'); hold on;
plot(X,y95,'b--'); hold on;

f1 = plot(X,yMa,'k-'); hold on;
f2 = scatter(Minot_Rig_B.Age,
Minot_Rig_B.PCI,30,'MarkerFaceColor','b','MarkerEdgeColor','b','MarkerFaceAlpha',
0.5,'MarkerEdgeAlpha', 0.5); hold on;
% f3 = scatter(McGuire_Rig_B.Age,
McGuire_Rig_B.PCI,30,'s','MarkerFaceColor','b','MarkerEdgeColor','b','MarkerFaceAlpha',
0.5,'MarkerEdgeAlpha', 0.5);

f4 = scatter(Dover_Rig_B.Age,
Dover_Rig_B.PCI,30,'MarkerFaceColor','g','MarkerEdgeColor','g','MarkerFaceAlpha',
0.5,'MarkerEdgeAlpha', 0.5); hold on;
f5 = scatter(SeymourJohn_Rig_B.Age,
SeymourJohn_Rig_B.PCI,30,'s','MarkerFaceColor','g','MarkerEdgeColor','g','MarkerFaceAlpha',
0.5,'MarkerEdgeAlpha', 0.5); hold on;
% f6 = scatter(Hurlburt_Rig_B.Age,
Hurlburt_Rig_B.PCI,30,'d','MarkerFaceColor','g','MarkerEdgeColor','g','MarkerFaceAlpha',
0.5,'MarkerEdgeAlpha', 0.5); hold on;
f7 = scatter(Moody_Rig_B.Age,
Moody_Rig_B.PCI,30,'^','MarkerFaceColor','g','MarkerEdgeColor','g','MarkerFaceAlpha',
0.5,'MarkerEdgeAlpha', 0.5); hold on;

% f8 = scatter(MtHome_Rig_B.Age, MtHome_Rig_B.PCI,30,'MarkerFaceColor',[0.8500 0.3250
0.0980],'MarkerEdgeColor',[0.8500 0.3250 0.0980],'MarkerFaceAlpha', 0.5,'MarkerEdgeAlpha', 0.5); hold
on;
f9 = scatter(Fairchild_Rig_B.Age, Fairchild_Rig_B.PCI,30,'s','MarkerFaceColor',[0.8500 0.3250
0.0980],'MarkerEdgeColor',[0.8500 0.3250 0.0980],'MarkerFaceAlpha', 0.5,'MarkerEdgeAlpha', 0.5); hold
on;
% f10 = scatter(Nellis_Rig_B.Age, Nellis_Rig_B.PCI,30,'d','MarkerFaceColor',[0.8500 0.3250
0.0980],'MarkerEdgeColor',[0.8500 0.3250 0.0980],'MarkerFaceAlpha', 0.5,'MarkerEdgeAlpha', 0.5); hold
on;



title('Rigid Bravo, Aprons');
xlabel('Age'); ylabel('Observed Condition'); grid minor;
% legend([f1,f2,f3,f4,f5,f6,f7,f8,f9,f10],{'Weighted Average','Minot','McGuire','Dover','Seymour
Johnson','Hurlburt','Moody','Mountain Home','Fairchild','Nellis'},'Location','southwest');
```

```
legend([f1,f2,f4,f5,f7,f9],{'Weighted Average','Minot','Dover','Seymour
Johnson','Moody','Fairchild'},'Location','southwest');
axis([0 (max(Data_Rig_B.Age)) 50 100]);

xt = 2.5;  %x-axis starting point for equation caption
yt = 55; %y-axis starting point for equation caption
caption = sprintf('y = %f * x + %f',m1a,intercept1);
text(xt, yt, caption, 'FontSize', 14, 'Color', 'k', 'FontWeight', 'bold');

figure(4) %FIGURE SHOWING COMBINED LINE WITH 1 LINE PER BASE
f1 = plot(X,yMa,'k-','LineWidth',2); hold on;

%Base #1 - Minot
xInput = [Minot_Rig_B.Age];
yInput = [Minot_Rig_B.PCI];
fit_Rig_B_Minot = fit(xInput, yInput,'poly1')
fit_Ca = coeffvalues(fit_Rig_B_Minot);
m1a = fit_Ca(1); intercept1 = fit_Ca(2);
Minot_Rig_B_fit = intercept1 + m1a*X;
f2 = plot(X,Minot_Rig_B_fit,'b'); hold on;
Minot_Total3 = horzcat(Minot_Total3,Minot_Rig_B_fit');
% Minot_Total3 = horzcat(Minot_Total3,zeroTemp);

%Base #2 - McGuire
% xInput = [McGuire_Rig_B.Age];
% yInput = [McGuire_Rig_B.PCI];
% fit_Rig_B_McGuire = fit(xInput, yInput,'poly1')
% fit_Ca = coeffvalues(fit_Rig_B_McGuire);
% m1a = fit_Ca(1); intercept1 = fit_Ca(2);
% McGuire_Rig_B_fit = intercept1 + m1a*X;
% f3 = plot(X,McGuire_Rig_B_fit,'b--'); hold on;
% McGuire_Total3 = horzcat(McGuire_Total3,McGuire_Rig_B_fit');
McGuire_Total3 = horzcat(McGuire_Total3,zeroTemp);

%Base #3 - Dover
xInput = [Dover_Rig_B.Age];
yInput = [Dover_Rig_B.PCI];
fit_Rig_B_Dover = fit(xInput, yInput,'poly1')
fit_Ca = coeffvalues(fit_Rig_B_Dover);
m1a = fit_Ca(1); intercept1 = fit_Ca(2);
Dover_Rig_B_fit = intercept1 + m1a*X;
f4 = plot(X,Dover_Rig_B_fit,'g'); hold on;
Dover_Total3 = horzcat(Dover_Total3,Dover_Rig_B_fit');
% Dover_Total3 = horzcat(Dover_Total3,zeroTemp);

%Base #4 - Seymour Johnson
xInput = [SeymourJohn_Rig_B.Age];
yInput = [SeymourJohn_Rig_B.PCI];
fit_Rig_B_SeymourJohn = fit(xInput, yInput,'poly1')
fit_Ca = coeffvalues(fit_Rig_B_SeymourJohn);
m1a = fit_Ca(1); intercept1 = fit_Ca(2);
SeymourJohn_Rig_B_fit = intercept1 + m1a*X;
f5 = plot(X,SeymourJohn_Rig_B_fit,'g--'); hold on;
```

```
SeymourJohn_Total3 = horzcat(SeymourJohn_Total3,SeymourJohn_Rig_B_fit');
% SeymourJohn_Total3 = horzcat(SeymourJohn_Total3,zeroTemp);

%Base #5 - Hurlburt
% xInput = [Hurlburt_Rig_B.Age];
% yInput = [Hurlburt_Rig_B.PCI];
% fit_Rig_B_Hurlburt = fit(xInput, yInput,'poly1')
% fit_Ca = coeffvalues(fit_Rig_B_Hurlburt);
% m1a = fit_Ca(1); intercept1 = fit_Ca(2);
% Hurlburt_Rig_B_fit = intercept1 + m1a*X;
% f6 = plot(X,Hurlburt_Rig_B_fit,'g-.'); hold on;
% Hurlburt_Total3 = horzcat(Hurlburt_Total3,Hurlburt_Rig_B_fit');
Hurlburt_Total3 = horzcat(Hurlburt_Total3,zeroTemp);

%Base #6 - Moody
xInput = [Moody_Rig_B.Age];
yInput = [Moody_Rig_B.PCI];
fit_Rig_B_Moody = fit(xInput, yInput,'poly1')
fit_Ca = coeffvalues(fit_Rig_B_Moody);
m1a = fit_Ca(1); intercept1 = fit_Ca(2);
Moody_Rig_B_fit = intercept1 + m1a*X;
f7 = plot(X,Moody_Rig_B_fit,'g:'); hold on;
Moody_Total3 = horzcat(Moody_Total3,Moody_Rig_B_fit');
% Moody_Total3 = horzcat(Moody_Total3,zeroTemp);

%Base #7 - Mountain Home
% xInput = [MtHome_Rig_B.Age];
% yInput = [MtHome_Rig_B.PCI];
% fit_Rig_B_MtHome = fit(xInput, yInput,'poly1')
% fit_Ca = coeffvalues(fit_Rig_B_MtHome);
% m1a = fit_Ca(1); intercept1 = fit_Ca(2);
% MtHome_Rig_B_fit = intercept1 + m1a*X;
% f8 = plot(X,MtHome_Rig_B_fit,'color',[0.8500 0.3250 0.0980],'color',[0.8500 0.3250 0.0980]); hold on;
% MtHome_Total3 = horzcat(MtHome_Total3,MtHome_Rig_B_fit');
MtHome_Total3 = horzcat(MtHome_Total3,zeroTemp);

%Base #8 - Fairchild
xInput = [Fairchild_Rig_B.Age];
yInput = [Fairchild_Rig_B.PCI];
fit_Rig_B_Fairchild = fit(xInput, yInput,'poly1')
fit_Ca = coeffvalues(fit_Rig_B_Fairchild);
m1a = fit_Ca(1); intercept1 = fit_Ca(2);
Fairchild_Rig_B_fit = intercept1 + m1a*X;
f9 = plot(X,Fairchild_Rig_B_fit,'--','color',[0.8500 0.3250 0.0980],'color',[0.8500 0.3250 0.0980]); hold on;
Fairchild_Total3 = horzcat(Fairchild_Total3,Fairchild_Rig_B_fit');
% Fairchild_Total3 = horzcat(Fairchild_Total3,zeroTemp);

%Base #9 - Nellis
% xInput = [Nellis_Rig_B.Age];
% yInput = [Nellis_Rig_B.PCI];
% fit_Rig_B_Nellis = fit(xInput, yInput,'poly1')
% fit_Ca = coeffvalues(fit_Rig_B_Nellis);
% m1a = fit_Ca(1); intercept1 = fit_Ca(2);
```

```
% Nellis_Rig_B_fit = intercept1 + m1a*X;
% f10 = plot(X,Nellis_Rig_B_fit,'-.','color',[0.8500 0.3250 0.0980],'color',[0.8500 0.3250 0.0980]); hold
on;
% Nellis_Total3 = horzcat(Nellis_Total3,Nellis_Rig_B_fit');
Nellis_Total3 = horzcat(Nellis_Total3,zeroTemp);

axis([0 (max(Data_Rig_B.Age)) 50 100]);
title('Rigid Bravo, Aprons');
xlabel('Age'); ylabel('Observed Condition'); grid minor;
legend([f1,f2,f4,f5,f7,f9],{'Weighted Average','Minot','Dover','Seymour
Johnson','Moody','Fairchild'},'Location','southwest');

%% CONTINUE using correct syntax for each family
%and methodology outlined in the notes at the beginning of this script
% repeat for all 6 families (2010). The first two are copied above.


%% Save matricies of Age vs. CI

%WHEN READY, uncomment to create variables for next step

% save('Minot_Total3','Minot_Total3');
% save('MtHome_Total3','MtHome_Total3');
% save('Fairchild_Total3','Fairchild_Total3');
% save('McGuire_Total3','McGuire_Total3');
% save('Dover_Total3','Dover_Total3');
% save('Nellis_Total3','Nellis_Total3');
% save('Hurlburt_Total3','Hurlburt_Total3');
% save('Moody_Total3','Moody_Total3');
% save('SeymourJohn_Total3','SeymourJohn_Total3')
```

```
%TITLE: STEP 2: Create Variables
%INPUT: Run "Cont_Function...v4_3" and have Base_Climate Data.csv files (with Equiv Passes added in)
%NOTE: This file uses dates 2010-2019. Use CreateVar_v2 & Cont_Function...v5 for 1985-2019
%OUTPUT: Base_Data.mat file for the PCA Analysis
%Captain Sarah Brown & Capt Evan Fortney
%Date: 25 Feb 2021
%2010-2019 NEW FAMILIES (Rig A,B,C,D, and Flex A,B,C,D)

clc; clear all; close all; warning off;

%% 1. Load in Dependent Variable - Run "Final_Project_Import_MLR script first

%2010 Import Lines for Pavement Data File
Minot = readtable('Minot_Climate_Traffic Data3.csv', 'HeaderLines',0);
MtHome = readtable('MtHome_Climate_Traffic Data3.csv', 'HeaderLines',0);
Fairchild = readtable('Fairchild_Climate_Traffic Data3.csv', 'HeaderLines',0);
McGuire = readtable('McGuire_Climate_Traffic Data3.csv', 'HeaderLines',0);
Dover = readtable('Dover_Climate_Traffic Data3.csv', 'HeaderLines',0);
SeymourJohn = readtable('SeymourJohn_Climate_Traffic Data3.csv', 'HeaderLines',0);
Nellis = readtable('Nellis_Climate_Traffic Data3.csv', 'HeaderLines',0);
Hurlburt = readtable('Hurlburt_Climate_Traffic Data3.csv', 'HeaderLines',0);
Moody = readtable('Moody_Climate_Traffic Data3.csv', 'HeaderLines',0);

% %1985 Import Lines for Pavement Data File
% GrandForks = readtable('GrandForks_Climate Data.csv', 'HeaderLines',0);
% Minot = readtable('Minot_Climate Data.csv', 'HeaderLines',0);
% MtHome = readtable('MtHome_Climate Data.csv', 'HeaderLines',0);
% Fairchild = readtable('Fairchild_Climate Data.csv', 'HeaderLines',0);
% WrightPatt = readtable('WrightPatterson_Climate Data.csv', 'HeaderLines',0);     %Import Line for
Pavement Data File
% McGuire = readtable('McGuire_Climate Data.csv', 'HeaderLines',0);
% Dover = readtable('Dover_Climate Data.csv', 'HeaderLines',0);
% SeymourJohn = readtable('SeymourJohn_Climate Data.csv', 'HeaderLines',0);
% Luke = readtable('Luke_Climate Data.csv', 'HeaderLines',0);
% Nellis = readtable('Nellis_Climate Data.csv', 'HeaderLines',0);
% Holloman = readtable('Holloman_Climate Data.csv', 'HeaderLines',0);
% MacDill = readtable('MacDill_Climate Data.csv', 'HeaderLines',0);
% Hurlburt = readtable('Hurlburt_Climate Data.csv', 'HeaderLines',0);
% Moody = readtable('Moody_Climate Data.csv', 'HeaderLines',0);

%% For 2010, use below code as is.

%% For 1985,
% 1. remove the '3' from Base_Total
% 2. remove the '4' from Base_Data on the 'save' line
% 3. add the commented bases (there will be 5 extra for 1985)

load Minot_Total3.mat
Minot_Data = table2array(Minot);
Minot_Data = horzcat(Minot_Data, Minot_Total3);
save('Minot_Data4','Minot_Data');

load McGuire_Total3.mat
```

```
McGuire_Data = table2array(McGuire);
McGuire_Data = horzcat(McGuire_Data, McGuire_Total3);
save('McGuire_Data4','McGuire_Data');

load Dover_Total3.mat
Dover_Data = table2array(Dover);
Dover_Data = horzcat(Dover_Data, Dover_Total3);
save('Dover_Data4','Dover_Data');

load SeymourJohn_Total3.mat
SeymourJohn_Data = table2array(SeymourJohn);
SeymourJohn_Data = horzcat(SeymourJohn_Data, SeymourJohn_Total3);
save('SeymourJohn_Data4','SeymourJohn_Data');

load Hurlburt_Total3.mat
Hurlburt_Data = table2array(Hurlburt);
Hurlburt_Data = horzcat(Hurlburt_Data, Hurlburt_Total3);
save('Hurlburt_Data4','Hurlburt_Data');

load Moody_Total3.mat
Moody_Data = table2array(Moody);
Moody_Data = horzcat(Moody_Data, Moody_Total3);
save('Moody_Data4','Moody_Data');

load MtHome_Total3.mat
MtHome_Data = table2array(MtHome);
MtHome_Data = horzcat(MtHome_Data, MtHome_Total3);
save('MtHome_Data4','MtHome_Data');

load Fairchild_Total3.mat
Fairchild_Data = table2array(Fairchild);
Fairchild_Data = horzcat(Fairchild_Data, Fairchild_Total3);
save('Fairchild_Data4','Fairchild_Data');

load Nellis_Total3.mat
Nellis_Data = table2array(Nellis);
Nellis_Data = horzcat(Nellis_Data, Nellis_Total3);
save('Nellis_Data4','Nellis_Data');

%% 1985 only locations
%
% load GrandForks_Total.mat
% GrandForks_Data = table2array(GrandForks);
% GrandForks_Data = horzcat(GrandForks_Data, GrandForks_Total);
% save('GrandForks_Data','GrandForks_Data');
%
% load WrightPatt_Total.mat
% WrightPatt_Data = table2array(WrightPatt);
% WrightPatt_Data = horzcat(WrightPatt_Data, WrightPatt_Total);
% save('WrightPatt_Data','WrightPatt_Data');
%
% load Luke_Total.mat
% Luke_Data = table2array(Luke);
```

```
% Luke_Data = horzcat(Luke_Data, Luke_Total);
% save('Luke_Data','Luke_Data');
%
% load Holloman_Total.mat
% Holloman_Data = table2array(Holloman);
% Holloman_Data = horzcat(Holloman_Data, Holloman_Total);
% save('Holloman_Data','Holloman_Data');
%
% load MacDill_Total.mat
% MacDill_Data = table2array(MacDill);
% MacDill_Data = horzcat(MacDill_Data, MacDill_Total);
% save('MacDill_Data','MacDill_Data');
```

```
%TITLE: STEP 3.a Pavement Principal Component Analysis (PCA)
%with CrossValidation - BOTH Climate and Aircraft Passes
%starting year can be adjusted
%INPUT: Needs to be run using the PCA_Execution Script and be in the same
%file folder as that script and the Base_Data.mat files
%*****NOTE: do NOT run this file directly. See above note.
%OUTPUT: Plots showing bases' model based on number of PCs selected, Scree
%Plot & Heat Map showing PC to IV correlation
%Captain Sarah Brown and Capt Evan Fortney
%Date: 25 Feb 2021
%IMPORTANT: this document should be Saved As:
%Pavement_PCA_crossval_climate_only_2010

%% Set Up Analysis
strcat(Base,'-',pvtFam) %when looking at the command window, it helps
%differentiate when a new family or base is running from the PCA_Execution script

start_year = 2010;  %enter fist year of data (2010 or 1985)

%% NOTE
% To perform CLIMATE ONLY analysis
% ctrl+F CLIMATE ONLY and substitute key phrases from comments

%%ii. Name each variable
Freeze = zscore(basedata(:,2));
Solar = zscore(basedata(:,3));
Wind = zscore(basedata(:,4));
Precip = zscore(basedata(:,5));
Snow = zscore(basedata(:,6));
EquivPasses = zscore(basedata(:,IVa));
%user selects Pavement family type in PCA_Execution.m script

IV = horzcat(Freeze,Solar,Wind,Precip,Snow,EquivPasses)
% For CLIMATE ONLY, use following
% IV = horzcat(Freeze,Solar,Wind,Precip,Snow)

[numobs, numc] = size(basedata);    %Measure the size of the data to use col and row as variables

%Set Dependent Variable (based on which Pavement Family you want
depend = basedata(:,DV);

%Construct Right-hand side variables (detrended IVs) for linear model
rhsvar = horzcat(ones(length(depend),1), Freeze,Solar,Wind,Precip,Snow,EquivPasses);

%% 2. LINEAR MODEL: to build a linear prediction model to predict DV using IVs, directly

betas = inv(rhsvar'*rhsvar)*rhsvar'*depend; %calculate beta coefficients
mod = rhsvar*betas; %calculate y_hat from coefficients and beta coefficients

year = start_year:1:start_year+(numobs-1);  %for plotting automate calculation of x-axis

%% 3. PCA MODEL: to build a linear prediction model to predict DV using ALL vs. first PCs of IVs
```

```
X = IV;

[COEFF,SCORE,latent] = pca(X);
%(*) COEFF = eigenvector, SCORE = PC, latent = eigenvalue
expvar(1:length(COEFF),1) = latent/ sum(latent);
% calculates the variance explained by each PC

%% 3a.  Create a linear model using all PCs
rhsvar2 = horzcat(ones(length(depend),1), SCORE);
betas2 = inv(rhsvar2'*rhsvar2)*rhsvar2'*depend;
mod2 = rhsvar2*betas2;

%% 3b.  Create a linear model using first PC only
rhsvar2a = horzcat(ones(length(depend),1), SCORE(:,[1]));
betas2a = inv(rhsvar2a'*rhsvar2a)*rhsvar2a'*depend;
mod2a = rhsvar2a*betas2a;

%% 4. Cross Validation (drop one year) use IVs as predictor
index = 1:numobs;
for i = 1:numobs
   ind = index~=i;
   dependt=depend(ind);       % drop one year of depend
   rhsvart=rhsvar(ind,:);     % drop one year of rhsvar
   betascv(:,i) = inv(rhsvart'*rhsvart)*rhsvart'*dependt;
   % find betas after dropping the year
   modcv(i) = rhsvar(i,:)*betascv(:,i);  % crossvalidated model
end

figure1 = figure('color', [1,1,1]);
plot(year,modcv,year,depend,'r');  % plot forecast and Cont. Function
xlim([start_year start_year+(numobs-1) ])
xlabel('Years')
ylabel('Asset Condition')
title({[Base,' - ',pvtFam],['ALL directly as Predictors, Drop-one-year Cross Validation']})
legend('Model','Cont. Function');

r2_cv_linear = corr(modcv',depend)^2;

str=['r^2 = ',num2str(r2_cv_linear)];
xt = 2012;  %x-axis starting point for equation caption
yt = 99; %y-axis starting point for equation caption
text(xt, yt, str, 'FontSize', 14, 'Color', 'k', 'FontWeight', 'bold');
hold off

close(figure1) %used so that the maximum number of figures is NOT reached
%when executing all family-location pairs

%% 5. Cross Validatation (drop one year) use N PCs as predictor(s)
index = 1:numobs;
betascv_pca = zeros(numc,numobs);
betastrack=[];
```

```
for i = 1:numobs
   ind = index~=i;
   dependtp=depend(ind);% drop one year of depend, temp variable for pca
   X = horzcat(Freeze,Solar,Wind,Precip,Snow,EquivPasses);
   % For CLIMATE ONLY, use following
   % X = horzcat(Freeze,Solar,Wind,Precip,Snow);
   [COEFFtp,SCOREtp,latenttp] = pca(X(ind,:));
   % (*) COEFF = EOF/eigenvector, SCORE = PC, latent = eigenvalue
   expvartp(1:length(COEFFtp),1) = latenttp/ sum(latenttp);
   expvartp_track(:,i) = expvartp;
%% PC Retention

%Starting point
pcn=0;

% Joffille's Rule (1972): if PC explains at least 70% of mean variance explained by all PCs
   for j=1:length(latent);
      if latent(j,1)>=0.7*(mean(latent))
         pcn=pcn+1;
      else
         pcn=pcn+0;
      end
   end %pcn: number of pc selected

% find the beta coefficient based on the number of pc selected
   rhsvartp = horzcat(ones(length(dependtp),1), SCOREtp(:,[1:pcn]));
   betascv_pca(1:(1+pcn),i) = inv(rhsvartp'*rhsvartp)*rhsvartp'*dependtp;
   % find beta after dropping the year, keep track of betas
   betascvtp = inv(rhsvartp'*rhsvartp)*rhsvartp'*dependtp;
   % temporary variable for PCA
   % find the appropriate PC for target/dropped year for prediction
   % the process is (1) find the detrended predictor variables of drop yr
   % by subtracting column means (means of all vars over non-dropped yrs)
   detrendtp = X(i,:)-mean(X(ind,:));
   % (2)multiply by the eigenvectors from the PCA filling period (*)
   PCtp = detrendtp*COEFFtp;
   % find all the PCs for dropped year (1x4)
   rhsvarPC = horzcat(1, PCtp(1:pcn));
   modcv_pca(i) = rhsvarPC*betascvtp;
end

%Comparison of forecast to Cont. Function data
figure2 = figure('color', [1,1,1])
subplot(2,1,1);
plot(year,modcv_pca,year,depend,'r');
xlim([start_year start_year+(numobs-1) ])
xlabel('Years')
ylabel('Asset Condition')
title({[Base,' - ',pvtFam],['Rule-based n = ',num2str(pcn),' PC(s) as Predictors'],['Drop-one-year Cross
Validation'],['Raw Model Output']})
legend('Model','Cont. Function','Location','southeast');
axis([2010 2019 70 100]);
r2_cv_pca = corr(modcv_pca',depend)^2;
```

```
str=['r^2 = ',num2str(r2_cv_pca)];
xt = 2011;  %x-axis starting point for equation caption
yt = 75; %y-axis starting point for equation caption
text(xt, yt, str, 'FontSize', 14, 'Color', 'k', 'FontWeight', 'bold');
% str2 = lm_PCA.NumObservations;
% yt2 = 82.5; %y-axis starting point for NumObs caption
% text(xt, yt2, str2, 'FontSize', 14, 'Color', 'k', 'FontWeight', 'bold');
hold on

%UNCOMMENT to save the model and DV outputs as files for figure making
% %Set the FileName to the Current Base/Pvt Family Type
% fileName1 = strcat(Base,'-',pvtFam,'_modelboth2010');
% fileName2 = strcat(Base,'-',pvtFam,'_DVboth2010');
%
% save(fileName1,'modcv_pca'); %save the model data
% save(fileName2,'depend'); %save the continuous function data

%% Comparison of NON INCREASING forecast to Cont. Function data

% If you don't want any post processing, comment the rest of this section
% If you don't want to force the intercept through (0,100),comment
modcv_pca(1)= 100;

slopes1 = [];
for i = 1:numobs-1;
   if (i < numobs);
      slope = modcv_pca(i+1) - modcv_pca(i);
   end
   slopes1 = horzcat(slopes1,slope);
end

slopes2 = [];
for i = 1:numobs-1;
   if (i < numobs);
      if (modcv_pca(i+1) > modcv_pca(i));
         modcv_pca(i+1)= modcv_pca(i);
      end
      slope = modcv_pca(i+1) - modcv_pca(i);
   end
   slopes2 = horzcat(slopes2,slope);
end

% figure('color', [1,1,1]) % only use when testing code line by line.
% Otherwise, this plot won't appear due to earlier subplot

% subplot(2,1,2); % by commenting, both lines will appear on 1 plot and
% display the difference through 'post processing'
plot(year,modcv_pca,year,depend,'r');
xlim([start_year start_year+(numobs-1) ]);
xlabel('Years');
ylabel('Asset Condition');
title({['Post-Processed']});
% when 'subplot(2,1,2) is commented, use this
```

```
% legend('Model','Cont. Function','Location','southeast');
legend('Raw Model','Cont. Function','Adjusted Model','Location','southeast');
axis([2010 2019 70 100]);
r2_cv_pca = corr(modcv_pca',depend)^2;
str=['adj r^2= ',num2str(r2_cv_pca)];
xt = 2014;  %x-axis starting point for equation caption
yt = 75; %y-axis starting point for equation caption
text(xt, yt, str, 'FontSize', 14, 'Color', 'k', 'FontWeight', 'bold');
% str2 = lm_PCA.NumObservations;
% yt2 = 82.5; %y-axis starting point for NumObs caption
% text(xt, yt2, str2, 'FontSize', 14, 'Color', 'k', 'FontWeight', 'bold');
hold off

% use when you just want to output HEAT plots
% close (figure2)

%UNCOMMENT to save the model and DV outputs as files for figure making
% %Set the FileName to the Current Base/Pvt Family Type
% fileName3 = strcat(Base,'-',pvtFam,'_NEGATIVEboth2010')
% save(fileName3,'modcv_pca'); %save the NON INCREASING model data



%% 6. Create a simple diagnostic linear model
fprintf([Base,' Linear Regression with PCs:'])
lm_PCA = fitlm((SCORE(:,1:pcn)),depend)
% Create a final linear model based based on the number of PCs retained

r2_lm_selected_pc = corr(depend,lm_PCA.Fitted);
RMSE = lm_PCA.RMSE;
% Obs = lm_PCA.NumObservations;
pVal = coefTest(lm_PCA) %model significance
pVal1 = lm_PCA.Coefficients.pValue(2); %significance of each principal component retained
pVal2 = lm_PCA.Coefficients.pValue(3);
try
pVal3 = lm_PCA.Coefficients.pValue(4); %if only 2 PCs retained, this will stop pVal3 from error
catch
   pVal3 = NaN;
end
try
pVal4 = lm_PCA.Coefficients.pValue(5); %if only 3 PCs retained, this will stop pVal4 from error
catch
   pVal4 = NaN;
end
pValVar = [pVal pVal1 pVal2 pVal3 pVal4];

% Scree Plot
figure('color', [1,1,1])
subplot(1,2,1)
plot(expvar,'-x')
xlabel('PCs')
ylabel('Variance Explained (%)')
xlim([1 size(IV,2)])
%title({[Base,' - ',pvtFam],['Scree Plot of PCs']})
```

```
title({[Base],['Scree Plot of PCs']})
xticks([1 2 3 4 5 6])
% For CLIMATE ONLY, use following
% xticks([1 2 3 4 5])
hold on

back_corr = corr(SCORE,IV);            % Cross correlation
yvalues = {'Freeze','Solar','Wind','Precip','Snow','EquivPasses'};
xvalues = {'PC 1','PC 2','PC 3','PC 4','PC 5','PC 6'};

% For CLIMATE ONLY, use following
% yvalues = {'Freeze','Solar','Wind','Precip','Snow'};
% xvalues = {'PC 1','PC 2','PC 3','PC 4','PC 5'};


% Heatmap of cross correlation
subplot(1,2,2)
heatmap(xvalues,yvalues,back_corr);
colormap('Autumn')
%title({[Base,' - ',pvtFam],['Heat Map Showing PC Correlation to IVs']})
title({[Base],['Heat Map Showing PC Correlation to IVs']})

%highlight the top 2 variables from each PC that was retained
important = abs(back_corr(:,1:pcn));
[m,i] = maxk(important,2);
[i_val, ~, ind_i_val] = unique(i);
i_valnew = ['Freeze';'*     ';'Wind  ';'Precip';'Snow  ';'Traff '];
% For CLIMATE ONLY, use following
% i_valnew = ['Freeze';'*     ';'Wind  ';'Precip';'Snow  ']; %change for traffic variables

% * = solar irradiance
% Traff = Equivalent Passes
i_new = i_valnew(ind_i_val);
i_new = reshape(i_new,size(i));

yvalues2 = {'Most Important','Second Most'};

%create tables showing important
if isnan(pVal4) == 1;
   if isnan(pVal3) == 1;
      if isnan(pVal2) == 1;
         if isnan(pVal1) == 1;
            disp('No Table');
         else
         T = array2table(i_new,'RowNames',{'Most Important','Second Most'},'VariableNames',{'PC1'});
         end
      else
         T = array2table(i_new,'RowNames',{'Most Important','Second
Most'},'VariableNames',{'PC1','PC2'});
      end
   else
   T = array2table(i_new,'RowNames',{'Most Important','Second
Most'},'VariableNames',{'PC1','PC2','PC3'});
```

```
    end
else
    T = array2table(i_new,'RowNames',{'Most Important','Second
Most'},'VariableNames',{'PC1','PC2','PC3','PC4'});
end

%determine if model and each variable is significant at ALPHA level
% alpha = 0.25 % added alpha to the PCA_Execution Script
if pVal > alpha;
    T.ModelSig = [0;0];
elseif pVal <= alpha;
    T.ModelSig = [1;1];
elseif isnan(pVal) == 1;
    T.ModelSig = [0;0];
end
if pVal1 >alpha;
    T.Sig1 = [0;0];
elseif pVal1 <= alpha;
    T.Sig1 = [1;1];
elseif isnan(pVal1) == 1;
    T.Sig1 = [0;0];
end
if pVal2 > alpha;
    T.Sig2 = [0;0];
elseif pVal2 <= alpha;
    T.Sig2 = [1;1];
elseif isnan(pVal2) == 1;
    T.Sig2 = [0;0];
end
if pVal3 >alpha;
    T.Sig3 = [0;0];
elseif pVal3 <= alpha;
    T.Sig3 = [1;1];
elseif isnan(pVal3) == 1;
    T.Sig3 = [0;0];
end
if pVal4 >alpha;
    T.Sig4 = [0;0];
elseif pVal4 <= alpha;
    T.Sig4 = [1;1];
elseif isnan(pVal4) == 1;
    T.Sig4 = [0;0];
end
T % displays the Table of significant variables in the command window
Coefficients = lm_PCA.Coefficients(:,1);
```

```
%TITLE: STEP 3.b PCA Execution Across Bases -
%CLIMATE VARIABLES ONLY (NOTE 3 shows how to perform both
%climate and aircraft passes)
%INPUT: Must be in same file folder as Base_Data.mat files &
%Pavement_PCA_crossval_climate_only_2010.m &
%Pavement_PCA_crossval_climate_only_v2.m scripts
%OUTPUT: Plot showing bases' model based on number of PCs selected, Scree
%Plot & Heat Map showing PC to IV correlation
%Captain Sarah Brown & Captain Evan Fortney
%Date: 25 Feb 2021
%2010-2019 analysis, Families (Rig A,B,C,D, and Flex A,B,C,D)
%1985-2019 analysis, Families
%%
clc; clear all; close all; warning off;

%% DIRECTIONS:
%(1) To test all pavement families at selected locations, comment out the
%bases you don't want. Be sure to edit the "R2_All" and "RMSE_All" to
%include the bases that aren't commented.

%(2) To test certain pavement families, change the initial "q" to just the
%selected family. The list of families is shown at the beginning of the loop

%% 2010-2019 FAMILIES
%DV = 18: Rigid Alpha, Primary Taxiways and Runway Ends
%DV = 19: Rigid Bravo, Aprons
%DV = 20: Rigid Charlie, Secondary Taxiways and Runway Interiors
%DOES NOT EXIST: Rigid Delta, Overruns/Shoulders
%DV = 21: Flexible Alpha, Primary Taxiways and Runway Ends
%DOES NOT EXIST: Flexible Bravo, Aprons
%DV = 22: Flexible Charlie, Secondary Taxiways and Runway Interiors
%DV = 23: Flexible Delta, Overruns/Shoulders

%% 1985-2010 FAMILIES
% DV = 22;   %Family #1: RIGID - PRIMARY - TAXIWAYS/APRONS
% DV = 23;  %Family #2: RIGID - PRIMARY - RUNWAYS
% DV = 24;  %Family #3: RIGID - SEC/TER - TAXIWAYS/APRONS
% DV = 25;  %Family #4: FLEXI - PRIMARY - TAXIWAYS/APRONS
% DV = 26;  %Family #5: FLEXI - PRIMARY - RUNWAYS
% DV = 27;  %Family #6: FLEXI - SEC/TER - OVERRUNS/SHOULDERS
% DV = 28;  %Family #7: FLEXI - SEC/TER - TAXIWAYS/APRONS

%% NOTE 1, 2010
%IVa is only used for the traffic analysis and refers to the Equivalent
%Passes column in the Base_Data file.
%% NOTE 2, 2010
%Even though the 6 valid families are represented in DV = 18 thru 23, the
%corresponding raw EquivPasses data is in a different order. You probably
%don't need to worry about it, but when calculating the different families,
%at one point the order was Rig A, Flex A, Rig B, Flex B... etc. Then I
%changed it to Rig A, Rig B, Rig C, Rig D, Flex A... etc. That is why the
%numbering is off between the DV and the IVa in the Base_Data.m files
%% NOTE 3, 2010
```

```
%To execute BOTH climate and traffic 2010, replace the following:
%Pavement_PCA_crossval_climate_only_2010 with
%Pavement_PCA_crossval_v2
%For each location in the for loop, below
%% NOTE 4, 1985
%There are no traffic pass data for 1985 analysis, ONLY climate
%Several extra installations (14 total) are included for 1985.
%There are only 9 installations for 2010 analysis

R2_All = [];
RMSE_All = [];

alpha = 0.25 %set this to whatever you want to test

for q = [18:23]
   % to test all 2010-2019 families, use q = [18:23]. For one family, just use q = [18], etc.
   % to test all 1985-2019 families, use q = [22:28].
   % for one family, just use q = [18], etc.
   DV = q
   %2010 analysis
   if(DV == 18)
      pvtFam = 'RIG A';
   elseif(DV == 19)
      pvtFam = 'RIG B';
   elseif(DV == 20)
      pvtFam = 'RIG C';
   elseif(DV == 21)
      pvtFam = 'FLEX A';
   elseif(DV == 22)
      pvtFam = 'FLEX C';
   elseif(DV == 23)
      pvtFam = 'FLEX D';
   end

k = q - 17;

%    %1985 analysis
%    if(DV == 22)
%       pvtFam = 'RIGID - PRIMARY - TAXIWAYS & APRONS';
%    elseif(DV == 23)
%       pvtFam = 'RIGID - PRIMARY - RUNWAYS';
%    elseif(DV == 24)
%       pvtFam = 'RIGID - SEC-TER - TAXIWAYS & APRONS';
%    elseif(DV == 25)
%       pvtFam = 'FLEXI - PRIMARY - TAXIWAYS & APRONS';
%    elseif(DV == 26)
%       pvtFam = 'FLEXI - PRIMARY - RUNWAYS';
%    elseif(DV == 27)
%       pvtFam = 'FLEXI - SEC-TER - OVERRUNS & SHOULDERS';
%    elseif(DV == 28)
%       pvtFam = 'FLEXI - SEC-TER - TAXIWAYS& APRONS';
%    end
% k = q - 21;
```

```
% close all

%Base #1: Minot
load Minot_Data4.mat
basedata = Minot_Data;
Base = 'Minot';
Pavement_PCA_crossval_climate_only_2010
%Pavement_PCA_crossval_climate_only_v2
%Use for 1985 Analysis
Coeff_Minot = Coefficients;
RMSE_Minot = RMSE;
R2_Minot = r2_cv_pca;
pVal_Minot = pVal;
% obs_Minot = Obs;

%Base #2: McGuire
load McGuire_Data4.mat
basedata = McGuire_Data;
Base = 'McGuire';
Pavement_PCA_crossval_climate_only_2010
%Pavement_PCA_crossval_climate_only_v2
%Use for 1985 Analysis
Coeff_McGuire = Coefficients;
RMSE_McGuire = RMSE;
R2_McGuire = r2_cv_pca;
pVal_McGuire = pVal;
% obs_McGuire = Obs;

%Base #3: Dover
load Dover_Data4.mat
basedata = Dover_Data;
Base = 'Dover';
Pavement_PCA_crossval_climate_only_2010
%Pavement_PCA_crossval_climate_only_v2
%Use for 1985 Analysis
Coeff_Dover = Coefficients;
RMSE_Dover = RMSE;
R2_Dover = r2_cv_pca;
pVal_Dover = pVal;
% obs_Dover = Obs;

%Base #4: Seymour Johnson
load SeymourJohn_Data4.mat
basedata = SeymourJohn_Data;
Base = 'Seymour Johnson';
Pavement_PCA_crossval_climate_only_2010
%Pavement_PCA_crossval_climate_only_v2
%Use for 1985 Analysis
Coeff_SeymourJohn = Coefficients;
RMSE_SeymourJohn = RMSE;
R2_SeymourJohn = r2_cv_pca;
pVal_SeymourJohn = pVal;
% obs_SeymourJohn = Obs;

%Base #5: Hurlburt
load Hurlburt_Data4.mat
basedata = Hurlburt_Data;
Base = 'Hurlburt';
Pavement_PCA_crossval_climate_only_2010
%Pavement_PCA_crossval_climate_only_v2
%Use for 1985 Analysis
Coeff_Hurlburt = Coefficients;
RMSE_Hurlburt = RMSE;
R2_Hurlburt = r2_cv_pca;
pVal_Hurlburt = pVal;
% obs_Hurlburt = Obs;

%Base #6: Moody
load Moody_Data4.mat
basedata = Moody_Data;
Base = 'Moody';
Pavement_PCA_crossval_climate_only_2010
%Pavement_PCA_crossval_climate_only_v2
%Use for 1985 Analysis
Coeff_Moody = Coefficients;
RMSE_Moody = RMSE;
R2_Moody = r2_cv_pca;
pVal_Moody = pVal;
% obs_Moody = Obs;

%Base #7: Mt Home
load MtHome_Data4.mat
basedata = MtHome_Data;
Base = 'Mt Home';
Pavement_PCA_crossval_climate_only_2010
%Pavement_PCA_crossval_climate_only_v2
%Use for 1985 Analysis
Coeff_MtHome = Coefficients;
RMSE_MtHome = RMSE;
R2_MtHome = r2_cv_pca;
pVal_MtHome = pVal;
% obs_MtHome = Obs;

%Base #8: Fairchild
load Fairchild_Data4.mat
basedata = Fairchild_Data;
Base = 'Fairchild';
Pavement_PCA_crossval_climate_only_2010
%Pavement_PCA_crossval_climate_only_v2
%Use for 1985 Analysis
Coeff_Fairchild = Coefficients;
RMSE_Fairchild = RMSE;
```

```
R2_Fairchild = r2_cv_pca;
pVal_Fairchild = pVal;
% obs_Fairchild = Obs;

%Base #9: Nellis
load Nellis_Data4.mat
basedata = Nellis_Data;
Base = 'Nellis';
Pavement_PCA_crossval_climate_only_2010
%Pavement_PCA_crossval_climate_only_v2
%Use for 1985 Analysis
Coeff_Nellis = Coefficients;
RMSE_Nellis = RMSE;
R2_Nellis = r2_cv_pca;
pVal_Nellis = pVal;
% obs_Nellis = Obs;

%% ONLY use the following 5 installations for 1985 analysis
% %Base #10: Grand Forks
% load GrandForks_Data.mat
% basedata = GrandForks_Data;
% Base = 'Grand Forks';
% Pavement_PCA_crossval_climate_only_v2
% Coeff_GrandForks = Coefficients;
% RMSE_GrandForks = RMSE;
% R2_GrandForks = r2_cv_pca;
%
% %Base #11: Wright Patterson
% load WrightPatt_Data.mat
% basedata = WrightPatt_Data;
% Base = 'Wright Patterson';
% Pavement_PCA_crossval_climate_only_v2
% Coeff_WrightPatt = Coefficients;
% RMSE_WrightPatt = RMSE;
% R2_WrightPatt = r2_cv_pca;
%
% %Base #12: Luke
% load Luke_Data.mat
% basedata = Luke_Data;
% Base = 'Luke';
% Pavement_PCA_crossval_climate_only_v2
% Coeff_Luke = Coefficients;
% RMSE_Luke = RMSE;
% R2_Luke = r2_cv_pca;
%
% %Base #13: Holloman
% load Holloman_Data.mat
% basedata = Holloman_Data;
% Base = 'Holloman';
% Pavement_PCA_crossval_climate_only_v2
% Coeff_Holloman = Coefficients;
% RMSE_Holloman = RMSE;
% R2_Holloman = r2_cv_pca;
%
% %Base #14: MacDill
% load MacDill_Data.mat
% basedata = MacDill_Data;
% Base = 'MacDill';
% Pavement_PCA_crossval_climate_only_v2
% Coeff_MacDill = Coefficients;
% RMSE_MacDill = RMSE;
% R2_MacDill = r2_cv_pca;

%% Outputs

% % Testing ONLY ONE BASE, any number of families
% R2_All(k) = (R2_Fairchild)
% RMSE_All(k) = (R2_Fairchild)

% % Testing 4 (or any number of) select locations
% R2_All(:,k) = [R2_Fairchild; R2_Dover; R2_Moody; R2_MtHome];
% RMSE_All(:,k)= [RMSE_Fairchild; RMSE_Dover; RMSE_Moody; RMSE_MtHome];

% Use this when running ALL, 2010 Analysis
R2_All(:,k) = [R2_Minot; R2_McGuire; R2_Dover; R2_SeymourJohn; R2_Hurlburt; R2_Moody;
R2_MtHome; R2_Fairchild; R2_Nellis];
RMSE_All(:,k)= [RMSE_Minot; RMSE_McGuire; RMSE_Dover; RMSE_SeymourJohn;
RMSE_Hurlburt; RMSE_Moody; RMSE_MtHome; RMSE_Fairchild; RMSE_Nellis];
pVal_All(:,k)= [pVal_Minot; pVal_McGuire; pVal_Dover; pVal_SeymourJohn; pVal_Hurlburt;
pVal_Moody; pVal_MtHome; pVal_Fairchild; pVal_Nellis];
% % TEST_All(:,k)= [TEST_Minot; TEST_McGuire; TEST_Dover; TEST_SeymourJohn;
TEST_Hurlburt; TEST_Moody; TEST_MtHome; TEST_Fairchild; TEST_Nellis];
```

```
% Use this when running ALL, 1985 Analysis
% R2_All(:,k) = [R2_Minot; R2_McGuire; R2_Dover; R2_SeymourJohn; R2_Hurlburt; R2_Moody;
R2_MtHome; R2_Fairchild; R2_Nellis; R2_GrandForks; R2_WrightPatt; R2_Luke; R2_Holloman;
R2_MacDill];
% RMSE_All(:,k)= [RMSE_Minot; RMSE_McGuire; RMSE_Dover; RMSE_SeymourJohn;
RMSE_Hurlburt; RMSE_Moody; RMSE_MtHome; RMSE_Fairchild; RMSE_Nellis; RMSE_GrandForks;
RMSE_WrightPatt; RMSE_Luke; RMSE_Holloman; RMSE_MacDill];
% pVal_All(:,k)= [pVal_Minot; pVal_McGuire; pVal_Dover; pVal_SeymourJohn; pVal_Hurlburt;
pVal_Moody; pVal_MtHome; pVal_Fairchild; pVal_Nellis; pVal_GrandForks; pVal_WrightPatt;
pVal_Luke; pVal_Holloman; pVal_MacDill];

% close all
end

%% Saving Variables
%Only use if interested to process data separately/later

% save('2010v2_2019_ClimateOnly_ %BASE% _TABLE signficant variables','T');

%make sure the name of the documents matches the "R2_All" variable above
%When READY, uncomment, edit names, and save variables
% save('R2_All_Climate2010v2', 'R2_All_Climate2010v2');
% save('RMSE_All_Climate2010v2', 'RMSE_All_Climate2010v2');
% writematrix(R2_All_Climate2010v2,'R2_ClimateOnly_2010v2.csv')
% writematrix(RMSE_All_Climate2010v2,'RMSE_ClimateOnly_2010v2.csv')
```

References

Abdi, H., and Williams, L. J. (2010). "Principal component analysis." *WIREs Computational Statistics*, 2(4), 433–459.

Adolf, M. (2010). "PCASE 2.09 User Manual." US Army Corps of Engineers, Transportation Systems Center and Engineering Research and Development Center.

AFI 32-1041. (2019). "Air Force Instruction 32-1041. Civil Engineering Pavement Evaluation Program. Department of the Air Force."

Allen, J. P., and Albert, B. C. (2014). *Sustainable Transportation: Strategy for Security, Prosperity, and Peace*. US Army War College.

Ameri, M., Mansourian, A., Heidary Khavas, M., Aliha, M. R. M., and Ayatollahi, M. R. (2011). "Cracked asphalt pavement under traffic loading – A 3D finite element analysis." *Engineering Fracture Mechanics*, Multiaxial Fracture, 78(8), 1817–1826.

American Society for Testing and Materials. (2012). "Standard Test Method for Airport Pavement Condition Index Surveys. American Society for Testing and Materials International, Report D5340-12."

Ankit, G., Kumar, P., and Rastogi, R. (2011). "Effect of Environmental Factors on Flexible Pavement Performance Modeling."

Bennett, M. (2019). "Factors Affecting Airfield Pavement Performance in the United States Air Force Enterprise Wide." Master of Science, The Pennsylvania State University.

Castillo, D., Gamez, A., and Al-Qadi, I. (2019). "Homogeneous versus Heterogeneous Response of a Flexible Pavement Structure: Strain and Domain Analyses." *Journal of Engineering Mechanics*, American Society of Civil Engineers, 145(9), 04019068.

Chih-Yuan, C., and Durango-Cohen, P. L. (2008). "Empirical Comparison of Statistical Pavement Performance Models." *Journal of Infrastructure Systems*, 14(2), 138–149.

Chinowsky, P. S., Price, J. C., and Neumann, J. E. (2013). "Assessment of climate change adaptation costs for the U.S. road network." *Global Environmental Change*, 23(4), 764–773.

Colorado State University. (2019). "About PAVER™." <http://PAVER™.coloradostate.edu> (Mar. 12, 2020).

Delorit, J. D., Schuldt, S. J., and Chini, C. M. (2020). "Evaluating an Adaptive Management Strategy for Organizational Energy Use Under Climate Uncertainty." *Energy Policy*, 142(111547).

Delorit, J., Gonzalez Ortuya, E. C., and Block, P. (2017). "Evaluation of model-based seasonal streamflow and water allocation forecasts for the Elqui Valley, Chile." *Hydrol. Earth Syst. Sci.*, 21(9), 4711–4725.

Evans, J. D. (1996). *Straightforward statistics for the behavioral sciences*. Straightforward statistics for the behavioral sciences, Thomson Brooks/Cole Publishing Co, Belmont, CA, US, xxii, 600.

Federal Aviation Administration. (2014). *Airport Pavement Management Program (PMP), Advisory Circular (AC)*. U.S. Department of Transportation.
Frangopol, D. M., Jung S. Kong, and Emhaidy S. Gharaibeh. (2001). "Reliability-Based Life-Cycle Management of Highway Bridges | Journal of Computing in Civil Engineering | Vol 15, No 1." *Journal of Computing in Civil Engineering*, 15(1).
Gendreau, M., and Soriano, P. (1998). "Airport pavement management systems: an appraisal of existing methodologies." *Transportation Research Part A: Policy and Practice*, 32(3), 197–214.
Greene, J., Shahin, M. Y., and Alexander, D. R. (2004). "Airfield Pavement Condition Assessment." *Transportation Research Record*, 1889(1), 63–70.
Haas, R. (2001a). "Reinventing the (Pavement Management) Wheel." Seattle, Washington.
Harvey, J. T., Meijer, J., Ozer, H., Al-Quadi, I. L., Saboori, A., and Kendall, A. (2016). *Pavement Life Cycle Assessment Framework*. U.S. Department of Transportation, Federal Highway Administration, 244.
Heymsfield, E., and Tingle, J. S. (2019). "State of the practice in pavement structural design/analysis codes relevant to airfield pavement design." *Engineering Failure Analysis*, 105, 12–24.
Ismail, N., Ismail, A., and Atiq, R. (2009). "An Overview of Expert Systems in Pavement Management." *European Journal of Scientific Research*, 30(1), 99–111.
Jolliffe, I. T. (Ed.). (2002). "Choosing a Subset of Principal Components or Variables." *Principal Component Analysis*, Springer Series in Statistics, Springer, New York, NY, 111–149.
Kemeny, V. (2018). "AFCEC's Airfield Pavement Evaluation Team wins One Air Force Award." *U.S. Air Force*.
Kjellstrom, T., Freyberg, C., Lemke, B., Otto, M., and Briggs, D. (2018). "Estimating population heat exposure and impacts on working people in conjunction with climate change." *International Journal of Biometeorology*, 62(3), 291–306.
Knost, B., and Mishalani, R. (2019). "Modeling the Accuracy of Airfield Pavement Deterioration Forecasts." NYU Abu Dhabi, Abu Dhabi.
Meihaus, J. C. (2013). "Understanding the Effects of Climate on Airfield Pavement Deterioration Rates." AIR FORCE INSTITUTE OF TECHNOLOGY WRIGHT-PATTERSON AFB OH GRADUATE SCHOOL OF ENGINEERING AND MANAGEMENT.
Múčka, P. (2016). "International Roughness Index Specifications around the World." *Road Materials and Pavement Design*.
Mulry, B., Jordan, M., and O'Brien, D. (2015). "Automated Pavement Condition Assessment Using Laser Crack Measurement System (LCMS) on Airfield Pavements in Ireland."
Parsons, T. A., and Pullen, B. A. (2016). "Relationship between Climate Type and Observed Pavement Distresses."
Parsons, T. A., and Pullen, B. A. (2017). "Characterization of Pavement Condition Index Deterioration Curve Shape for USAF Airfield Pavements."
Sahagun, L. K., Karakouzian, M., Paz, A., and Fuente-Mella, H. de la. (2017). "An Investigation of Geography and Climate Induced Distresses Patterns on Airfield

Pavements at US Air Force Installations." *Mathematical Problems in Engineering*, 2017.
Sawant, V. (2009). "Dynamic Analysis of Rigid Pavement with Vehicle-Pavement Interaction." *International Journal of Pavement Engineering*, 10(1), 63–72.
Seiler, W. J., Darter, M. I., and Garrett, J. H. (1991). "An Airfield Pavement Consultant System (AIRPACS) for Rehabilitation of Concrete Pavements." ASCE, 332–353.
Shafabakhsh, G. A., and Kashi, E. (2015). "Effect of Aircraft Wheel Load and Configuration on Runway Damages." *Periodica Polytechnica Civil Engineering*, 59(1), 85–94.
Shahin, M. Y. (1994). "Analyzing Consequences of Pavement Maintenance and Rehabilitation Budget Scenarios." *Transportation Research Record*, (1455).
Shahin, M. Y. (2005). *Pavement Management for Airports, Roads, and Parking Lots*. Springer, NY, USA.
Shahin, M. Y., Nunez, M. M., Broten, M. R., Carpenter, S. H., and Sameh, A. (1987). "New Techniques for Modeling Pavement Deterioration." *Transportation Research Record*, (1123), 40–46.
Shahin, M. Y., and Rozanski, F. M. (1978). "Development of a computerized system for pavement maintenance management." *Transportation Research Record*, 674.
Sidess, A., Ravina, A., and Oged, E. (2020). "A model for predicting the deterioration of the pavement condition index." *International Journal of Pavement Engineering*, Taylor & Francis, 0(0), 1–12.
Taylor, M. A. P., and Philp, M. L. (2015). "Investigating the impact of maintenance regimes on the design life of road pavements in a changing climate and the implications for transport policy - ScienceDirect." *Transport Policy*, 41, 117–135.
US DoD. (2001a). "UFC 3-260-02 Pavement Design for Airfields." 538.
US DoD. (2001b). "UFC 3-260-03 Airfield Pavement Design." 271.
van Vuuren, D. P., Edmonds, J., and Kainuma, M. (2011). "The representative concentration pathways: an overview." *Climatic Change*, 109(5).
Wang, H., and Al-Qadi, I. L. (2011). "Impact of non-uniform aircraft tire pressure on airfield pavement responses." First Congress of Transportation and Development Institute, Chicago, Illinois, United States.
White, T. D., Zaghloul, S. M., Anderton, G. L., and Smith, D. M. (1997). "Pavement Analysis for Moving Aircraft Load." *Journal of Transporation Engineering*, 123(6), 436–446.

REPORT DOCUMENTATION PAGE

Form Approved
OMB No. 074-0188

PLEASE DO NOT RETURN YOUR FORM TO THE ABOVE ADDRESS.

1. REPORT DATE *(DD-MM-YYYY)*	2. REPORT TYPE	3. DATES COVERED *(From – To)*
25-03-2021	Master's Thesis	Sept 2019 – March 2021

TITLE AND SUBTITLE

Improving Airfield Pavement Degradation Prediction Skill with Local Climate and Traffic

5a. CONTRACT NUMBER

5b. GRANT NUMBER

5c. PROGRAM ELEMENT NUMBER

6. AUTHOR(S)

Fortney, Evan M., Captain, USAF

5d. PROJECT NUMBER

5e. TASK NUMBER

5f. WORK UNIT NUMBER

7. PERFORMING ORGANIZATION NAMES(S) AND ADDRESS(S)

Air Force Institute of Technology
Graduate School of Engineering and Management (AFIT/ENV)
2950 Hobson Way, Building 640
WPAFB OH 45433-8865

8. PERFORMING ORGANIZATION REPORT NUMBER

AFIT-ENV-MS-21-228

9. SPONSORING/MONITORING AGENCY NAME(S) AND ADDRESS(ES)

Air Force Civil Engineer Center (AFCEC/DS) - Mr. John (Dale) Clark
2261 Hughes Ave
JBSA Lackland, TX 78236-9853
john.clark.7@us.af.mil

10. SPONSOR/MONITOR'S ACRONYM(S)

AFCEC

11. SPONSOR/MONITOR'S REPORT NUMBER(S)

12. DISTRIBUTION/AVAILABILITY STATEMENT

DISTRUBTION STATEMENT A. APPROVED FOR PUBLIC RELEASE; DISTRIBUTION UNLIMITED.

13. SUPPLEMENTARY NOTES

14. ABSTRACT

Airfield pavements are a critical component of the global transportation network that provide a platform for national defense. Preventative and corrective maintenance activities are founded upon accurate expectations of degradation. The leading pavement management software creates degradation predictions from pavement groups using age as the IV and current state conditions as the DV. For this work, a framework is created and implemented that utilizes a PCR model to build upon accepted practices for degradation modeling to enhance and possibly augment future prediction capabilities. The model was applied to pairs of location and pavement family and reveals several findings: the selected climatic variables describe 74-93% of pavement degradation across 1,995 pavement sections constructed between 1985-2019; the effects from climatic factors are nonstationary; and environmental factors are more impactful than aircraft passes, with between 2-15% improvement of model skill in the pavement family that supports the most aircraft operations when comparing two datasets of 266 pavement sections between 2010-2019. The created framework discovered that freeze-thaw, solar irradiance, precipitation, and sustained wind were commonly significant factors in describing degradation variability and can be applied to any large airport with data availability to determine local sources of degradation and improve pavement design sustainability.

15. SUBJECT TERMS

Pavement Degradation, Degradation Prediction, Principal Component Regression, Climate Change

16. SECURITY CLASSIFICATION OF:			17. LIMITATION OF ABSTRACT	18. NUMBER OF PAGES	19a. NAME OF RESPONSIBLE PERSON
a. REPORT	b. ABSTRACT	c. THIS PAGE			Steven J. Schuldt, AFIT/ENV
U	U	U	UU	144	19b. TELEPHONE NUMBER *(Include area code)* (937) 255-6565x4645 Steven.Schuldt@afit.edu

Standard Form 298 (Rev. 8-98)
Prescribed by ANSI Std. Z39-18